# Synthesis and Performance Evaluation of Nanocomposite SAPO-34/Ceramic Membranes for $CO_2/N_2$ Mixture Separation

**MSc RESEARCH DISSERTATION**

*Prepared by*

**Kgaphola Kedibone Lawrence (303858)**

School of Chemical and Metallurgical Engineering, Faculty of Engineering and the Built Environment, University of the Witwatersrand, Johannesburg, South Africa

Supervisor: Prof. M.O. Daramola

Co-supervisor: Prof. I. Sigalas

August 2017

**Declaration**

I, Kedibone Lawrence Kgaphola, declare that this dissertation is my own unaided work under the supervision of Prof M.O. Daramola and Prof I. Sigalas. It is being submitted for the degree of Masters of Science in Chemical Engineering at the University of the Witwatersrand, Johannesburg. It has not been submitted for any degree or examination at any other university.

Name: Kedibone Lawrence Kgaphola

Signature

Date

**ABSTRACT**

Global warming, resulting from emission of greenhouse gases (GHGs), is the cause of drastic climate changes that threatens the economy and living conditions on the planet. Currently, recovery and mitigation of these greenhouse gases remains a technological and scientific challenge. Various recovery processes for the mitigation of GHGs have been reported including among others carbon capture and storage (CCS). The most mature and applied technology in CCS process involves the absorption of carbon dioxide on amine based solvents. However, studies have shown that this process has several drawbacks that include low stability and high energy required to strip off the absorbed $CO_2$ and regenerate the solvent. This presents an opportunity for the development of new materials for $CO_2$ capture such as zeolite membranes.

Previous studies have shown that the separation of $CO_2$ can be achieved with high selectivity at low temperatures using thin-film SAPO-34 membranes (thin layers on supports). This is because $CO_2$ adsorbs strongly on the membranes compared to other gases found in flue gas. In the thin-film membranes supported on ceramic or sintered stainless steel, thermal expansion mismatch may occur at higher operating temperatures resulting in loss of membrane selectivity due to the formation of cracks. A new method is required to overcome the aforementioned problems, thereby enhancing the separation application of the membranes at higher temperatures.

The effective separation and capture of $CO_2$ from the coal-fired power plant flue gas is an essential part in the CCS process (Figueroa et al., 2016; Yang et al., 2008). Currently, the capture stage is a huge contributor to the overall cost of CCS (Yang et al., 2008). This is due to the high-energy intensity and inefficient thermal processes applied in the separation and capture in various industrial applications (Yang et al., 2008).

This work presents the use of nanocomposite SAPO-34 zeolite membranes synthesized via the pore-plugging hydrothermal method for the separation of $CO_2$ during post-combustion $CO_2$ capture. The SAPO-34 membranes used were supported on asymmetric α-alumina as membrane supports. The membranes were characterized with a combination of dynamic and static physicochemical techniques such as Basic Desorption Quality Test (BDQT), X-ray diffraction (XRD) spectroscopy, Scanning Electron Microscopy (SEM), Fourier Transform

Infrared (FTIR) spectroscopy and thermogravimetric analysis (TGA). The characteristic peaks at 2θ = 21°, 26°, and 32° on the XRD pattern confirmed the presence of SAPO-34 with a rhombohedral crystalline structure. The SEM images showed the formation of the cubic crystalline which were consistent with the reported morphology of SAPO-34. FTIR spectra showed the presence of the essential double-6 membered rings (D6R) and $TO_4$ structural groups in surface chemistry of crystalline materials further confirming the presence SAPO-34. The TGA confirmed that the membranes possessed high thermal stability.

To assess the feasibility of the synthesis process, the nanocomposite zeolites were grown within the tubular supports. The SEM images of the cross-section of the membrane confirmed the presence of the zeolites within the pores of the support confirming the fabrication of nanocomposite membranes by the pore-plugging synthesis method. The permeation tests used a dead-end filtration mode to measure the single gas permeance and the ideal selectivity of $CO_2$ and $N_2$ were calculated.

The BDQT was essential in the study of the quality of the as-synthesized nanocomposite membranes. The quality of the membranes increased with an increase in the synthesis layers of the membranes. However, with an increase in synthesis layers, the membrane thickness also increases. The membrane thickness affected the gas permeance for $CO_2$ and $N_2$ significantly. The permeance of the $N_2$ gas decreased from 10.73 $x10^{-7}$ $mol.s^{-1}.m^2Pa^{-1}$ after the first synthesis to 0.31 $x10^{-7}$ $mol.s^{-1}.m^2Pa^{-1}$ after seven synthesis layers. Alternatively, the more adsorbing gas $CO_2$ decreased from 12.85 $x10^{-7}$ $mol.s^{-1}.m^2Pa^{-1}$ to 2.44 $x10^{-7}$ $mol.s^{-1}.m^2Pa^{-1}$. The performance of these zeolite membranes depends significantly on the operating conditions. Hence, we studied extensively the influence of the various operating conditions such as temperature, feed pressure and feed flowrate in this work.

Results indicated that the membrane separation performance in this study is largely dependent on the temperature. In addition, the ideal selectivity decreased significantly with an increase in temperature. High temperatures results in less adsorption of the highly adsorbing $CO_2$ gas, the permeance reduces significantly, while the permeance of the less adsorbing $N_2$ increased slightly. The feed flow rate has less effect on the adsorbing gas while the non-absorbing gas increased resulting in a decrease in the ideal selectivity as well. The nanocomposite membranes in this study have a low flux compared to their thin film counterparts. An increase in feed pressure significantly increased the flux significantly as well as the ideal selectivity.

Maxwell-Stefan model simulation was done in this study to describe the permeance of pure $CO_2$ single gas permeance as a function of temperature. This model considered explicitly the adsorption-diffusion mechanism, which is the transport phenomenon, involved in the transport of $CO_2$ through the zeolite membrane. The description of the support material was included in the model as well. However, the model was only applied to the $CO_2$ gas permeation well within the experimental data. We then compared the model was with the experimental results and a good correlation was observed.

In conclusion, SAPO-34 nanocomposite zeolite membranes were obtained at low temperatures (150 °C) with a short synthesis time (6 h). In addition, the high thermal stability of the as-synthesized SAPO-34 membranes makes them ideal for high temperature $CO_2$ separation such as the intended post-combustion carbon capture. The BDQT revealed that the quality of the membranes was related to the thickness of the membranes. Therefore, better membrane quality was obtained with relatively thicker membranes. The separation performance evaluation was conducted on the membrane with the greatest quality. Our findings demonstrate that the performance of the membranes depends extensively on the operating conditions.

## Dedications

I would like to dedicate this work to my girlfriend Thandiwe Pule and my friend Olawale Oloye for being my lab partners through the late nights in the lab, weekends we spent on research. I also dedicate this work to my mother Rosina Kgaphola, for supporting me all the time when I wanted to study further and understanding that one degree is just not enough. To my niece and nephews, I hope to raise the bar higher for everyone seeking academic excellence; bear in mind the bar can never be high enough. I dedicate this work to anyone who is interested in the carbon capture and storage. I hope whenever anyone goes through this work questions the ideas reported in this study in order to improve carbon capture techniques and share more ideas through science and technology.

To all my Leaders from The Knockando Hall of Residence, this one is for you. Special dedication goes to Edward “Lord Jemba” Nyakorh for helping me appeal my exclusion from the University during my undergraduate days; Mduduzi “Kakaramba” Skhosana for making an accountable leader; my best friend Brian Mthulisi Moyo for being there through thick and thin… I cannot not mention you all, for it would take the entire Dissertation to list everyone who played a critical role in shaping up my academic life. To all of you, I would like to thank you…”DANKIE, KE YA LEBOGA”

**Acknowledgements**

I would like to thank God. Through Him, everything is possible.

I would also like to thank the following:

The Department of Science and Technology/ National research foundation Centre of Excellence in Strong Materials (DST/NRF CoE-SM) for the financial support for this work.

The University of the Witwatersrand for the facilities and excellent academics on the campus.

My supervisors, Prof M.O. Daramola and Prof I. Sigalas. Without you, this work would not have been possible. Thank you for the endless patience, guidance and support.

My colleagues and friends at the University of the Witwatersrand.

The Wits School of Chemistry for the FTIR spectroscopy and TGA analyses.

The School of Chemical and Metallurgical Engineering for the SEM analyses.

## PUBLICATIONS AND PRESENTATIONS

### Journal Publications

1. **Kedibone, K**., Daramola, M., O., Sigalas, I. Synthesis and Characterization of Nanocomposite SAPO-34/Ceramic Membranes for Post-Combustion $CO_2$ Capture, Asia-Pacific Journal of Chemical Engineering (manuscript in press)
2. **Kgaphola, K.,** Oloye, O., Daramola, M. O., Sigalas, I., Deng, Z., Membrane Materials for $CO_2$ Capture: a short overview (manuscript in preparation).

### Conference Proceedings

3. **Kgaphola, K.**, Daramola, M. O., Sigalas, I., 2016. Synthesis and Characterization of Nanocomposite SAPO-34/Ceramic Membrane for Post-combustion $CO_2$ capture. Unpublished paper at: 3rd National Conference on Global Change, Southern Sun Hotel, Durban, 5th December 2016.
4. **Kgaphola, K.**, 2016. The South African Carbon Emission mitigation: Challenges and Opportunities. Unpublished paper at: 2nd Annual South African International Science Forum, SFSA2016, CSIR Convention centre, Johannesburg, South Africa, 7-8th December 2016.
5. **Kgaphola, K.**, Daramola, M. O., Sigalas, I., 2016. Synthesis and Characterization of Nanocomposite SAPO-34/Ceramic Membrane for Post-combustion $CO_2$ capture. Unpublished paper at: International Conference on Environment, Materials and Green Technology. VUT Southern Gauteng Science and Technology Park, South Africa, 25th November 2016.
6. **Kgaphola, K.**, Synthesis and Evaluation of Nanocomposite SAPO-34/Ceramic Membranes for $CO_2/N_2$ Mixture Separation. Unpublished paper at: 6th International Conference on Nanoscience and Nanotechnology in Africa (NanoAfrica), UNISA Science Campus, Florida, South Africa, 5th April 2016.
7. **Kgaphola, K**., 2016. Synthesis and Evaluation of Nanocomposite SAPO-34/Ceramic Membranes for $CO_2/N_2$ Mixture Separation. Unpublished paper at: 7th Cross-Faculty Postgraduate Symposium, Wits University, Johannesburg, South Africa, 1st March 2016.
8. **Kgaphola, K**., Daramola, M. O., Sigalas, I, 2015. Synthesis and Evaluation of Nanocomposite SAPO-34/Ceramic Membranes for $CO_2/N_2$ Mixture Separation.

Unpublished paper at: 42nd National Convention of the South African Chemical Institute (SACI). Southern Sun Elangeni Hotel, Durban, South Africa, 29th November – 05 December 2015.

9. **Kgaphola**, **K.**, Daramola, M. O., Sigalas, I., 2015. Synthesis and Evaluation of Nanocomposite SAPO34/Ceramic Membranes for $CO_2/N_2$ Mixture Separation. Unpublished paper at: 21st Anniversary Seminar of the School of Chemical and Metallurgical engineering, Wits University, South Africa, 23th September 2015.
10. **Kgaphola, K**., 2015. Breaking the Wall of Industrial $CO_2$ Emissions. Unpublished paper at: The Falling Walls Johannesburg innovator of the year competition hosted by AT Kearny, Wits University, South Africa, 18th September 2015.
11. **Kgaphola, K.**, Daramola, M. O., I., Sigalas, I., 2015. Synthesis, Characterization and Performance Evaluation of Nanocomposite SAPO-34/Ceramic Membranes for $CO_2/N_2$ Mixture Separation. Unpublished paper at: Proposal presented at the 6*th* national student colloquium on clean coal, carbon, energy and the environment. Wits University, South Africa, 30th June 2015.

**TABLE OF CONTENTS**

ABSTRACT ..... iii
Dedications ..... vi
Acknowledgements ..... vii
NOMENCLATURE ..... xvi
Abbreviations and acronyms ..... xvi
Greek ..... xvii
1. Introduction ..... 2
1.1 Background and motivation ..... 2
1.2 Problem statement and aim of research ..... 5
1.3 Aim ..... 6
1.4 Research questions ..... 6
1.5 Research objectives ..... 7
1.6 Expected research outcomes and benefits ..... 7
1.7 Dissertation outline ..... 8
2 Literature review ..... 10
2.1 Introduction ..... 10
2.2 Energy ..... 10
2.1 Importance of energy ..... 11
2.2.2 Energy consumption statistics ..... 11
2.3 Renewable energy resources ..... 14
2.3.1 Bioenergy ..... 14
2.3.2 Direct solar energy ..... 15
2.3.3 Geothermal energy ..... 15
2.3.4 Hydropower energy ..... 16
2.4 Non-renewable energy sources ..... 16
2.4.1 Natural gas ..... 17
2.4.2 Fossil fuels ..... 17
2.4.3 Coal ..... 17
2.4.4 Nuclear energy ..... 18
2.4.5 Implications of fossil-fuel based energy production ..... 18
2.5 Carbon capture and storage (CCS) ..... 20
2.5.1 Carbon Capture methods ..... 22
2.6 $CO_2$ separation and capture techniques ..... 29
2.6.1 Adsorption ..... 32

2.6.2 Cryogenics ..... 33
2.6.3 Membrane separation ..... 34
2.7 Membrane separation technology ..... 36
2.7.1 Types of membranes ..... 37
2.7.2 Polymeric membranes ..... 38
2.7.2 Inorganic membranes ..... 39
2.7.3 Mixed matrix membranes ..... 41
2.7.4 Inorganic membranes in comparison with other types of membranes ..... 42
2.7.5 Zeolite membranes ..... 44
2.7.6 Challenges associated with the existing synthesis methods ..... 51
2.8 Recent development for zeolite membranes ..... 53
2.9 Applications of inorganic membrane in CO2 capture ..... 55
2.10 Single gas permeation mechanisms ..... 56
2.10.1 Single gas permeation tests through the SAPO-34 membranes ..... 58
2.11 Applications of nanocomposite inorganic membrane in $CO_2$ capture ..... 59
3 Experimental Procedures ..... 62
3.1 Introduction ..... 62
3.2 Synthesis of zeolite membranes ..... 62
3.3 The pore-plugging synthesis for nanocomposite membranes ..... 63
3.4 The support ..... 63
3.5 Experimental methods ..... 65
3.5.1 Development of the SAPO-34 pore-plugging protocol ..... 65
3.5.2 Preparation of nanocomposite membranes ..... 66
3.5.3 Membrane synthesis ..... 66
3.6 Static characterization techniques ..... 70
3.6.1 X-ray Diffraction ..... 70
3.6.2 Scanning electron microscopy and EDS ..... 70
3.6.3 Thermogravimetric analysis ..... 70
3.6.4 Fourier Transform Infrared Spectroscopy (FTIR) ..... 71
3.7 Membrane calcination ..... 71
3.8 Dynamic characterization ..... 73
3.8.1 Single gas permeation before calcination ..... 73
3.8 Basic desorption quality test ..... 73
3.9 Single gas permeation tests ..... 75
3.10 Gas separation performance ..... 76

4 Nanocomposite SAPO-34/Ceramic membranes: Synthesis, Static and Dynamic Characterization ..... 78
4.1 Introduction ..... 78
4.2 Nanocomposite membrane synthesis and characterization ..... 78
4.3 Membrane quality evaluations ..... 78
4.4 Results and discussion ..... 78
4.4.1 FTIR spectroscopy results ..... 78
4.4.2 TGA analysis ..... 80
4.4.3 XRD analysis ..... 81
4.4.5 SEM analysis ..... 85
4.5 Basic Desorption Quality Test ..... 93
4.6 Concluding remarks ..... 94
5 Nanocomposite ceramic/SAPO-34 membranes: the effects of operating conditions on the separation performance ..... 97
5.1 Introduction ..... 97
5.2 Results and discussion ..... 97
5.2.1 Error analysis in measured values ..... 97
5.2.2 Single gas permeation tests through the SAPO-34 membranes ..... 97
5.3 Comparison of obtained results to selected zeolite membranes reported in literature ..... 101
5.4 Maxwell-Stefan modelling for the SAPO-34 membranes ..... 105
5.5 The effect of temperature on the separation performance ..... 106
5.5.1 The effect of pressure on the separation performance ..... 109
5.5.2 The effect of flow rate on the separation performance ..... 112
5.6 Concluding remarks ..... 114
6 Conclusions and general outlook ..... 117
6.2 Recommendations ..... 118
7.1 References ..... 120
Appendix 1 ..... 144

**LIST OF FIGURES**

Figure 2.1 Global energy consumption projections by yearly region in British thermal units (Btu) (adopted from the IEO 2016).....12

Figure 2.2 Global energy resource consumption by year in Btu (adopted from IEO 2016).....13

Figure 2.3: A bar chart illustration of the global energy-related $CO_2$ emissions (adopted from WEC 2016).....19

Figure 2.4 CCS flow diagram showing various stages of the CCS stages .....21

Figure 2.5 The main carbon capture methods (adopted from Olajire, 2010) .....23

Figure 2.6 A typical CO2 capture process diagram using MEA absorption technique (adopted from Osman et al., 2013).....28

Figure 2.7 Reported carbon capture techniques (adapted from Olajire, 2010).....30

Figure 2.8 Schematic Illustration of the adsorbent based CO2 capture process (adapted from Yang et al., 2008) .....32

Figure 2.9 A process flow diagram of a typical cryogenic $CO_2$ separation method (Adapted from Yang et al., 2008).....34

Figure 2.10 A two stage membrane process flow diagram for $CO_2$ separation (adapted from Zhang et al., 2014). .....36

Figure 2.11 The pore opening structure of SAPO-34 zeolite (adapted from Dent & Smith, 1958). .....60

Figure 3.1 Ceramic membrane tube with graphite O-rings (note 10 mm sealed endings) (picture not to scale). .....64

Figure 3.2 The cross-sectional view of the asymmetric ceramic support. .....64

Figure 3.3 Experimental flow diagram illustrating the experimental procedure. .....65

Figure 3.4 Experiment method for the synthesis of SAPO-34/ceramic membranes .....67

Figure 3.5 A Teflon-lined stainless autoclave components used for the synthesis of SAPO-34 .....68

Figure 3.6 Temperature program diagram for the nanocomposite membrane synthesis.....69

Figure 3.7 Stainless steel membrane reactor module include the graphite ring and the membrane.....71

Figure 3.8 Cross-section view of the assembled membrane reactor module (not to scale).....72

Figure 3.9 The temperature program for the pretreatment method. .....73

Figure 3.10 Heating oven used for the calcination of the membranes under $N_2$ atmosphere..72

Figure 3.11 Schematic representation of the BDQT experimental setup. .....75

Figure 4.1 FTIR spectrum of the SAPO-34 crystals.....79

Figure 4.2 TGA profiles of the as-synthesized SAPO-34 crystals .....81

Figure 4.3 XRD results of the as-synthesized SAPO-34 compared with the calculated reference.....83

Figure 4.4 XRD results of the as-synthesized SAPO-34 compared with the supported zeolite membranes as well as the calculated reference.....84

Figure 5.1 Single gas permeance as function of number of synthesis stages .....100

**LIST OF TABLES**

Table 2.1 Fossil fuel-powered emission levels. ..... 19

Table 2.2 Direct comparison of the costs associated with and without $CO_2$ capture in coal-fired power plants (IEA greenhouse gas programme). ..... 25

Table 2.3 Comparison of advantages and disadvantages of current capture technologies ..... 26

Table 2.4 Current and potential extension of carbon capture technologies. ..... 27

Table 2.5 Advantage and disadvantages of current $CO_2$ separation methods ..... 31

Table 2.6 Comparison of inorganic and organic membranes ..... 43

Table 2.7 Examples of synthetic zeolite membranes (Bekkum et al., 2007; Szostak, 1998) .. 45

Table 2.8 Selected gas separation membrane application (Adapted from Ismail et al., 2002) 47

Table 2.9 Summary the most common zeolite synthesis techniques. ..... 49

Table 4.1 FTIR functional group identification and interpretation ..... 80

Table 5.0.1 Room temperature single gas permeation properties ..... 99

Table 5.2 Comparison of $CO_2/N_2$ Separations through selected Zeolite Membranes ..... 104

## NOMENCLATURE

### Abbreviations and acronyms

| | |
|---|---|
| SAPO-34 | Siliconaluminohoshate-34 |
| SDA | structure directing agent |
| CCS | Carbon capture and storage |
| BDQT | Basic desorption quality test |
| GHG | Greenhouse gas |
| EOR | Enhance oil recovery |
| IZA | International zeolite association |
| IEA | International energy agency |
| WEO | World energy outlook |
| IGCC | Integrated gasification combined cycle |
| ESA | Electrical swing adsorption |
| PSA | Pressure swing adsorption |
| TSA | Temperature swing adsorption |
| LTA | Linde type A |
| CVD | Chemical vapor deposition |
| DDR | Deca-dodecasil 3R |
| D6R | Double six membered ring |
| OECD | Organization of Economic Cooperation Development |
| $\Pi_i$ | Permeance of gas component *i* |

| | |
|---|---|
| PPH | pore-plugging hydrothermal synthesis |
| SEM | Scanning electron microscopy |
| XRD | X-ray diffraction |
| FTIR | Fourier-transform infrared spectroscopy |
| TGA | Thermogravimetric analysis |
| $\Delta P$ | Transmembrane pressure |
| A | Total membrane area |
| R | Ideal gas constant |
| $C_{sat}$ | Saturated concentration of the gas |
| $D_0^{\infty}$ | Stefan–Maxwell diffusivity |
| L | Membrane equivalent thickness |
| $P_R$ | Retentate pressure |
| $P_p$ | Permeate pressure (Pa) |
| $P_0$ | Atmospheric pressure |
| $\Delta S_{ads}°$ | Adsorption entropy |
| $\Delta H_{ads}°$ | Adsorption enthalpy |
| $E_D$ | Diffusion activation energy |
| ZSM-5 | Zeolite socony mobil-5 |

**Greek**

| | |
|---|---|
| $\alpha_{i/j}$ | ideal selectivity estimated from permeances |
| $\theta$ | adsorption fractional coverage |
| $\varepsilon$ | porosity |
| $\tau$ | tortuosity factor |
| $\rho$ | density |

# Chapter One

## Introduction

# 1. Introduction

In this chapter, motivation, justification, and research objectives are highlighted. The industrial and scientific benefits from this study are outlined as well.

## 1.1 Background and motivation

The current energy crisis as well as global warming which is associated with $CO_2$ emissions has resulted in a high demand for energy efficiency as well as energy saving techniques. Currently, the dominant sources of energy around the globe results from burning fossil fuels. These energy sources are both environmentally unfriendly as they result in the emissions of $CO_2$ that causes global warming. Carapellucci and coworkers (2003) stated that more than 40% of the total anthropogenic $CO_2$ emissions is due to fossil-fuel powered industries.

Consequently, these chemical industries are highly encouraged by various government policies across the globe to improve on their energy efficiency to reduce $CO_2$ emissions. Scientific studies have reported that one of the ways to reduce $CO_2$ emissions in these fossil fuel powered industries is by the carbon capture and sequestration (CCS), also referred as carbon capture and storage (Merkel *et al.*, 2010). The CCS technology includes; (i) the capture of $CO_2$ from emission sources, (ii) transportation of the captured $CO_2$ to storage sites and finally, (iii) the storage of the captured $CO_2$ at various suitable storage sites.

The most essential part of the CCS processes is the carbon capture as it has a high contribution to overall cost of the energy production. Most researchers have reported various methods to capture the $CO_2$ from their emission points (Merkel et al., 2010; Yang et al., 2008). The capture methods are classified as:

i. Pre-combustion capture: This involves recovering $CO_2$ in the synthesis gas after conversion of CO into $CO_2$ in the stream before the combustion of the fuel and applies primarily to gasification plants;
ii. Oxy-combustion: This involves the combustion of fuel in pure oxygen mixed with recycled exhaust gases, which produces predominantly $CO_2$ and water. The water can be removed by condensation, while the $CO_2$ can be removed inexpensively;
iii. Post-combustion capture: This involves removing $CO_2$ from other exhaust gases produced after the combustion process and applies primarily to coal-fired power plants.

Currently, the most industrially matured technology for $CO_2$ capture is the amine absorption using various amine based solvents. However, this technology is energy intensive because of the energy required to regenerate the spent solvent when the absorbed $CO_2$ is stripped off. The most energy-efficient and recyclable methods were found to be the membrane and the adsorption technologies (Camus et al., 2006). Energy efficient technologies warrant further investigations to replace the currently applied energy intensive technologies.

The most commercially applied membrane technology in industrial processes are the polymeric membranes (Powell & Qiao 2008; Yang et al., 2008). These membranes were reported to have high $CO_2/N_2$ selectivity required for the separation and capture of $CO_2$ (Yang et al. 2008). The membranes presented a high reproducibility as well as promising separation performance characteristics (Olajire, 2010; Yang et al., 2008). However, these membranes are thermally and chemically unstable resulting in the inability to withstand extreme operating conditions (Daramola et al., 2010; 2012; Olajire, 2010; Yang et al., 2008). The key requirements in the membrane technology for industrial processes is high chemical, thermal and mechanical stability (Yang et al., 2008). Inorganic membranes can overcome the limitations associated with the polymeric membranes.

Several studies have explored various zeolite and zeolite based membranes supported on ceramic or sintered stainless steel (thin-films membranes) such as Zeolite Socony Mobile Five (ZSM-5), Zeolite A (LTA), Chabazite (CHA), Deca-dodecasil 3R (DDR), Silicon Aluminum Phosphate (SAPO-34) and Faujasite (FAU) in the $CO_2$ separation and capture processes (Carreon *et al.*, 2008; Crawford, 2013; Prakash, 1994; Sato & Nakane, 2007). These various materials have been reported to have different pore dimensions, which are essential for the separation of the $CO_2$ from other gas molecules (Carreon *et al.*, 2008; Crawford, 2013; Prakash, 1994; 1999).

For instance, it has been reported in the above-mentioned studies that $CO_2$ can be selectively separated from light gaseous mixture such as $CO_2/H_2$, $CO_2/CH_4$ and $CO_2/N_2$ using thin-film membranes. The separation of these gases can be achieved at a wide range of temperatures from relatively low to exceptionally high temperatures (Baker, 2002; Merkel *et al.*, 2010; Yang *et al.*, 2008; Zhao *et al.*, 2008). These highly desirable separations should be achieved because $CO_2$ has high affinity for the various zeolites, resulting in a strong adsorption of $CO_2$ on the zeolites (Yang *et al.*, 2008).

As for the $CO_2/N_2$ mixture, the high selectivity is governed by the preferential adsorption of $CO_2$ at relatively low temperatures. At high temperatures it is however governed by diffusion resulting in $CO_2$ (0.33 nm kinetic diameter) having a higher permeance than $N_2$ (0.36 nm kinetic diameter) due to their difference in diffusivities through the membranes (Baker et al., 2002; Figueroa et al., 2010; Yang et al., 2008). However, in Thin-film membranes, thermal expansion mismatch between the zeolites and the supports may occur at higher operating temperatures resulting in loss of membrane selectivity due to cracks formation that enhances the permeance of wanted gases. This phenomenon is more enhanced in membranes supported on stainless steel because of a high disparity between the thermal expansion of the membrane and that of the stainless steel (Daramola et al., 2015). This limitation acts as a barrier for membranes to be applied in industrial high temperature applications. A new method is required to overcome the aforementioned problems, thereby enhancing the separation application of the membranes at higher temperatures.

Shortcoming associated with thin-film membranes can be overcome by using nanocomposite zeolite membranes, where by the zeolite crystal are grown and embedded within the pores of the supports instead of a thin film on top of the supports (Daramola et al., 2015; Miachon et al., 2006). Desirable advantages of the nanocomposite architecture includes limiting the defects to the size of the support pores and higher mechanical and thermal stability (Miachon et al., 2006). These membranes have shown promising membrane separation performance as reported in previous studies (Daramola et al., 2015; Deng et al., 2010; Miachon et al., 2006; 2007).

Hence, this current work explored the pore-plugging hydrothermal synthesis method to produce nanocomposite zeolite membranes. This method was recently reported to have an enhanced reproducibility when producing nanocomposite zeolite membranes (Daramola et al., 2010; 2012; Miachon et al., 2006; 2007). The resulting nanocomposite membranes are protected by the support against any abrasions during membrane handling (Alshebani *et al.*, 2006; Daramola *et. al.*, 2012).

Additionally, the nanocomposite membranes were reported to have a desirable compensation for the thermal expansion missmatch between the supports and the zeolite membranes (Miachon, *et. al*, 2006). These desirable advantages encourage further studies to explore the nanocomposite membranes in industrial applications. Hence, this research focused on using nanocomposite SAPO-34 zeolite membranes for post-combustion $CO_2$ capture. SAPO-34

materials are referred to as synthetic microporous and crystalline zeolite-like materials (Crawford, 2013; Hong *et al.,* 2007). Previous work has shown that SAPO-34 materials are effective in the separation of high purity $CO_2$ from a $CO_2/N_2$ gas mixture (Li & Fan, 2010; Poshusta *et al.*, 1998). However, these studies focused on the thin-film zeolite membranes (thin layer of zeolite membrane on top of a ceramic support). The thin-film membranes have been reported to have limitations that hinder industrial applications such as cracks formation because of the thermal expansion mismatch at high temperatures as well as abrasion during membrane handling. Thus, the development of alternative fabrication that can overcome the limitations is essential. Nanocomposite membrane architecture has been reported to overcome these limitations but nanocomposite SAPO-34 membranes are yet to be explored extensively in post-combustion $CO_2$ capture.

Thus, the main objective of the current study was to investigate the possibility of developing nanocomposite SAPO-34 membranes for the post-combustion $CO_2$ capture in coal-fired power plant flue gas. Having in-depth knowledge to overcome limitation associated with reported thin-film membrane separation techniques; this work utilized the pore-plugging synthesis technique (Alshebani *et al.,* 2008; Miachon *et al*., 2006; Li *et al*., 2008; Daramola *et al.,* 2012) to produce nanocomposite SAPO-34 membranes within α-alumina supports. Furthermore, this work investigated the quality and the performance of the as-synthesized membranes for post-combustion $CO_2$ capture through single gas permeation tests and separation of $CO_2/N_2$ gas mixture.

### 1.2 Problem statement and aim of research

The increasing concentration of $CO_2$, a well-known Greenhouse Gas (GHG), in the atmosphere due to large emission sources has received a considerable attention in recent studies as it is linked to global warming (Olajire, 2010; Yang et al., 2008). The resulting global warming is a major course of drastic climate changes which threatens the economy and living conditions on the planet (IEA, 2016). Currently, recovery and mitigation of this particular greenhouse gas remains a technological and scientific challenge (Yang et al., 2008). Various recovery processes have been reported, amongst them the CCS (Daramola et al., 2015; Olajire, 2010; Yang et al., 2010). CCS has been proposed as a method with a high potential at reducing $CO_2$ emissions, from stationary and mobile point sources. The most mature and applied technology in CCS process involves the absorption of carbon dioxide on amine based solvents (Yang et al., 2008). However, studies have shown that this process has

several drawbacks which include low stability and high energy required to strip off the absorbed $CO_2$ and regenerate the solvent. This presents an opportunity for the development of various zeolite membranes for $CO_2$ capture.

Various authors reported SAPO-34 zeolite membranes with a high chemical and thermal stability (Li et al., 2004; 2010; Prakash et al., 1998). These studies have shown that the separation of $CO_2$ can be achieved with high selectivity at low temperatures using thin-film SAPO-34 membranes, which are normally thin layers on supports, because of the preferential adsorption of $CO_2$ on the surface of the membranes than the other gases found in the flue gas (Li et al., 2010; 2012). In the thin-film membranes supported on ceramic or sintered stainless steel, thermal expansion mismatch may occur at higher operating temperatures resulting in loss of membrane selectivity due to cracks formation. A new method is required to overcome the aforementioned problems, thereby enhancing the separation application of the membranes at higher temperatures. In this study a new synthesis method, the pore-plugging hydrothermal synthesis, was explored to produce nanocomposite SAPO-34 membranes for post-combustion $CO_2$ capture.

Thus, the current study aims to utilize nanocomposite ceramic SAPO-34 membranes in the separation of $CO_2$ and $N_2$ for post combustion $CO_2$ recovery processes. In this SAPO-34, membranes were synthesized within the pores of a ceramic support by the pore-plugging hydrothermal synthesis technique. We evaluated the separation performance and operational stability of the as-synthesized nanocomposite SAPO-34 membranes in post-combustion $CO_2$ capture using a $CO_2$ single gas as a model. Moreover, we also investigated the effect of operational parameters such as feed pressure, temperature, and feed flow rate as well.

### 1.3 Aim

The aim of this study is to use an unconventional pore-plugging hydrothermal synthesis technique in order to synthesize nanocomposite SAPO-34 membrane within the pores of a ceramic support and evaluate them for post-combustion $CO_2$ capture.

### 1.4 Research questions

The research questions that this work seeks to answer are:

a. Can nanocomposite SAPO-34/ceramic membrane be synthesized via pore-plugging hydrothermal synthesis technique?

b. What will the separation performance of the nanocomposite SAPO-34/ceramic membranes during the separation of $CO_2/N_2$ gas mixture be?
c. What will be the effect of operating conditions on the separation performance of SAPO-34/ceramic membranes during the separation of $CO_2/N_2$ gas mixture be?

### 1.5 Research objectives

The objectives of this research work are:

a. To investigate the formation of pure SAPO-34 crystals via the pore-plugging hydrothermal technique and to characterize the synthesized crystals.
b. Using the developed material in (a) to prepare nanocomposite SAPO-34/Ceramic membranes via pore-plugging technique and to characterize the as-synthesized membranes using static and dynamic characterization techniques.
c. To evaluate the separation performance of the as-synthesized nanocomposite SAPO-34/ceramic membranes using single gas $CO_2$ and $N_2$ permeation experiments and compare the results with literature findings.
d. To evaluate the effects of operating conditions (temperature, pressure and feed flow rate) on the separation performance of the as-synthesized membranes.

### 1.6 Expected research outcomes and benefits

Results obtained from this research project will highlight the development and implementation of nanocomposite SAPO-34 membranes in post-combustion $CO_2$ capture from coal-fired power plants.

This research project highlights the possibility of combining the membrane separation technology with the current carbon capture and storage processes. This study further highlights the desirable properties associated with the synthesis of nanocomposite SAPO-34 membranes by the pore-plugging technique on the separation performance of $CO_2/N_2$ gas mixture. Moreover, the study provides a detailed report on effects of operating conditions on the separation performance of the as-synthesized.

In this dissertation, relatively new ideas were developed and tested. Therefor, the novel contribution of this research study that could be built upon is the separation performance of nanocomposite SAPO-34/ceramic tubular zeolite membranes for post-combustion $CO_2$

capture in coal-fired power plants. The study of nanocomposite SAPO-34 membranes for post combustion has not been extensively reported in open literature.

The outcome from this research study opens a platform to investigate scale-up processes for industrial applications of nanocomposite SAPO-34 membranes as well as other various nanocomposite architecture based zeolite membranes. The research ideas developed in this study were presented at national and international conference proceedings.

### 1.7 Dissertation outline

**Chapter 1** discusses the motivation and the objectives of the study. In this introduction, detailed concepts of the research problems were outlined along with solutions to the problems that were mentioned.

**Chapter 2** discusses the state-of-the-art technologies for the mitigation of the anthropogenic $CO_2$ through a literature review. The emphasis was placed on the challenges and opportunities presented by the various separation technologies.

**Chapter 3** describes the preparation and characterization of the SAPO-34 zeolite membranes with more emphasis on the nanocomposite SAPO-34 zeolite membranes. This chapter also outlines the instrumentation as well as experimental procedures used to produce the results that are described in this dissertation.

**Chapter 4** concentrates mainly on the analysis of the data obtained from the X-ray diffraction (XRD), scanning electron microscope (SEM), fourier transform infrared spectrometer (FTIR) and thermal gravimetric analysis (TGA) of the SAPO-34 membranes compared with literature.

**Chapter 5** focuses on the analysis of the separation performance of the as-synthesized SAPO-34 nanocomposite zeolite membrane in single gas permeation tests as well as $CO_2/N_2$ gas mixture separation.

**Chapter 6** provides the general conclusions of this research study and future work recommendation.

# Chapter Two

## Literature Review

# 2 Literature review

## 2.1 Introduction

The current global energy crisis caused by an exponential growth in population with high-energy demands calls for energy efficient technologies to be implemented in industrial processes (Olajire, 2010; Yang *et al.,* 2008). High energy demands from conventional nonrenewable sources of energy such as the combustion of fossil fuels are environmentally unfriendly (Merkel et al., 2010; IPCC, 2014). Scientific studies have shown that more than 40% of $CO_2$ emissions, a well-known Green House Gas (GHG), is due to fossil-fuel powered industries (Carapellucci & Millazzo, 2003; Merkel *et al.*, 2010; Yang *et al.*, 2008). Among other GHGs, $CO_2$ is a major contributor to global warming due to its high emissions which have been reported to have a contributing factor of approximately 60% (Albo *et al.,* 2010). Global warming is a major cause of drastic climate change which threatens the economy, the ecology and living conditions on the planet (Daramola *et al.,* 2010; 2015 Olajire, 2010).

On the other hand, utilizing energy efficient technologies as well as switching to non-fossil fuel based energy sources can reduce the greenhouse gas emissions (Yang *et al.,* 2008). For instance, renewable energy (RE) sources, nuclear and carbon capture and storage (CCS) could be used in energy production to reduce GHG emissions (IPCC, 2014; Merkel et al., 2010; Yang et al., 2008). These options along with selected viable technologies that can be applied to mitigate $CO_2$ emission are discussed in detail in this chapter.

## 2.2 Energy

Energy can be defined as the property of matter, which can be converted into work, radiation or work. Though energy itself cannot be created or destroyed, it can be converted from one form into another. Work and heat are the essential forms of energy required by the global society. These forms are currently being used for the production of electricity. However, this are not the most primitive forms of energy that are readily available for the world consumption. The conversion of natural energy resources to heat and work is essential prior to consumption.

The definition of energy emphasizes the fact that energy conversion is essential for the energy utilization. However, during this conversion bi-products are generated as waste. These wastes include GHG emissions. The GHG emissions produced in the energy sector represents approximately two-thirds of all anthropogenic GHG emissions (IEA, 2016). The GHG

emissions has seen a rise in the past century making it difficult to tackle the climate change problem. On a global scale, the need for energy outweighs the global climate change concerns.

## 2.1 Importance of energy

The supply of energy plays an important economic, social and environmental role. Not all energy is supplied on a commercial platform. Traditionally biomass, which provides energy required for heating and cooking in developing countries in non-commercial. Currently, universal access to commercial energy sources remains a challenge. For many countries, especially developing countries in Africa and Asia, the electrification pace lags behind the increase growth in demand. It is essential to address this paramount challenge without further delays, particularly taking into account the impact that an access to electricity has on people's lives and well-being, social development and economic growth. This includes access to basic social services such as health, housing and education. The rising energy demand results in a high consumption and depletion of most nonrenewable energy resources. However, the energy industry has been able to meet this growth globally assisted by continuous increases in reserves' assessments and improving energy production and consumption technologies.

### 2.2.2 Energy consumption statistics

The International Energy Outlook 2016 (IEA, 2016) has reported a significant increase in the global population which leads to an exponential increase in energy demand over a 28-year period projection from 2012 – 2040. Figure 2.1 shows that most of the energy demands come from the developing nations outside the Organization for Economic Cooperation and Development (non-OECD). The non-OECD has experienced more than a 70 % increase in energy demand in the projected 28-year period (IEA, 2016; WEC, 2016).

On the other hand, the OECD nations counterparts are currently experiencing slower growth in their economies and are expected to have an energy demand rise of about 18 % in coming years (IEA, 2016; WEC, 2016).

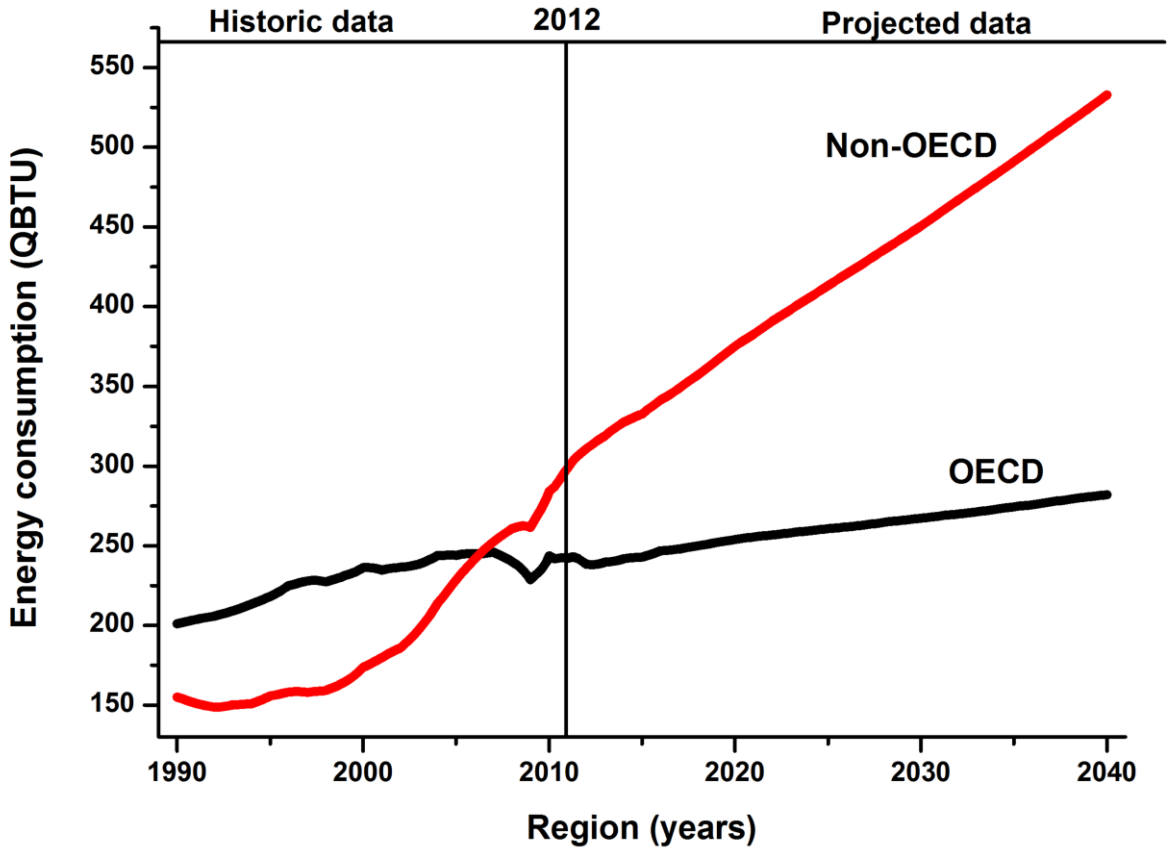


Figure 2.1 Global energy consumption projections in British thermal units (Btu) (adopted from the IEO 2016)

The increase in economic growth results in improvements in infrastructure that influences the global energy demands (WEC, 2016). As a nation develops, living standards improve and the energy demands grow rapidly as a result of the demand for better housing which requires increasing number of electrical appliances.

The increase in population leads to an increase in transportation and a growing capacity in the production of goods and services to sustain the improving life-style. These changes in the economy lead to a high demand for energy and often the supply cannot meet the demand (IEA, 2016). On a global scale, as more countries develop, the resulting energy consumption dramatically increases leading to the depletion of the unsustainable energy resources (IEA, 2016; WEC, 2016). The past two decades have experienced exceptional changes in the consumption of energy resources (WEC, 2016). The GHG emissions that resulted in this tremendous increase in energy production and consumption contributed significantly to the GHG atmospheric concentrations (IPPC, 2014). A special report by the IPCC concluded that the observed increase in the global average GHG concentrations since the 20-centuy is due to anthropogenic greenhouse gases from energy production (IPCC, 2016).

The unsustainable and environmentally hazardous fossil fuels currently dominate the global energy resources (Daramola, 2016; IEA, 2016; WEC, 2016). This led to serious concerns about the sustainability of these sources and reduction in environmental hazards caused by the emission of greenhouse gases (IPCC, 2014; WEC, 2016; Yang et al. 2008). Hence, the increase in the use of the less carbon-intensive energy sources such as renewable energy sources and nuclear power. Figure 2.2 illustrates the global energy consumption by source associated with the International Energy Organization projection (IEO, 2016).

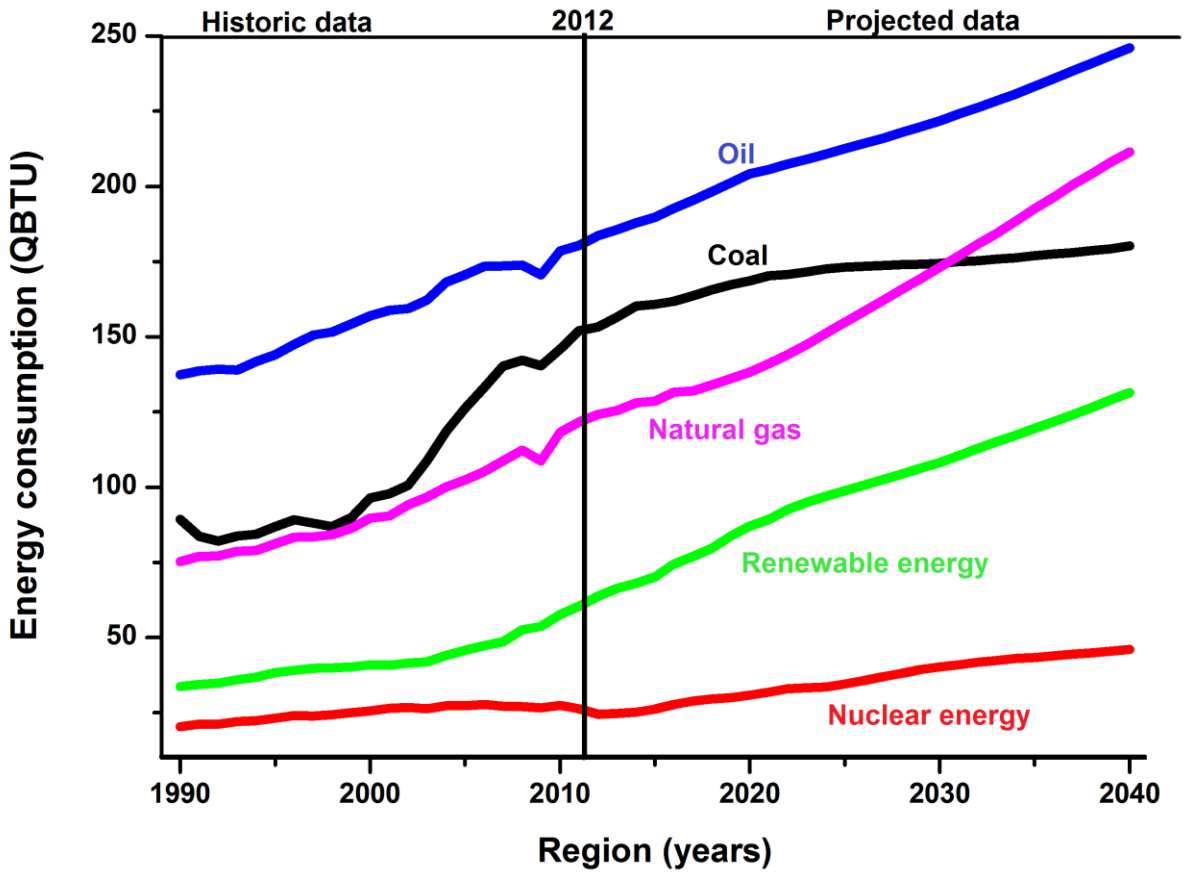


Figure 2.2 Global energy resource consumption by year in Quadrillion British Thermal Units (QBTU) (Adopted from IEO 2016)

As a result of various government incentives and policies encouraging the use of less carbon intensive fuels source, the renewable energy consumption is projected to have the highest increment rate, followed by the nuclear and natural gas from 2012 to 2040 (IEA, 2016; WEC, 2016). The consumption of coal is estimated to have the lowest increment rate as there as shift to more non-fossil fuel based energy consumption sources (IEA, 2016). The oil consumption has received a steady increment over the years as it is highly used in the transportation sector which has seen an exponential growth in recent years (IEA, 2016).

Although the fossil fuels are highly carbon-intensive, they remain a predominant source of fuel (WEC, 2016). On the other-hand, alternative energy resources such as renewable and nuclear have challenges that need to be addressed (WEC, 2016). Multiple options are required to lower the GHG emissions while meeting the global energy demands. These various energy resource present various challenges and development opportunities that need to be addressed. Renewable energy sources have been reported to provide exceptional benefits required to reduce GHG emissions (IPCC, 2014; WEC, 2016; Yang et al., 2008)

### 2.3 Renewable energy resources

When considering lowering the major GHG emissions such as $CO_2$, renewable energy is the way to go for future energy generation (Kumar et al., 2017; Prakash & Saravanan, 2014; WEC, 2016). This is a growing technically mature energy production option with a near zero GHG emission (IPCC, 2014).

The World Energy Council (2016) reported that the unprecedented changes in the energy consumption contributed to the high amount of GHG emissions. This report supported a statement in a discussion paper by Abolhosseini and co-workers (2014) that stated that many countries have started to install facilities that produce power by renewable energy sources.

Global policies encourage the deployment of renewable energy in a wide range of applications such as; renewable feeds stocks, electricity production, thermal and mechanical energy as well as fuel production to service the multiple energy needs (Abolhosein et al., 2014; IPCC, 2014; Prakash & Saravana, 2016). Renewable energy spans from and is not limited to bioenergy, direct solar energy, geothermal and hydropower. Although these renewable energy sources presents an alternative to the fossil fuel as far as $CO_2$ emissions mitigation is concerned they present various challenges that limit their application as a replacement for fossil fuels.

#### 2.3.1 Bioenergy

Bioenergy represents the transformation of various biological feedstocks, including agricultural and livestock residues, forest, plantations, organic solid waste, and other organic wastes into energy (IPCC, 2014; WEC, 2016). The feedstock can either be collected from the natural surroundings or it can be grown for bioenergy purposes (Hennenberg et al., 2010). In some cases, a combination of feedstocks produce electricity or heat as well as gaseous, liquid or solid fuels (IPCC, 2016).

Bioenergy is the largest renewable energy source, which has accounted for 10 % of the global energy supply (WEC, 2016). Bioenergy has shifted from the traditional indigenous energy source to one of the traded commodities globally (IPCC, 2014; WEC, 2016). However, the primary source of bioenergy remains biomass (WEC, 2016). Maes & Passel (2014) argued that the continued use of bioenergy is not sustainable as it often leads to deforestation. This argument was further supported by various reports which argued that bioenergy results in a limitation to ecology and biodiversity (Larkum et al., 2010; Pedroli et al., 2013; van Vuuren et al., 2009). Furthermore, IPCC reported that the main disadvantage of bioenergy is that it depends on the local and regional fuel supply (IPCC, 2014).

### 2.3.2 Direct solar energy

Solar energy technologies are globally installed to harness the direct radiation from the sun and convert it into thermal energy (Grangvist et al., 2007; Mor et al., 2006; Baetens et al., 2010). This is done either through active or passive means using photovoltaics (PV) and solar power concentrations (Baetens et al., 2010; IPCC, 2014). The costs of solar power are constantly declining with new market for the solar energy industry constantly emerging with a backup from policy and regulatory incentives (WEC, 2016).

The solar energy storage technologies are constantly improving with new technologies such as Perovskite cell being commercialized (WEC, 2016). The solar energy comes across as a temporal energy source due to the predictable solar energy output profiles, which are only suitable for small-scale energy demands (Soangi et al., 2011; IPCC, 2014).

### 2.3.3 Geothermal energy

Geothermal energy comprises drilling and accessing the thermal energy from the earth's crust, which is then extracted from geothermal reservoirs by wells, amongst other means (Barbier et al., 2002; Dickson & Fanelli, 2013 Lund & Freeston, 2001). Once this energy is extracted to the surface then fluids at various temperatures are used to generate electricity (Armstead, 1978; Dickson & Fanelli, 2013; Milora et al., 1976).

The geothermal energy compared to other renewables, contributes to a small proportion of the global energy consumption. Limitations of geothermal energy include but are not limited to higher installation cost and relatively long development periods (Dickson & Fanelli, 2013; WEC, 2016). Thus, most governments are reluctant to invest in geothermal energy as compared to other renewable energy sources (WEC, 2016).

### 2.3.4 Hydropower energy

For hydropower energy generation, energy from moving water is harnessed at lower elevations. Hydropower may vary from dam projects with reservoirs, river-runs, and streams (Akpinar et al., 2013; Stickler et al., 2013; WEC, 2016). The variety give the hydropower generation to cater for a larger demand of energy. Innovative technologies in the hydropower generation include:

(I) Increased scale of turbines, conventional as well as pumped hydropower

(II) Advanced hydropower control technologies

The controlled output of the energy production is essential to meeting the peak hour demands and help balance the energy with a large amount of generation (IPCC, 2016; Sipahutar et al., 2013). Hydropower has had successful synergies with the other energy generation methods to improve energy supply (Akpinar et al., 2013; Stickler et al., 2013). The role of Hydro power is expected to increase soon because of its a high potential renewable energy source (WEC, 2016). However, the current drought being experienced because of global warming provides a limitation to hydropower generation.

## 2.4 Non-renewable energy sources

Although the consumption of renewable energy resources is expected to grow faster than fossil fuels, fossil fuels are reported to still account for more than 78 % of the energy use in the case study by the IEA (2016). Natural gas has seen the fastest growth in consumer (IEA, 2016). Global natural gas includes the shale gas and coalbed methane (Sloan, 2003). Even though there is a serious concern about the environmental pollution caused by fossil fuels, oil based fuel sources remain the largest source of energy consumption globally (Anastas & Warner, 2016; Crutzen et al., 2008; Howarth & Santoro, 2011).

The unpredictable oil prices have led to a growing confidence in the consumption of coal as it comes across as the most abundant energy source (IEA, 2016; Shafiee & Topal, 2009; WEC, 2016). Coal is widely used as a source of electricity, which has resulted in high amounts of anthropogenic GHG emissions (Leo et al., 2009; Zedtwitz & Steinfeld, 2003). Implantation of energy efficient technologies could result in continued use of coal as a fuel source while mitigating greenhouse emissions (Leo et al., 2009).

### 2.4.1 Natural gas

Natural gas has been reported to account for the largest increase by an energy source in the global energy consumption (IEA, 2016). The WEC (2016) reported it as a fossil fuel energy source that has the highest potential in the global transition into cleaner, secure and affordable energy (Brandt et al., 2014; Dicks, 1996). Recent advances in technologies on the supply side have altered the global landscape and created a new prospect for affordable and secure supplies of natural gas (Howarth & Santoro, 2011; WEC, 2016).

The new emerging natural gas reserves interconnected with the integration of global natural gas markets make natural gas a desirable source of energy (Sloan, 2003). Thus, creating a better gas-to-gas pricing, trade, and consumer bargaining power (WEC, 2016). The abundance of natural gas resources and the robust production contributes to the highly competitive position of natural gas among other energy resources (IEA, 2016).

Natural gas contributes highly to electric power sector as well as the industrial sector, which are the two sectors that have a high contribution to the global energy consumption. There are major concerns about methane as a source of fuel such as the high greenhouse gas footprint limiting further the development of natural energy production (Allen et al., 2013; Brandt et al., 2014; Howarth & Santoro, 2011).

### 2.4.2 Fossil fuels

Oil remains the dominant source of fuel in the world, (IEA, 2016) and it accounts for more than 32 % of the total energy consumption. Although the price of oil is unpredictable, the growth in population will support the oil demand for future generations hence increasing the oil consumption (Urry, 2013; WEC, 2016). Most of the energy consumption is projected to increase due to the growth in transportation sectors.

### 2.4.3 Coal

The WEC (2016) reported that at this point the consumption of coal is well over 7 700 Mt. The consumption is essential in a variety of sectors from iron and steel production, liquid fuel as well as electricity production. Coal currently accounts over 40 % of the world's electricity production with projections and forecasts showing that it will continue to be used for electricity generation for at least three more decades (IEA, 2016; WEC, 2016). The projections places coal as the second most important source of fuel (IEA, 2016; Miller, 2004; WEC, 2016).

Energy security needs are met in cases where coal is mined and used in the same country as it is termed a predominant source of fuel (Leo et al., 2009; Zedtwitz & Steinfeld, 2003 WEC, 2016). Coal is a very dirty fuel as it is responsible for majority of environmental pollution experienced today. The WEC (2016) reported that pollution from coal combustion is due to subcritical and inefficient technology applications in over 75 % of the global coal plant (Thielemann et al., 2007; WEC, 2016).

An increase in plant efficiencies by using CCS technologies could see a global increase in energy production from the average 33 % to 40 % (Leo et al., 2009). This could result in a cut of about 1.7 billion tons of $CO_2$ emissions annually (IEA, 2016; Longwell et al., 1995, WEC, 2016). Although there has been major competition from renewable energy, coal consumption has been reported to have increased by 64 % from 2000 to 2014 (WEC, 2016), thus classifying coal as one of the fastest growing source of energy.

### 2.4.4 Nuclear energy

Nuclear energy has shown potential to be a replacement for the combustion of fossil fuels. The low fuel cost associated with nuclear energy makes it the lowest-cost electricity production alternative in the market. There is an increasing need to minimize the global GHG emission. However, the nuclear accidents such as the Fukushima one in 2011 has resulted in the nuclear retreat in most countries.

Nuclear energy is often deemed as unsafe due to the catastrophic accidents previously experienced at various nuclear plants. Moreover, the use of nuclear in most countries needs constant regulation, as it is associated with weapons of mass destruction. Hence, nuclear energy is often the last option to be considered when mitigating greenhouse gas emissions.

### 2.4.5 Implications of fossil-fuel based energy production

Generation of energy from fossil fuels contribute a relatively high amount of anthropogenic $CO_2$. It has been reported that over 85 % of the world's energy is supplied by the combustion of fossil fuels, Table 2.1 shows a comparison of the world's leading fossil fuels used in energy production (Yang et al., 2008). Currently a large portion of $CO_2$ emissions come from the fossil-fuel fired power plants with coal-fired plant being the main contributors (Figure 2.3).

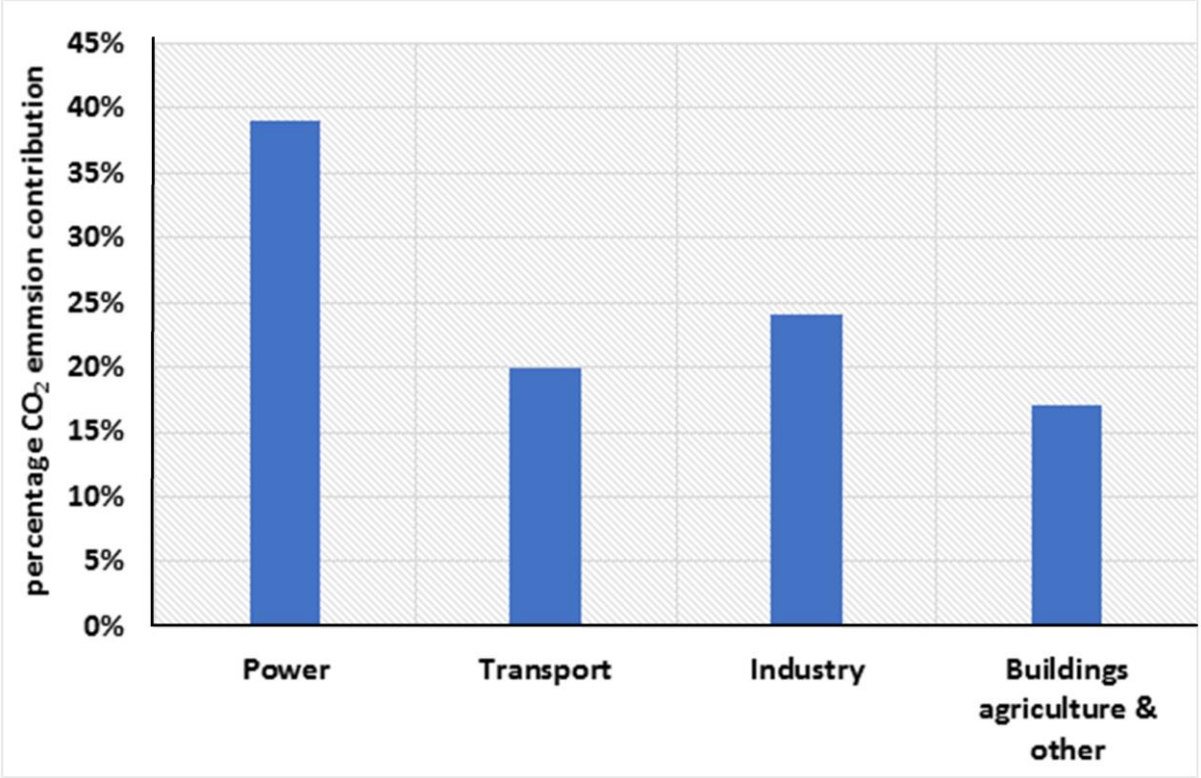


Figure 2.3: A bar chart illustrating global energy-related $CO_2$ emissions (adopted from WEC 2016)

The power generation industry is highly dominated by natural gas and coal as they offer relatively abundant and secure source of fuel (Mason et al., 2016; WEC; 2016). This is due to the high abundancy of coal and natural gas in most developing as well as developed countries (WEC, 2016). Table 2.1 shows the pollution penalty associated with the fossil fuel-fired power plants.

Table 2.1 Fossil fuel-powered emission levels (quadrillion Btu).

| **Pollutant emitted** | **Oil (Btu)** | **Natural gas (Btu)** | **Coal (Btu)** |
|---|---|---|---|
| $CO_2$ | 164 000 | 117 000 | 208 000 |
| CO | 33 | 40 | 208 |
| $NO_x$ | 448 | 92 | 457 |
| $SO_2$ | 1122 | 1 | 2591 |
| Particulates | 84 | 7 | 2744 |
| Mercury | 0.007 | 0.00 | 0.016 |
| Total | 165 687 | 117 140 | 214 000 |

Source: IEA (2016)

There have been major environmental issues associated with the emissions of greenhouse gases from this energy production method (Olajire, 2010; Yang et al., 2008; WEC, 2016). Studies in the recent years have shown that the increase in GHG emissions has led to global warming (Boot-Handford, 2010; Yang et al., 2008). Greenhouse gas pollutants include methane and chlorofluorocarbons (CFCs) which have a relatively higher greenhouse effect per unit mass of gases (Yang et al., 2008). However, $CO_2$ is the major contributor to global warming as it is emitted during the combustion of fossil fuels (Figueroa, 2016; Yang et al., 2008).

The resulting global warming is a major cause of unpredictable climate changes, melting of the ice poles, raising sea levels, droughts, increase in global temperatures that we are experiencing currently (Boot-Handford et al., 2010, Fegueroa et al., 2010; Yang et al., 2008). Global warming threatens the food security, ecology, biodiversity, economy as well as agricultural resources (Fegueroa et al., 2010; Yang et al., 2010).

There are a few options that can help reduce $CO_2$ emissions in the atmosphere and they include:

i. Reducing the energy intensity in order to decrease carbon emission by utilizing energy efficient technologies (Yang et al., 2010).
ii. Switching from fossil fuel to renewable energy sources.
iii. Developing carbon capture technologies to prevent the emission of $CO_2$ (Fegueroa et al., 2010; Yang et al., 2008).

Amongst the three options, the implementation of carbon capture technologies is the most feasible option (Olajire, 2010; Yang et al., 2010; Zhang et al., 2010). Thus, application of carbon capture technologies, either by retrofitting capture plants to existing power plants or building new plants with CCS technologies, in the energy generation sector shows a high potential for the mitigation of the effect of greenhouse gas emission (Yang et al., 2010).

### 2.5 Carbon capture and storage (CCS)

Carbon capture and storage (CCS) or carbon capture and utilization (CCUS) has been reported as an integrated suite of technologies with high potential to reduce GHG e.g. $CO_2$ emissions into the atmosphere (Daramola et al., 2010; 2015; Gibbins & Chalmers, 2008; Rackley, 2009). Figure 2.4 illustrates the major elements of CCS.

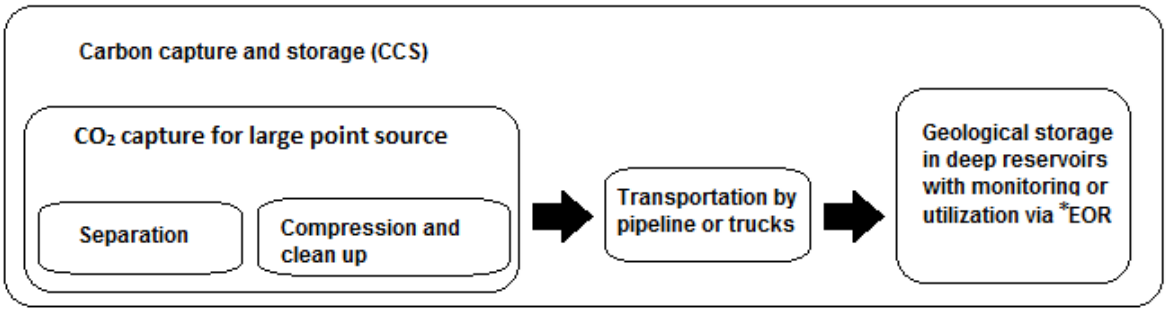


Figure 2.4 Schematic illustration of CCS *EOR=Enhanced Oil Recovery

CCS is made up of three major elements and these are discussed below:

a) **Capture** – At this stage $CO_2$ is separated from various gases produced at fossil fuel powered energy production facilities such as the cement plants, coal and natural gas power plants, chemical and petrochemical plants and many others. The $CO_2$ is then compressed at high pressures (Daramola et al., 2010; Hester, 2009).

b) **Transport** – After complete compression of the $CO_2$, it is then transported either by pipelines or trucks to a selected storage site (Daramola et al, 2010; Hester, 2010).

c) **Storage** – A geological storage site is identified and assessed for appropriate scales to support $CO_2$ storage. This could either be an underground storage (into selected rock formations which are typically saline formation and depleted hydrocarbon reservoirs which could be about a kilometer deep) or deep ocean reservoirs (Daramola et al., 2010; Hester, 2010). Alternatively, the compressed $CO_2$ can be utilized in enhanced oiled recovery by injecting it in similar depth ranges. Similarly, other utilization options include using the $CO_2$ as feed stocks for various chemicals (Benson et al., 2012; Haszeldine, 2009). The $CO_2$ utilization in the chemical industry processes is still at an early stage and currently energy intensive. Therefore, more research and development is required (Azar et al., 2006; Luthje, 2010).

The CCS technologies can be fitted with various types of new fossil-fired power plants (Daramola et al., 2010; 2016; Luthje, 2010). The same applies for retrofitting these technologies onto existing operational power plants, in most cases, without affecting the combustion cycle (Heszeldine, 2009; Luthje, 2010). CCS technologies have been applied on a large-scale within the fertilizer and natural gas industries for decades now (Haszeldine,

2009; WEC, 2016). However, the first large-scale application within the electricity sector has only been realized recently (Anderson & Newell, 2004; WEC, 2016). The Boundary Dam power station in Canada was reported as the first plant to utilize CCS in 2014 and two additional power station are set to be operational in 2016-2017 (WEC, 2016).

The CCS technologies are yet to be extended to industrial processes that manufacture cement, steel, paper and pulp, natural gas and chemicals processing. These industries have been reported to emit significant amounts of $CO_2$ into the atmosphere which account for more than 25 % of the global emissions (WEC, 2016). Application of CCS technologies in these fields can result in a significant reduction in anthropogenic GHG emission (Herszog & Golomb, 2004; Luthje, 2010).

The main limitation of CCS application extension is the cost associated with the separation and capture stage (Daramola et al., 2010; 2016; Yang et al., 2008). Carbon capture technologies with significant $CO_2$ mitigation while delivering energy with high efficiency remains a paramount challenge.

### 2.5.1 Carbon Capture methods

$CO_2$ in fossil fuel powered industries is released during the combustion and conversion processes when energy is generated (Azar et al., 2006; Herzog & Golomb, 2004). For instance, in coal-fired industries, the emitted $CO_2$ is somewhat dilute as it is released along with other components of the flue gas (Herzog & Golomb, 2004). This makes $CO_2$ capture very challenging. In other energy generation systems, such as coal gasification energy (where coal is converted to methane, hydrocarbon liquids, or chemicals) the $CO_2$ levels are much higher and can be easily separated and captured (Azar et al., 2006; Herzog & Golomb, 2004; Haszeldine, 2009).

Anthropogenic carbon dioxide mitigation techniques includes using either one of the following methods: pre-combustion, oxyfuel combustion or post combustion capture. Figure 2.5 illustrates the various carbon capture processes (Daramola et al., 2010; Luthje, 2010; Olajire, 2010).

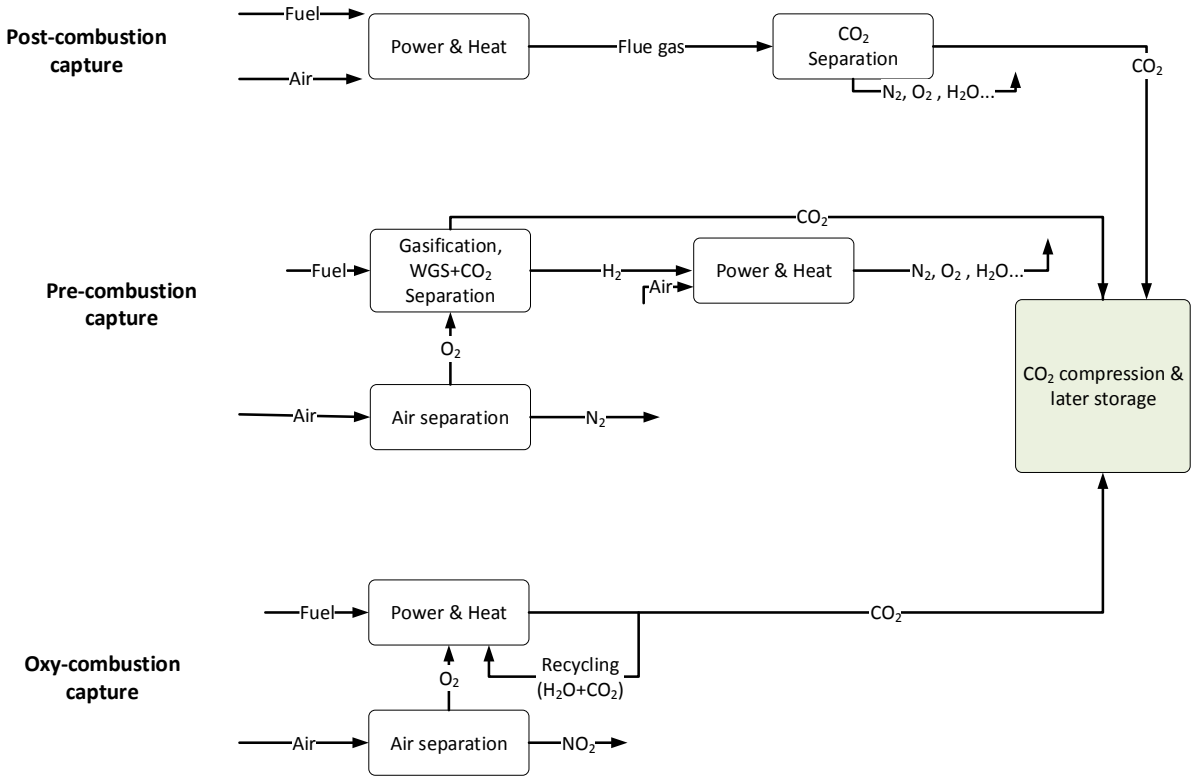


Figure 2.5 The main carbon capture methods (adopted from Olajire, 2010)

### 2.5.1.1 Pre-combustion capture processes

In this process, various types of fuel can be gasified either by reformation or by partial combustion with stoichiometric amounts of oxygen. Often some steam is used in power generation (Olajire, 2010; Azar et al., 2006). This process takes place at high pressures (40 – 70 atm) to produce synthesis gas mixture which is CO and $H_2$ (Olajire, 2010). Steam (water) is then added to the mixture in the presence of various catalyst to complete the water-gas shift reaction. A reduction in temperature promotes the production of $CO_2$ and $H_2$ (Olajire, 2010). The $CO_2$ can then be separated and captured while the hydrogen-rich solution can be used as a clean source of fuel (Azar et al., 2006; Olajire, 2010; Luthje, 2010). The separation plant needs to be integrated with the combustion process from the beginning (Olajire, 2010; WEC, 2016). For this reason, pre-combustion capture can only be implemented on new power plants (WEC, 2016).

### 2.5.1.2 Oxy-fuel combustion capture processes

This process involved the separation of oxygen from the air. The separated oxygen is then used in the combustion of fuel (Pires & Martins, 2011; Boot-Handford et al., 2014). This results in the production of sequestration ready exhaust gases made of water vapor and $CO_2$ (Boot-Handford et al., 2014; Olajire, 2010). The $CO_2$ can be separated easily in high purity with this capture process compared to other processes. Just like the pre-combustion capture,

new designs must be developed to incorporate this capture method with the combustion cycle (WEC, 2016).

#### 2.5.1.3 Post combustion capture process

Post combustion involves separating $CO_2$ from other components of the flue gas after the combustion cycle (Boot-Hanford et al., 2014; McCoy & Rubin, 2008). This process is also referred to as the downstream method, which is analogues to flue gas desulphurization (FGD), processes (Olajire, 2010). Flue gas components includes; $N_2$, $NO_x$, $SO_2$, $H_2O$ and $CO_2$. However, the major components of flue gas are $CO_2$ and $N_2$. Hence bench top studies showcase the need to separate a $CO_2/N_2$ mixture selectively.

Separation units are fitted at the tail end of power plant exhausts. This makes it ideal for CCS units to be fitted across all existing power plants, making the post combustion capture most desirable compared to its competitors. Further, Yang and co-workers (2008) reported that for over 60 years, post combustion capture units have been operational.

#### 2.5.1.4 Comparison of the current capture methods

There has been a major progression in carbon capture in recent years. This led to a major confidence in the carbon capture technologies which has further led to the building and operation of large scale capture units around the world (Boot-Handford et al., 2014; WEC, 2016). The major limitation in these capture technologies is the energy penalties associated with the separation and capture of $CO_2$ (Daramola et al., 2010; 2015; WEC, 2016).

Research effort are essential in the reduction of the separation costs because in the power generation process alone about 70-90 % of the overall costs of CCS projects is driven by capture process (Daramola et al., 2015; Olajire et al., 2010; WEC, 2016). Table 2.2 shows the comparison of the costs of $CO_2$ capture methods in coal-fired power plants while Table 2.3 show direct comparison of the advantages and disadvantages associated with each capture technology. Moreover, the current and potential applications summary of these technologies are presented in Table 2.2.

Table 2.2 Direct comparison of the costs associated with and without $CO_2$ capture in coal-fired power plants (IEA greenhouse gas programme).

| **Technology** | **Thermal Efficiency (%LHV)** | **Capital cost ($/kW)** | **Electricity cost (c/kWh)** | **Cost of $CO_2$ capture ($/t$CO_2$)** |
|---|---|---|---|---|
| No capture | 44.0 | 1410 | 5.4 | - |
| Pre-combustion | 31.5 | 1820 | 6.9 | 23 |
| Oxy-combustion | 35.4 | 2210 | 7.8 | 36 |
| Post-combustion | 34.8 | 1980 | 7.5 | 34 |

*The costs for carbon capture included the costs of compression by 110 bar while excluding the costs of storage and transportation. LHV = lower heating value.

Table 2.3 Comparison of advantages and disadvantages of current capture technologies

| **Capture method** | **Advantages** | **Disadvantages** | **References** |
|---|---|---|---|
| Pre-combustion | Relatively high concentration of $CO_2$<br>Pure $CO_2$ recovered<br>Essential for $H_2$ fuel source | Pre-cooling of gas before capture<br>Efficiency depends on the water gas shift reaction<br>Applicable mainly to new plants<br>Few gasification plants are in operation<br>Costly equipment<br>Extensive support required | Olajire, 2010<br>Herm et al., 2011<br>Figueroa et al., 2008<br>Haszeldine, 2009 |
| Oxy-fuel combustion | $NO_x$ emissions eliminated due to absence of nitrogen in the combustion stage | High energy required to separate pure $O_2$ from the air<br>Large $O_2$ production required (may be costly)<br>Cooling $CO_2$ recycle required to maintain the temperatures within the limits resulting in;<br>Decrease in process efficiency<br>Added auxiliary load | Olajire, 2010<br>Figueroa et al., 2008<br>Yang et al., 2008 |
| Post-combustion | Can be retrofitted to existing power plants<br>Power-plants designs<br>Can be applied to a variety of power plants | High energy associated with solvent generation<br>Loss of solvent<br>Flue gas contains dilute $CO_2$ at ambient pressure<br>Low $CO_2$ partial pressure | Olajire, 2010<br>Sumida et al., 2011<br>Mason et al., 2015<br>Figueroa et al., 2008 |

Table 2.4 Current and potential extension of carbon capture technologies.

| Capture method | Current application | Potential | References |
|---|---|---|---|
| Pre-combustion | Mature operation in: Integrated gasification combined cycle (IGCC), Ammonia production and Solvent separation. $H_2$-rich fuel turbines. | High $CO_2$ concentration but requires extensive support. Reduction in compression cost/loads. Fuel processing needed. | Babu et al., 2015 Olajire et al., 2010 Zhen et al., 2016 Figueroa, 2016 |
| Oxyfuel combustion | Small scale test rigs. Mature in $O_2$ production. | Higher $CO_2$ concentration. Processes high amounts of flue gas to avoid high combustion temperatures. Potential for $O_2$ separation membranes at low energy. Novel IGCC turbines with no gas shift reaction Can be either retrofitted or repowered to power plants | Olajire, 2010 Yang, 2008 Mason et al., 2015 Figueroa, 2016 |
| Post combustion | Amine scrubbing with 100% efficiency Small power plants in operation globally | Applicable to all existing coal-fired power plants. Low $CO_2$ partial pressures. Very high performance. Lower operating cost possible. The only limitation is the conventional MEA solvent Membranes offer lower energy separation process. | Liang et al., 2015 Del Rio et al., 2016 Olajire et al., 2010 Zang et al., 2014 Yang et al., 2008 |

Among the three most common carbon capture methods, the main limitation has been the cost associated with the separation and capture of $CO_2$ from other gases. For instance, the most common and widely applied separation method is to use an amine based solvent such as monoethanolamine (MEA) for the absorption of flue gas $CO_2$. This method has been reported to have up to 100 % efficiency in separating $CO_2$ resulting in relatively pure $CO_2$ streams (Olajire, 2010; Yang et al., 2008).

The $CO_2$ is selectively absorbed by passing the flue gas through the amine solvent. The solvent is normally in flowing in a counter current to the flue gas. This resulting in the $CO_2$ rich solvent exiting on the bottom of the absorber while the remaining flue gas components flow out on the opposite side (Figure 2.6). The $CO_2$ rich solvent is then heat and sent for stripping where the $CO_2$ is then removed from the solvent.

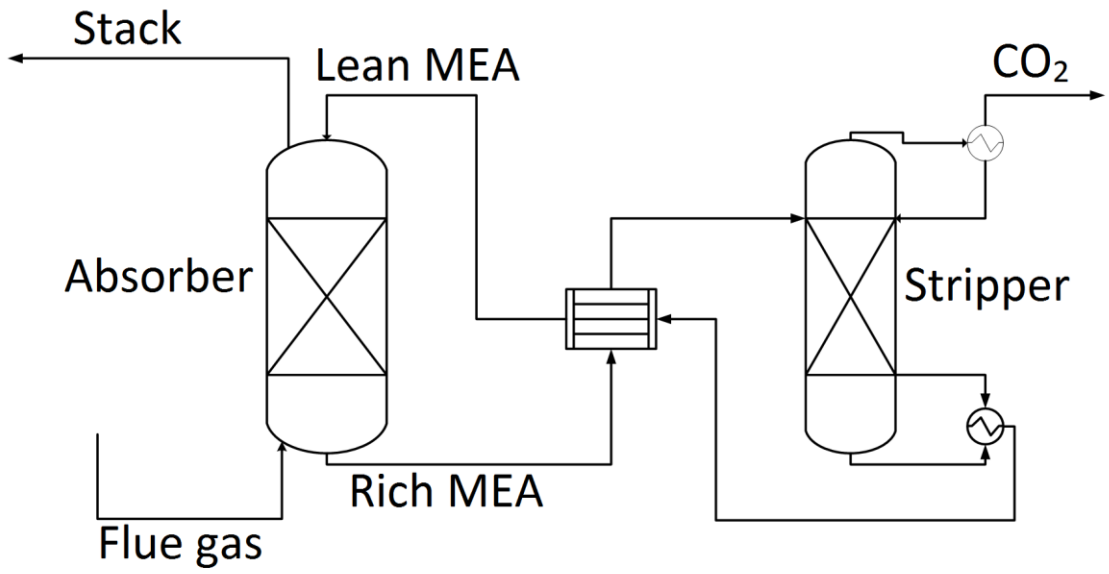


Figure 2.6 A typical $CO_2$ capture process diagram using MEA absorption technique (adopted from Osman et al., 2013)

Although this is a widely applied CCS technology, it has major limitations including and not limited to the following:

I. High energy associated with the absorption/stripping of $CO_2$ using conventional thermal methods.
II. Low $CO_2$ loading capacity.
III. Corrosion of the capture equipment.

IV. Degradation of the amine solvent by other components of the flue gas (Boot-Handford et al., 2010; Olajire, 2010, Yang et al., 2008).

These drawbacks present an ideal opportunity for an alternative method to be applied in CCS technologies (Olajire, 2010; Yang et al., 2008). Moreover, reports suggests that this method has been a major limitation on post combustion capture (Olaijire, 2010; Yang et al., 2010). Alternative separation methods with high energy efficiency warrants further investigation to make CCS a feasible option for $CO_2$ mitigation (Bont-Handford et al., 2010, Figueroa et al., 2010, Olajire, 2010).

### 2.6 $CO_2$ separation and capture techniques

The current inefficient separation techniques using amine solvent has been estimated to increase the cost of electricity by 50 % if old power plants are to be integrated with CCS technology (Olajire et al., 2010; Yang et al., 2008). Reducing the cost of capture remain a paramount challenge faced by CCS schemes to ensure that CCS processes are acceptable in the power production industry (Olajire, 2010).

Alternative separation techniques that have been investigated as potential replacements for the commercialized energy intensive MEA absorption/scrubbing technique include; (i) adsorption; (ii) Cryogenics; (iii) membrane separation (Boot-Hanford et al., 2010, Fegueroa et al., 2010, Olajire et al., 2010). The choices of separation method depend mostly on the physical and chemical properties such as adsorption coefficients, which influence the interaction with $CO_2$ in the presence of other gases. Flow Chart 2.1 illustrates $CO_2$ capture techniques reported in literature. This current study contributes to the ceramic/zeolite membranes process as highlighted in blue in the chart. Table 2.5 summarizes the key characteristics and limitations of widely applied $CO_2$ separation and capture methods.

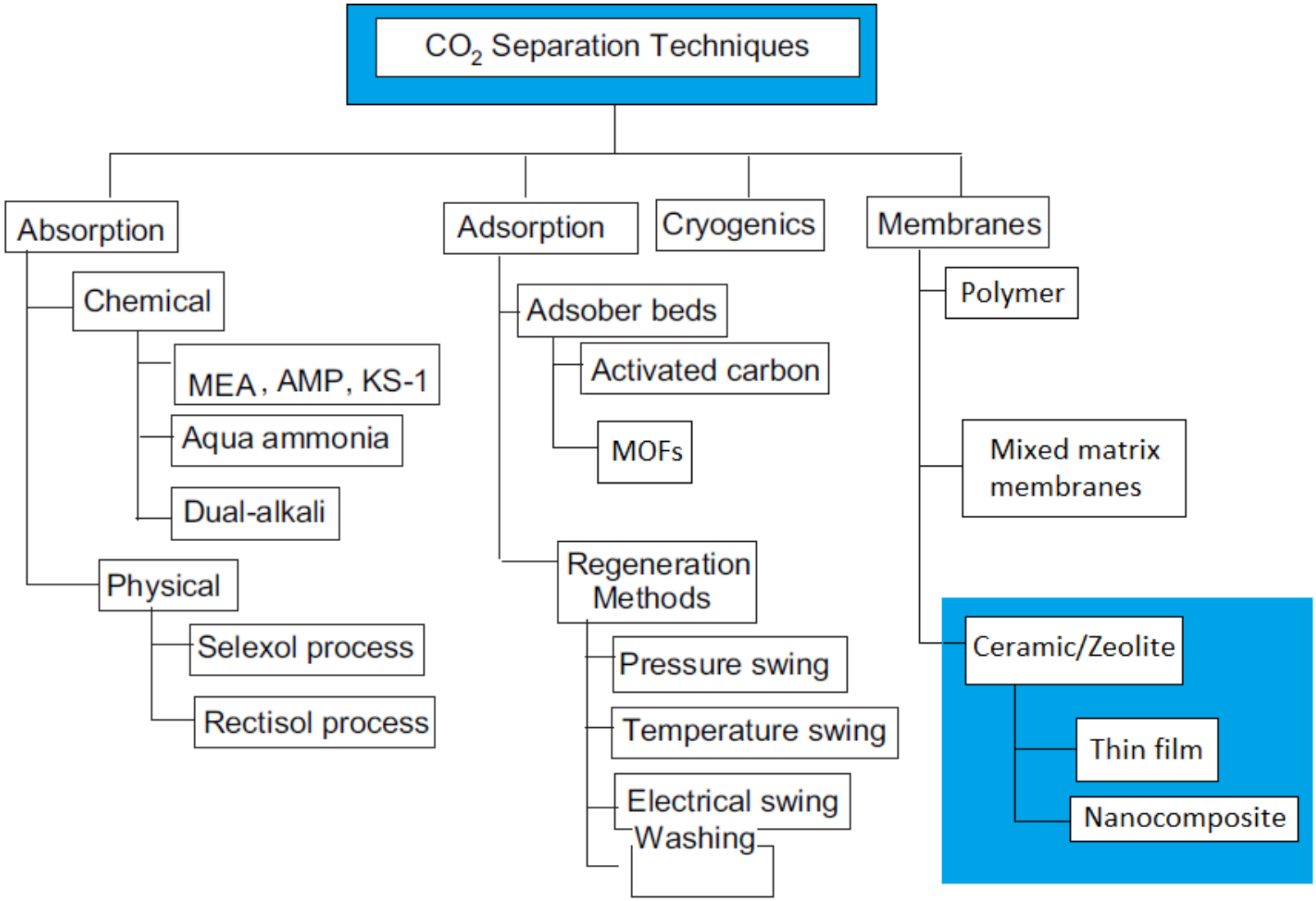


Flow Chart 2.1 Reported carbon capture techniques (adapted from Olajire, 2010)

Table 2.5 Advantage and disadvantages of current $CO_2$ separation methods

| **$CO_2$ separation technique** | **Type of method** | **Application status** | **Advantages** | **Disadvantages** | **References** |
|---|---|---|---|---|---|
| Absorption | MEA<br>Chilled ammonia<br>Pressure swing adsorption<br>Temperature swing adsorption<br>Metal organic frameworks | Commercialized<br>Research and development | >98% $CO_2$ separation efficiency<br>Commercialized for 60 years<br>High recovery<br>High loading capacity<br>Wide temperature & $CO_2$ concentrations range<br>High stability<br>High purity | Solvent degradation<br>High energy cost during solvent regeneration<br>Low carbon loading capacity<br>Require flue gas to be cooled<br>Energy intensive when $CO_2$ reacts with the adsorbent<br>No field demonstrations | Olajire, 2010<br>Yang et al., 2008<br>Daramola et al., 2010 |
| Membrane | Polymer<br>Inorganic<br>Zeolite | Commercialized | Low energy consumption<br>No solvent regeneration<br>No waste streams<br>Good for bulk separation<br>Low capital and operation cost | Costly ceramic supports<br>Low stability in polymer membranes<br>Moderate product purity | Olajire, 2010<br>Haszeldine, 2009<br>Herzog, 2001 |
| Mixed matrix membranes | Amine solvents in membranes | Research and development | Thermally and chemically stable<br>Low capital cost | Aggregation and sedimentation of particles during preparation<br>Poor zeolite polymer interface | Olajire, 2010<br>Yange et al., 2008 |
| Cryogenics | Cryogenic<br>Liquefaction | Commercialized | >98% $CO_2$ separation efficiency<br>High purity | Energy intensive<br>Complex operations | Olajire, 2010<br>Haszeldine, 2009<br>Herzog, 2001 |

### 2.6.1 Adsorption

The adsorption process is mainly based on the same principle as the amine absorption/stripping technique described in Table 2.5 but it uses porous solid adsorbents such as metal organic frameworks (MOFs), activated carbon and zeolites (Yang et al., 2008). However, during the adsorption process, $CO_2$ is attached to the surface of the adsorbent (Olajire, 2010; Yang et al., 2008). The attachment determines the kinetics of the process and it is either by either a physical or chemical means (Olajire, 2010).

The adsorbent is responsible for the selective removal of $CO_2$ from the gas stream. The $CO_2$ is recovered by desorption which usually done by lowering the pressure or increasing the temperature (Yang et al., 2010). Figure 2.7 illustrates the adsorbent-based capture process. In this process, the flue gas is cooled and then sent to the carbonation reactor, which is usually a packed bed reactor (Osman et al., 2014). $CO_2$ is adsorbed on the surface of the absorbent either chemical or physically depending on the reaction kinetics (Osman et al., 2014; Yang et al., 2008). The $CO_2$ loaded adsorbent is transferred to a regenerator where it is heated and then the $CO_2$ is released (Osman et al., 2014; Yang et al., 2008).

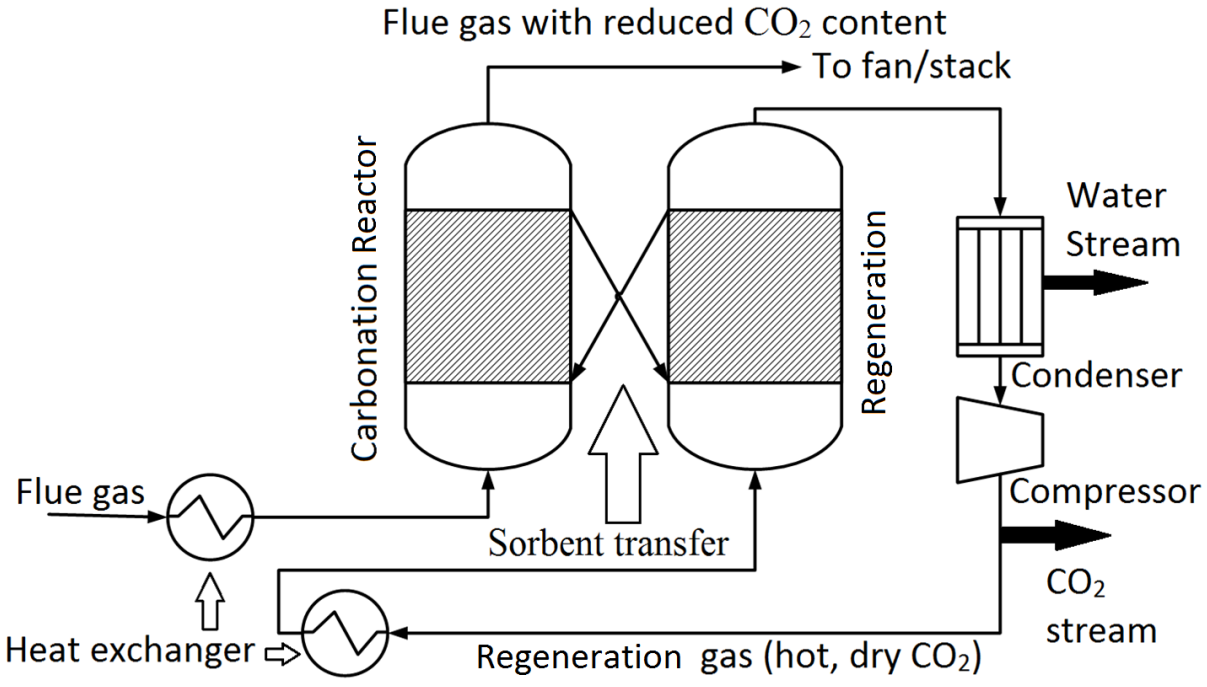


Figure 2.7 Schematic illustration of the adsorbent based $CO_2$ capture process (adapted from Yang et al., 2008)

This process in currently in the research phase to improve loading capacity as well as rapid absorption and is yet to see commercialization (Olajire, 2010). This process is also reported to be energy intensive and good adsorbent are still to be developed (Yang et al., 2010).

### 2.6.2 Cryogenics

Cryogenic separation, better known as $CO_2$ anti-sublimation, involves separating $CO_2$ from flue gas by a phase change through cooling the flue gas to a point whereby $CO_2$ exist either as a liquid or solid phase (Haszeldine, 2009; Herzog, 2001; Olajire, 2010). The phase change occurs in the presence of higher pressure (630 kPa to 7396 kPa) at temperatures between 217 K and 304 K (Herzog, 2001).

Figure 2.8 illustrates the process flow diagram for a typical cryogenic separation method. The flue gas is cooled by a heat exchanger which also removes moisture resulting in a dry gas consisting mainly of $CH_4$, $CO_2$, $N_2$, $O_2$ as well as trace amounts of $SO_2$, Hg and HCl (Haszeldine, 2009; Herzog, 2001). The remaining flue gas is further exposed to yet another heat exchanger whereby the temperatures are further lowered to around the freezing point of $CO_2$. At this point a flash point unit removes $SO_2$ and other trace amounts of flue gas components. A pressure difference is required for the separation based on how volatile they are. The remaining flue gas which is now made up of only $CO_2$ and $N_2$ is then cooled down even further by an expander. This is known to course partial freezing of $CO_2$; $CO_2$ can then be recovered from the flue gas. The resulting flue gas is then recycled with fresh flue gas stream while the recovered $CO_2$ is heated in the heat exchange and produce in a liquid form at high pressures. At this point $N_2$ can also be separated in a gaseous phase.

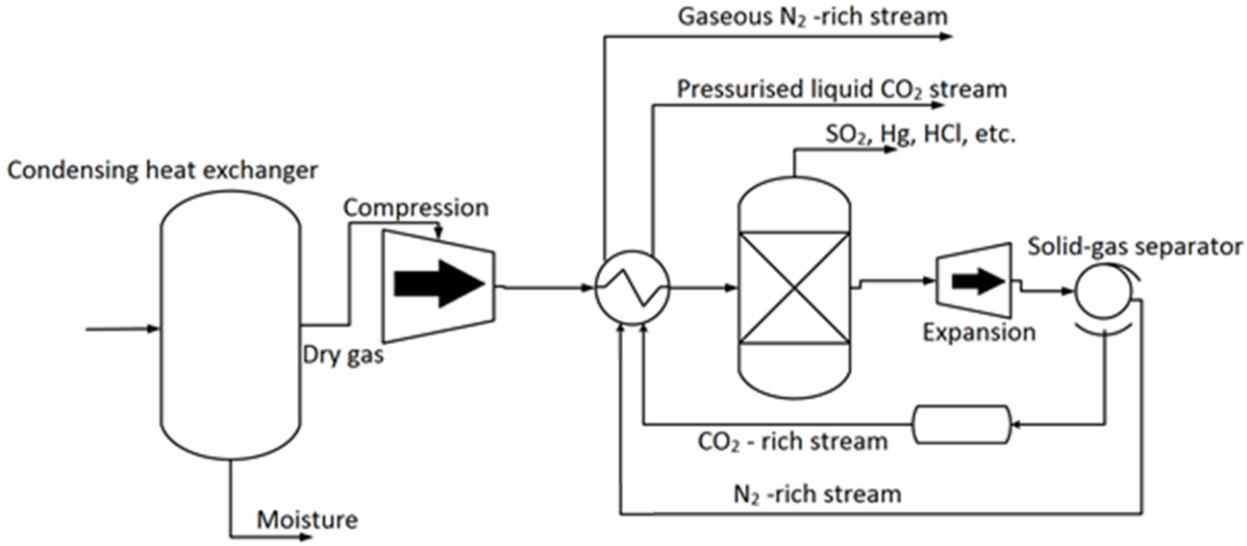


Figure 2.8 A process flow diagram of a typical cryogenic $CO_2$ separation method (Adapted from Yang et al., 2008)

The process of cooling and heating under high pressures is found to be very inefficient and costly as high energies are required by these processes (Haszeldine, 2009; Herzog, 2001). The process has been under a lot of development in recent years to correct this inefficiency (Haszeldine, 2009; Herzog, 2001). This results in liquefaction being a desired alternative to the high-pressure processes (Haszeldine, 2009; Herzog, 2001). In this case flue gas is cooled to significantly low temperatures (136-194 K), although the energy costs associated with liquefaction are lower, the overall operating costs of the cryogenic separation remains the major limitation for this technology (Haszeldine, 2009; Herzog, 2001; Olajire, 2010).

### 2.6.3 Membrane separation

It has been established that most chemical production plants, across the entire chemical industry, consist of a reaction unit which is followed by a separation unit (Daramola et al., 2012). McLeary and his coworkers (2005) stated that the integration of reaction and separation units which utilized membrane reactors has received increasing attention during the past 30 years (Mcleary et al., 2005). This combination delivers more compact and less capital-intensive processes with substantial savings in energy consumption (Mcleary et al., 2005). Most of the energy is consumed in the conventional separation units, which apply energy-intensive thermally

driven separation processes such as absorption, adsorption and cryogenics (Caro & Noack, 2008).

Low temperature separation methods appear to be more attractive. This statement was supported by Daramola and his coworkers (2012) who stated that energy prices has led to a high interest in energy efficient and energy saving technologies to be applied in industry. When membranes are applied in $CO_2$ separation capture from flue gas, no heating or cooling is required. Figure 2.9 illustrates a two stage membrane separation process flow diagram. The two stage membrane system is applied here to enhance the efficiency of the system.

Membrane separation technology comes across as one of the most innovative and rapidly increasing fields with a variety of application in science and engineering. Baker (2002) reported that in the last three decades the membrane gas separation business has developed into a business with over $ 150 million turnover per year. This is due to reports that the membrane separation process offers a more environmentally friendly, low energy consumption, versatile technologies and relatively simple operation (Baker, 2002; Daramola et al., 2012; Wenten, 2002; Yang et al., 1999; 2008).

In comparison to conventional separation processes such as cryogenic distillation, absorption and adsorption, often require a phase change in the gas to be separated in order to facilitate the separation method. This phase change is often a gas-to-liquid during the capturing process as well as liquid to gas during the recovery process. Wenten and his co-workers (2002) reported that the phase changes associated with all these processes add up significantly to the costs of the separation process. On the other hand, membrane technology requires no such phase change (Baker, 2002; Yang et al., 1999; 2008). For instance, as seen in Figure 2.10, $CO_2$ can easily pass through membranes while other components of the flue gas are retained due to their lower permeability (Figueroa, 2016; Olajire, 2010; Yang et al., 2008). The vacuum pumps are usually added in order to improve the mass transport on the permeate side. The operating conditions such as the partial pressures, membrane areas, and capture load distribution may be optimized to meet specific capture requirements (Yang et al., 2008; Zhang et al., 2014).

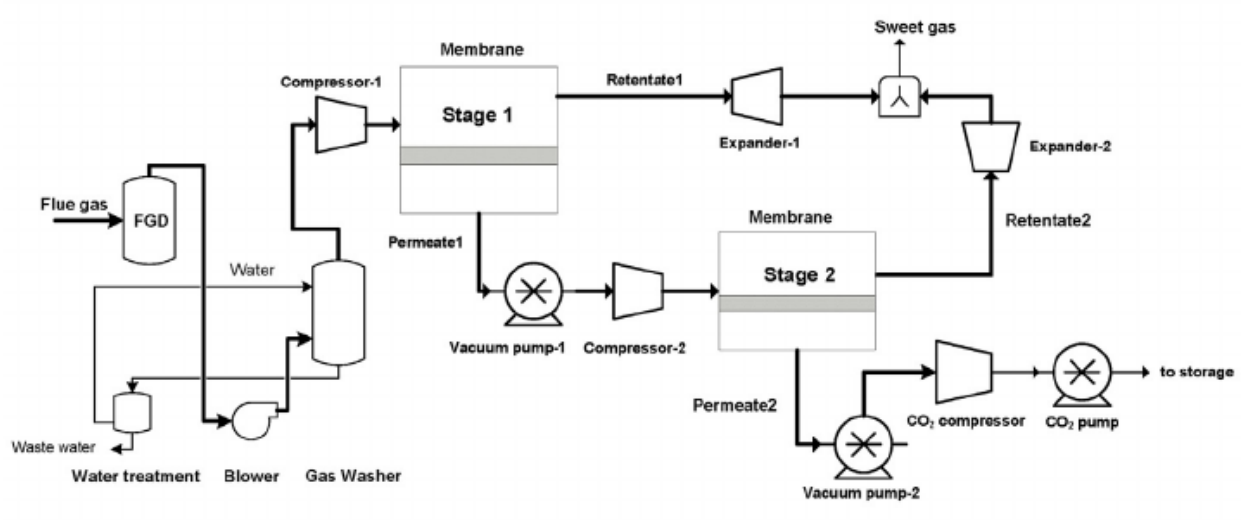


Figure 2.9 A two stage membrane process flow diagram for $CO_2$ separation (adapted from Zhang et al., 2014).

Moreover, Caro and Noack (2008) have established that the energy required by some industrial large-scale separation tasks can be an order of magnitude lower when using membranes versus traditional thermal separations (Koros, 2004). Various membranes have been explored and reported for the $CO_2$ separation and capture (Olajire, 2010; Yang et al., 2008).

This dissertation is focused on the development of ceramic nanocomposite zeolite membrane for $CO_2$ separation processes for desirable cost effective carbon capture plants. A reduction in the energy cost associated with the current carbon capture methods would bring great benefits to the CCS process.

### 2.7 Membrane separation technology

A membrane can be defined as a selective barrier that can separate two phases with the ability to separate gases or liquids. Membranes often achieve desirable selectivity with the aid of a driving force which could either be a difference in pressure, difference in chemical compositions, or even an electrical potential (Mulder, 1996). Membranes are categorized by either structure or morphology, which are essential for the transport mechanism during the separation process (Moulder, 1996).

The three main categories of membranes are the following; (i) organic/polymer, (ii) mixed matrix membranes and (iii) porous inorganic membranes. The key criteria that should be met by

these membranes in order to be applied in the separation and capture of $CO_2$ are stability, selectivity and permeability (Ismail & Lai, 2003; Yang et al., 2008). The selectivity is critical in processes where a high purity is required as it affect the product recovery directly (Ismail & Lai, 2003). Baker (2002) established that to obtain high permeations the membrane layer needs to be extremely thin. This applies to composite thin-film membranes.

The major challenge associated with membranes is achieving a high permeance while retaining a desirably high selectivity (Daramola et al., 2012; Yang et al., 2008). Tin and his co-workers (2003) reported that extremely superior membranes are able to maintain their separation properties as well as high durability in chemically harsh environments. However, no such membranes exist as there is always a permeability and selectivity trade-off limitation associated with membrane processes (Ismail et al., 2002; Koros & Mahajan, 2000; Yang et al., 2008). Previous studies have been focused on improving the permeability while keeping an acceptable selectivity through the membranes (Caro et al., 2000; Ismail and Lai 2003, Yang et al., 2008; Caro & Noack, 2008).

As a result, various scientists have reported various thin layer membranes with the feasibility of separating $CO_2$ from flue gas (Caro, 2010; Caro & Noack 2008; Figueroa et al., 2010; Olajire, 2010; Yang et al., 2008). In these studies, it was found that the high selectivity for $CO_2/N_2$ separations makes them ideal for post combustion $CO_2$ capture (Figueroa et al., 2010; Olajire, 2010; Yang et al., 2008). Furthermore, desirable properties of any membrane include the following; high heat resistance, high corrosion resistance and uniform porosity (Yang et al., 2008). However, the various types of membranes present desirable opportunities as well as challenges which often limit their industrial applications.

### 2.7.1 Types of membranes

Membranes can also be divided into either non-biological or biological (referred to as biomembranes, which are an enclosing or separating membrane that acts as a selectively permeable barrier within living things. They are not discussed here). The non-biological membranes can be further classified into naturally occurring or manmade/fabricated membranes. The fabricated membranes can further be divided to either polymeric, or inorganic membranes.

### 2.7.2 Polymeric membranes

Polymer membranes are the most widely studied membranes for gas separations due to their high flux as well as the relatively easy reproducible production (Powell & Qiao, 2006; Yang et al., 2008). The polymeric membranes have been reported to have an ability to be spun into hollow asymmetric fibers and modules, due to their solution processability as well as segmental flexibility (Basu et al., 2004; Clarizia, 2013; Koros, 2002; Freemantle, 2005). The hollow fiber configurations possess higher surface areas and relative low production costs which are essential for scaled up industrial applications (Bernado & Clarizia, 2013; Freemantle, 2005; Koros, 2002). As a result, polymeric membranes have been dominant in the gas separation industries (Basu et al., 2004; Figueroa et al., 2008; Merkel et al., 2010).

Polymer membranes are classified into either porous membrane which utilizes ultra- and microfiltration to separate molecules based on their kinetic diameters or non-porous dense membranes which utilizes solution-diffusion as a gas transport mechanism (Figueroa et al., 2008; Powell & Qiao, 2006; Yang et al., 2008). The fabrication of these membranes results in organic polymers with various molecular weight and cross-linking these polymeric chains (Mulder, 1996; Ismail et al., 2002; Powel & Qiao, 2006). Polymers often used are cellulose acetate, aromatic polyamides and fluorocarbon polymers. Moreover, the synthesis methods of these membranes involve either stretching, sol-gel process, phase inversion or sintering (Ismail et al., 2002; Koros, 2002; Mulder, 1996; Pandey & Chauhan, 2001).

Scholes and his co-workers (2010) stated that the separation performance in these membranes can be enhanced by; (i) either increasing the solubility of $CO_2$ in the non-porous membranes or, (ii) by changing the polymeric composition. Further, the diffusion of $CO_2$ can be increased by changing the polymer packing within the polymer membranes. This statement was support by Powell & Qiao (2006) in their full review on polymeric membrane applications in carbon capture.

The selectivity of the desired gases may be governed by the sizes of channels formed by selected polymeric chains as well as the solubility of the desired gas within the polymers (Figueroa et al., 2008; Powell & Qiao, 2006). Hence the choice of the polymeric chains when targeting specific molecular sizes is of critical importance (Powell & Qiao, 2006 Yang et al., 2008). In most cases

where $CO_2$ solubility is high the resulting selectivity that is exceptionally high while the permeability is below acceptable values (Yang et al., 2008).

Certain polymeric chains result in larger vacancies being formed; these membranes have a high permeability with a low selectivity (Yang et al., 2008). A complete study on gas separations with polymeric membranes was discussed in detail by Maier (1998).

Polymer membranes with considerably high selectivity and permeability which makes them desirable for $CO_2/N_2$ as well as $CO_2/CH_4$ mixture separations often have poor chemical and thermal resistance (Figueroa et al., 2008; Powell & Qiao, 2006; Yang et al., 2008). This has been attributed to the compaction, which results in a significant decrease in membrane thickness over time, as well as plasticization which leads to swelling resulting in an increase in permeability of the polymers (Freemantle, 2005; Ismail et al., 2002; Yang et al., 2008).

Moreover, polymer membranes were found to have a high permeability and selectivity trade off which hinders applications whereby a high purity product is required (Bernado & Clarizia, 2013; Powell & Qiao, 2008; Yang et al., 2008). This presents a limitation for the extension of polymeric membrane application for industrial processes more especially their potential applications in $CO_2$ separation for CCS purposes.

However, Baker and Lokhandwala (2008) reported that perflouropolymers composite membranes were produced with an improved resistance to impurities making them ideal for $CO_2$ separation processes. Moreover, exceptional transport properties were reported on polymer intrinsic membranes (Baker & Lokhandwala, 2008; Powell & Qiao, 2008; Yang et al., 2008). Although polymeric membranes are highly preferred due to their low capital cost, they are likely to foul and thus always facing competition from inorganic membranes which have been reported to overcome the abovementioned limitations (Bernardo & Clarizia, 2013).

### 2.7.2 Inorganic membranes

In order to overcome the above mentioned limitations associated with polymeric membranes, inorganic membranes have been highly explored in gas separation processes (Daramola et al., 2010; 2012; Yang et al., 2008). Although they are considerably more expensive than their polymeric counter parts, they possess desirable properties such as relatively higher stability, gas fluxes and uniform pores resulting in higher selectivity (Pandey & Chauhan, 2001; Salomon et

al., 2000; Tsai et al., 2000). Inorganic membranes consists of a macroporous supports which provide mechanical strength to the overlaying brittle membrane materials while minimizing mass-transfer resistance (Figueroa et al., 2008; Tsai et al., 2000; Yang et al. 2008). Depending on the type of support, they are often the higher drivers of the cost of the membrane fabrication (Daramola et al., 2010; 2012; Salomon et al., 2000 Tsai et al., 2000). Traditionally membranes are made of a porous top thin layer formed on top of a porous support which could either be a metal or a ceramic support (Daramola et al., 2010; Figueroa et al., 2006; Yang et al.; 2008).

However, the cost limitation has not hindered further research as studies have focused more on the gas properties of inorganic membranes as well as an extension of their applications (Barbeiri et al., 2002; Salomon et al., 2000; Tsai et al., 2000; Daramola et al., 2010; 2012). As a result, the inorganic membranes have been categorized into either porous or dense (non-porous) membranes.

The dense inorganic membranes are made of thin layer metal or solid electrolytes, such as vanadium, palladium, palladium alloys and zirconia (Figueroa et al., 2008; Meinema et al., 2005; Yang et al. 2008). These membranes have desirable separation performance for oxygen or hydrogen gas separations (Al-Mufachi et al., 2015, Alimov et al., 2014). The mass transport in these membranes is facilitated mostly by solution-diffusion when metals are involved or by charged particles in electrolytic membranes (Figueroa et al., 2008).

However, the low permeability with low chances of improvement, across the dense membranes limits their industrial applications. Hence, porous membranes are highly preferred instead of dense membranes (Ismail & David, 2001; Meinema et al., 2005; Yang *et al.,* 2008). Moreover, Alimov and his co-workers (2014) reported that the dense membranes mostly readily form oxide layer which hinder the separation process severely. These limitations have hinder further extension of application of the dense membrane into other gas separation process such as CCS technologies (Yang et al., 2008; Zhao et al., 2008).

Having realised the cost implications associated with porous membranes as well as the low permeability associated with Dense in organic membranes, other studies focused on the

improvement of polymeric membranes (Caro, 2011; Ismail et al., 2002; Jia et al., 1991; 1992; Perez et al., 2009). This resulted in the incorporation of inorganic materials with the organic polymer material resulting in what is termed mixed matrix membranes (MMMs) (Caro, 2011; Li et al., 2013; Yang et al., 2008). These membranes presented an opportunity to overcome some of the limitations associated with both organic and inorganic membranes.

### 2.7.3 Mixed matrix membranes

In this type of membranes, the polymeric membranes were incorporated with specific inorganic materials such as zeolites during their fabrication (Ismail et al., 2002; Powell & Qiao, 2006; Yang et al., 2008). This latest development in membrane technology may also consist of carbon molecular sieves as well as MOFs embedded in the matrix of the polymeric material (Caro, 2011; Ismail, 2002).

It has been highlighted in various studies that the MMMs have a high potential to enhance the permselectivity and productivity compared to existing membranes (Caro, 2011; Ismail et al., 2002; Jia et al., 1991; 1992; Yang et al., 2008). In simple terms, the MMMs membranes are reported to have excellent separation performance. They overcome the selectivity and permeability trade-off, which has been the major limitations associated with polymeric membranes (Ismail et al., 2009; Yang et al., 2008). Moreover, the resulting MMMs were found to exhibit good adhesion properties between the polymer matrix and inorganic composite (Jia et al., 1992; Li et al., 2013). This results in membranes with improved gas separation properties at high temperature (Li et al., 2013; Yang et al., 2008). Jia and his co-workers (1991) reported that polydimethylsiloxane (PDMS) membranes which were filled with significant amount of silicalite-1 showed an increase in the permeabilities of $H_2$, $O_2$ and $CO_2$ while on the other hand permeabilities of $N_2$, $CH_4$ and butante decreased.

Duval and his co-workers (1993) extended the preparation methods from PDMS to ethylene rubber (EPDM), nitrile butadiene rubber (NBR) and polychloropene (PCP). In each of these cases, both zeolites as well as carbon molecular sieve were explored. The results supported the initial study by Jia and his co-workers (1991; 1992), as the separation performance was for $CO_2/CH_4$ mixture increased significantly compared to either pure polymeric membranes or inorganic membranes (Duval et al., 1993).

The membranes take advantage of the high separation performance associated with the inorganic part of the membrane while utilizing the economical processing associated with polymer materials (Li et al., 2010; 2013 Yang et al., 2008). Moreover, the MMMs have enhanced mechanical properties compared to conventional polymeric membranes (Ahmed et al., 2012 Li et al., 2013).

Currently the challenge is comes with the synthesis of defect free and optimized MMMs which generally results from incompatibility associated with the interface between the polymer and the filler particles (Yang et al., 2008). Although many attempts have been made to fabricate defect-free MMMs, this remains a critical challenge (Yang et al., 2008). This is due to the different physico-chemical properties associated with the organic and inorganic membranes (Li et al., 2013).

In a recent study, Shen and coworkers (2015) stated that for membranes to be applied in industrial flue gas $CO_2$ capture, the $CO_2/N_2$ selectivity of >70 along with a minimum $CO_2$ permeability of about 100 Barrers for a membrane with a thickness of about 1 µm (Shen *et al.*, 2015). MMMs are reported to demonstrate selectivity and permeability greater than mentioned minimum requirement for industrial application. However, in a recent review, Shen and coworkers (2015) stated that the MMMs have not been applied commercially.

### 2.7.4 Inorganic membranes in comparison with other types of membranes

In the search to find better membranes for CCS applications, porous inorganic membranes still appear more desirable compared to the rest. Table 2.6 summarizes the direct comparison of polymer membranes, mixed matrix and inorganic membranes. The advantages associated with inorganic membranes make them more attractive for industrial applications. This led to increased interest in researchers investigating various gas separations using these membranes, more especially the porous inorganic membranes (Centeno et al., 2004; Fuertes 2000; Ismail & David, 2001; Rao & Sircar, 1993).

However, the development of porous inorganic membranes goes as far back as prior to 1945 (Keizer & Verweiji, 1996). The initial purpose of these membranes were to separate uranium isotopes primarily for military or nuclear applications (Keizer & Verweiji, 1996; Soria, 1995; Luque et al., 2008). Various alternative applications were later reported by the Pall Corporation

(then called Ceraver) with a product called Membralox as well as Ceraflo Pty Ltd (then called Norton) who produced Ceraflo (Keizer & Verweiji, 1996; Soria, 1995; Luque et al., 2008).

Ismail and David (2001) reported that the potential of the porous inorganic membranes was not extensively studied until the high quality porous membranes were used in industrial process on a large scale to replace the organic polymer membranes. The inorganic membranes are constantly compared (Table 2.6) with other types of membranes in attempts to fabricate industrial applicable membranes (Fuertes & Centeno, 1998; Ismail & David, 2001).

Table 2.6 Comparison of inorganic, organic membranes and mixed matrix membranes

| **Inorganic membranes** | **Organic membranes** | **Mixed matrix membranes** |
|---|---|---|
| High thermal & chemical stability | No thermal and chemical stability | Poor polymer/zeolite membrane contact |
| No swelling | Swelling and deformation | Possible swelling |
| Relatively high uniform pore openings | No uniform pore openings | May result in blocked pores |
| High production costs | Low production cost | no cost estimates |
| Very brittle | Not brittle | Not brittle |
| Less commercial application | More commercialized | Under research and development |

Currently, intense research efforts have been devoted to the development of porous membranes that provide enhanced selectivity, thermal stability and chemical stability as compared to polymer membranes (Ismail & David, 2001). The focus in this recent development is given to molecular sieving materials such as silica, carbon and zeolite membranes, as they appear to be desirable in gas separation as they overcome the selectivity versus permeability trade-off (Fuertes & Centeno, 1998, Ismail & David, 2001; Pandy & Chauhan, 2001; Yang et al., 1999; 2008; Koresh & Soffer, 1986).

However, silica-based membranes can selectively separate hydrogen in various gas mixtures but the permeability and selectivity between molecules with similar sizes, such oxygen and nitrogen was found to be inefficient (Hayashi *et al.,* 1997; Ismail & David, 2001; Meinema et al., 2005; Saufi & Ismail, 2004). Conversely, carbon membranes are essential for separating nitrogen in high purity from air (Ayral et al., 2008; Centeno et al., 2004; Gavalas et al., 1989). Hence, they are not desirable where similar-sized gas mixtures are consent as well separating $CO_2$ from other gases and it is more feasible to use zeolite membranes in these cases (Tsai et al., 2000; Yang et al., 2008; Yildrim & Hughes, 2003).

Porous inorganic membranes often act as molecular sieves for larger molecules and particles in cases where by their pore sizes are greater than 0.3 nm (Verweij, 2003; Soria, 1995). Various porous membranes have been categorized by the IUPAC as:

- Microporous (pore opening diameter of < 2 nm)
- Mesoporous (2 < pore opening diameter of  < 50 nm)
- Macroporous ( pore opening diameter > 50 nm)

Consequently, microporous membranes are made up mainly by materials such zeolites, amorphous silica and carbon membranes as they consist of an interconnected pore structure (Verweij, 2003). The size of these pores as well as the adsorption characteristics results in higher selectivity and higher fluxes are essential for the separation of various molecules.  The most applied of this microporous membranes are zeolite membranes. Their applications have been varied from separation of smaller molecules such as $H_2$ and $N_2$ to bigger molecules such as $H_2O$ from reaction mixtures as well as isomer separation such as p-xylene from o-xylene (Daramola et al., 2010; 2012; Lin et al., 2002; Luque et al., 2008; Soria, 1995; Verweij, 2003).

### 2.7.5 Zeolite membranes

Zeolites are natural minerals which have been known since the 1700's. Union Carbide pioneered the synthetic zeolite and molecular sieve materials in the late 1940's after an initiation of research on adsorption for purification, separation and catalysis (Barrer, 1978; Bowen et al., 2004; Ruthven, 1984; Yang, 1987).  This led to the first successful synthesis of pure Zeolite A and X in 1950 and the first synthetic zeolite publication in 1956 (Barrer, 1979). In this publication by Breck and coworkers (1956) it was concluded that the zeolite type A had a cubic

structure with cavities of 11.4 Å separated by circular openings of 4.2 Å. Moreover, the zeolites had a high adsorbent capacity and readily separated the molecules by their respective shapes and sizes (Berck *et al.*, 1956).

The zeolite community has received high attention recently with over 150 reported zeolites frameworks. They are highly distinguished by their chemical compositions (Feng *et al.*, 2015). Zeolite and zeolite-like materials have ordered porous molecular sieve layers which are believed to be important materials in the separation technologies with novel emerging applications (Snyder & Tsapatsis, 2007). The molecular sieve layers are applied as membranes which are used in ultrafiltration and microfiltration of liquid and gaseous mixtures of molecules (Caro & Noack, 2008; Freemantle, 2005).

Various zeolite membranes have been prepared and reported to have variable pore opening diameter which are essential for separation purposes (Bowen et al., 2004; Lin & Duke, 2013; Au & Yeung, 2001). Examples of the zeolite membranes that have been studied are listed in Table 2.7. The zeolite membranes are mostly identified using three letter code that confirms the framework structural types as commissioned of the International Zeolite Association.

Table 2.7 Examples of synthetic zeolite membranes (Bekkum et al., 2007; Szostak, 1998)

| **Zeolite name** | **Structure group** | **Average pore dimensions (nm)** | **References** |
|---|---|---|---|
| Linde Type A | LTA | 0.4 | Yang et al., 2008 |
| Faujusite | FAU | 0.74 | Lassinantti et al., 2000 |
| Modernite | MOR | 0.65 | Lin et al., 2004 |
| Ferrierite | FER | 0.53 | Matsufuji et al., 2002 |
| Chabazite | CHA | 0.42 | Sakamoto et al., 1989 |
| Sillicalite-1 | MFI | 0.55 | Crawford, 2013 |
| Hydorxy Sodalite | H-SOD | 0.57 | Khajavi et al., 2007 |

These membranes have been summarized in various reviews (Caro & Noack, 2000; 2008; Daramola *et al*., 2012; Li & Yang, 2008). The small pore diameters associated with these membranes make them ideal for separation by the molecular sieving technique (Caro & Noack, 2008 Skoulidas et al., 2003).

Zeolites have been traditionally applied as catalyst and adsorbents (Bowen et al., 2004). Currently, continuous polycrystalline zeolites (zeolite like materials) are being applied as zeolite membranes in various separation processes (Lin & Duke, 2013; Skoulidas et al., 2003). The zeolite membranes are made up of small pores (e.g. SAPO-34 & NaA), medium pores (e.g. MFI & Silicalite-1) and large pores (e.g. FAU) as seen in Table 2.7 (Au & Yeung, 2001). The zeolite membrane separation applications are advantageous due to the ordered crystalline structures as compared to the disordered polymer counterparts. The results in the ability to tailor make the zeolite membranes to suite a desired applications (Skoulidas et al., 2003). Table 2.8 highlights selected common membrane gas separation applications in industrial processes. An extensive review in membrane applications was given by Baker (2002).

Table 2.8 Selected gas separation process and corresponding membrane applications (Adapted from Ismail et al., 2002)

| Gas separation process | Industrial application |
|---|---|
| $O_2/N_2$ | Nitrogen enrichment from compressed air |
| | Nitrogen generation from compressed air |
| | Generating oxygen from compressed air |
| $H_2$/Hydrocarbon | Hydrogen recovery in refinery |
| $H_2/N_2$ | Hydrogen recovery from ammonia gas purging |
| $H_2$/CO | CO and $H_2$/CO ratio adjusted synthesis gas |
| | High purity hydrogen for proceses |
| $CO_2/CH_4$ | Natural gas processing |
| | Methane gas recovery from landfill gas and biogas |
| | $CO_2$ recovery for EOR flooding |
| $CO_2/N_2$ | $CO_2$ removal from natural gas liquids |
| | $CO_2$ recovery from flue gases |
| $CO_2$/Air | $CO_2$ separation for breathing systems |

#### 2.7.5.1 Existing zeolite membrane synthesis methods

In the above-mentioned reports, the synthesis procedures were thoroughly investigated to find economically viable synthesis routes. Thus, several synthesis strategies have been proposed and developed to achieve the preparation of zeolite membranes (Miachon *et al.*, 2006). The methods, as described in open literature, mainly involve two synthesis routes which are either based on the previously synthesised zeolite crystals or zeolite layer crystallization on supports (Daramola *et al.*, 2012).

Typical supports that have been used are porous inorganic tubes or disks made up of alumina, stainless steel, stainless steel grids, wire gauze packings, monoliths, metal nonporous plates, glass, ceramic and steel beads. However, the choice of the support depends on the desired application. For instance, Gorgojo and his co-workers (2008) reported membranes that exhibit high selectivity, a high degree of operational flexibility, low energy consumption and considerably low commercial costs which makes them ideal for industrial catalytic processes. Contrary, ceramic supports are preferred for gas separation. The synthesis of various zeolite membranes has been undergoing massive developments recently. Among the various reported synthesis techniques, the most dominantly reported are simple single stage hydrothermal synthesis, Chemical vapour transport and the secondary growth method (also referred to as the secondary seeded growth) (Tavolaro & Drioli, 1999; Caro, 2011; Chiang & Chao, 2001; McCleary et al., 2006). Table 2.9 summarizes the most commonly used synthesis techniques.

Table 2.9 Summary the most common zeolite synthesis techniques.

| Synthesis method | **Description** | **References** |
|---|---|---|
| Liquid-phase single step hydrothermal synthesis technique | Single step deposition of precursor solution on top of a ceramic support. The sol-gel technique is followed by crystallization during the heating process. | Matsuka et al., 1994<br>Davis & Sing, 2002<br>Yang et al., 2008 |
| Vapour phase transport synthesis technique | Two-step method which involves coating the support with precursor solution, followed by exposure to heat which results in further vapour deposition during crystallization | Yang et al., 2008<br>Figueroa et al., 2010 |
| Secondary seeded growth synthesis technique | Two-stage technique which involves seed synthesis, followed by coating on the supports and consequently hydrothermal synthesis. | Yang et al., 2008<br>Chau et al., 2000<br>Zhang et al., 2008 |

### 2.7.5.2 Simple single stage, hydrothermal synthesis method

Liquid-phase, hydrothermal synthesis; is a single step process during which both nucleation and growth of the zeolite material take place in the presence of the support (Davis *et al.,* 1990; Daramola *et al.,* 2012; Lin & Duke, 2013; Miachon *et al.,* 2006). The single step method is the most preferred as it is the simplest procedure. The procedure involves subjecting the previously prepared precursor solution and the support material to a single stage heating for a specified amount of time.

The products are then washed, dried and subjected to characterization. It was found that at short synthesis time; the nuclei and zeolite crystals are found on the support. On the other hand, at longer synthesis time, the nuclei disappear and the zeolite crystal surfaces, while the crystals continue to grow. As the reaction proceeds, the concentration of reactants is reduced, heterogeneous nucleation gets halted and only crystal growth proceeds (Vareltzis et al., 2003; Wang and Lin, 2012; Zhu et al., 2013).

Furthermore, for the simple hydrothermal synthesis method, the nuclei coexist with crystal for a long time during the synthesis of the zeolite materials (Yu et al., 2011). However, the nuclei amount and distribution homogeneity on the support is difficult to control as it depends mainly on the support surface (Miachon et al., 2006). In certain cases the nucleation formation was found to compete with the crystal growth process which leads to thick zeolite membrane layers (Bonhomme et al., 2003; Daramola et al., 2012; Kanezashi et al., 2006; Miachon et al., 2006).

### 2.7.5.3 Chemical vapour transport

The chemical vapour transport method favours nucleation process by a dry-gel conversion (Hong et al., 2011; Ping et al., 2012). This is a two-step synthesis technique involving coating a support with aluminium then followed by coating with an amorphous gel containing silica; these steps will then be followed by crystallization under autogenous pressure which occurs in the second step (Daramola *et al.,* 2012*;* Matsufuji *et al*., 2000; Miachon *et al.,* 2006; Xu *et al.*, 1990).

The vapour phase transport synthesis may result in crack formation in the amorphous gel layer, which leads to irreproducible membranes (Aoki et al., 1998; Daramola et al., 2012; Miachon et al., 2006).

### 2.7.5.4 Second growth synthesis

The secondary growth synthesis technique has been reported to provide an enhanced reproducibility and quality which is due to decoupling of the crystal growth and the nucleation process (Tang et al., 2010; Daramola et al., 2012). Various seeding techniques such as dip coating, spin coating among others have been proposed in open literature (Gouzinis et al., 1998; Miachon et al., 2006). The procedure involves, a two-step synthesis technique that involves an initial seeding step, during which previously synthesised zeolite crystals are deposited on the surface of the supports followed by hydrothermal synthesis (Bonilla *et al.,* 2001; Daramola *et al.,* 2012.; Gouzinis *et al.,* 1998; Miachon *et al.,* 2006).

For this process Tsapatsis and co-workers (1999) changed the pH of the synthesis solution to match the zeta potential of alumina supports and thus enhance the seeding process. On the other hand, Hedlund and Sterte (1999) reported that the seeding process can be enhanced by using cationic polymers and the seed are thus attached to the surface by electrostatic forces. In the latter case, the seeding technique is based on cationic polymers and was used successfully in the synthesis of ZSM-5 membranes on non-porous planes like gold plates (Hedlun & Sterte, 1999).

The quality of the membranes depends significantly on the quality of the seeds and the seeding method. The current seeding techniques may result in non-uniform seed distribution on the support (Daramola et al., 2012). The seed characteristics can affect the zeolite orientation and may influence the transport properties of the membranes (Miachon et al., 2006). The process often result in irreproducible zeolite membranes.

### 2.7.6 Challenges associated with the existing synthesis methods

The main aim of all three of these synthesis methods is to; (1) generate reproducible thin, zeolite layers with no defects or grain boundaries, (2) provide relatively easy scale up preparation process for commercial applications and (3) easy membrane assembly and handling for plant operations. The exsisting synthesis methods make it difficult to obtain crack-free zeolite membranes and thus limiting further application.

The drawbacks associated with the suggested synthesis techniques present an opportunity for an alternative synthesis technique to be applied for the synthesis of zeolite membranes. Miachon

and coworkers (2006) reported an alternative technique for the synthesis of zeolite membranes to overcome these drawbacks. This technique is referred to as the pore-plugging hydrothermal synthesis technique (Miachon *et al.,* 2006).

This new synthesis technique involves growing the zeolite membranes within the pores of the ceramic supports, until the entire pores are blocked by the zeolite crystals (Miachon *et al*., 2006; 2008; Daramola *et al*., 2009; 2010). Thus, the active zeolite crystals are located inside the pores of the support. The resulting membranes are then referred to as nanocomposite membranes. The nanocomposite membranes obtained lead to high separation selectivity in various studies when compared to their thin-film counter parts (Daramola *et al*, 2009; 2010; 2011; van Dyk *et al.*, 2005).

In the nanocomposite architecture membranes, the active phase is embedded within the pores of the porous support via pore-plugging hydrothermal synthesis. This architecture has been achieved by pore-plugging hydrothermal synthesis described by some authors as temperature controlled crystallization. The following outlines the process involved in this synthesis;

(a) the Formation of solution whose constituent is a mixture of zeolite active materials, the chemical precursor, and bringing it in contact with the porous support,
(b) Embedding the pores of the support with crystals by employing a non-isothermal temperature program using a multi-stage succession processes,
(c) Eliminating the residual chemical precursor by washing.

Interruption time is always introduced in the non-isothermal synthesis procedure to promote the growth of the nuclei or nutrient diffusion in the porous structure. Zeolite crystal size is subjected to the pore dimensions of host, thereby, limit differences in thermal expansion.

The active phase in a nanocomposite architecture is within the pores of the porous support, and the transport of molecules occurs within these phases. This then enhances higher separation performance (selectivity) and protects the membrane layer from abrasion and shock. These properties make nanocomposite architecture membrane better than the thin-film membranes.

Mass transfer within the nanocomposite membranes at high temperature is governed by the zeolite pores instead of the intercrystalline openings that may be found in the layered thin-film configuration (Li *et al.*, 2008). Intensive studies have been conducted on the nanocomposite membranes and they have shown desirable separation applications for example; xylene isomer separation (Daramola *et al.*, 2009; 2010; van Dyk *et al.*, 2005) and ammonia recovery (Camus *et al.*, 2007). These membranes were combined with catalysts in membranes reactors in industrial applications such as isobutene dehydrogenation (Ciavarella *et al.*, 2001; Miachon *et al*., 2007) and xylene isomerization (van Dyk *et al.*, 2005; Miachon *et al*., 2007; Daramola *et al.*, 2009; 2010; 2011).

However unlike their thin-film membrane counterparts, the nanocomposite membranes have a few reported disadvantages. The main disadvantages are high costs associated with the membrane supports and low flux (Daramola et al., 2010; Yang et al., 2008). In nanocomposite membranes, the flux can be increased by increasing the transmembrane pressure, resulting in high pressure requirements to achieve desirable separation performance which hinders scale-up processes for industrial applications. High flux nanocomposite membranes remains a scientific challenge. Moreover, the synthesis of nanocomposite membrane is currently only feasible for bench top processes and has not yet been modelled for scale-up processes.

### 2.8 Recent development for zeolite membranes

There have been high developments in the zeolite research area presenting a lot of research opportunities. There is high desire to apply zeolite membranes in industrial processes as they have desirable properties for industrial separation process. However, currently industrial applications have been limited as only a handful has emerged in the last decade (Figueroa, 2016). Rangnekar and coworkers (2015) stated that this limitation is mainly due to membranes having low flux and high fabrication cost which make the membranes economically unviable. This has been a paramount scientific challenge for the past 3 decades in the membranes research area (Yang et al., 2008).

A lot of attempts have been made to overcome this constraint; one of which would be reduction in membrane thickness (Daramola *et al.*, 2012; Rangnekar *et al.* 2015). Reports have stated that sub-micron (<1 μm) membrane thickness have a high industrial application potential (Tsapatsis,

2011). However, Rangnekar and coworkers (2015) highlighted that very thin film membrane will result in transport within the membranes being dominated by pore entry resistance instead of the intracrystalline transport. This means high quality supports are required to have very low resistance to permeation (Rangnekar *et al.* 2015). Currently, there have not been many reports that focus on the effect of the supports on the very thin membranes that have lately emerged.

The recent developments of ultra-thin membranes (sub-1 µm) have been reported to eliminate the low flux constraint in the zeolite membranes. As reported by Korelskiy and co-workers (2012), these membranes have a higher industrial potential. In their study, they were able to synthesize 0.5 µm MFI membranes which resulted in about 100 times higher flux for n-butanol/water separation by pervaporation than their previous work (Korelskiy *et al.*, 2012).

This sub-1 µm membrane synthesis approach was recently explored further by Agrawal and coworkers (2015) which supported the claims earlier made by Korelskiy and co-workers (2012). However, in both these cases the separation factor was found to drop at high temperatures (150 °C) (Argrawal et al., 2015; Korelsiy et al., 2012).

Moreover, Sjöberg and coworkers (2013) have also previously reported the synthesis of sub-micron MFI zolite membranes. In their study, they obtained 0.7 µm thin membranes which were subjected to $CO_2$ separation from synthesis gas derived from black liquor, a known by product found in paper processing industry (Sjoberg et al., 2013). The authors reported very high $CO_2$ permeance. However, the permeance and selectivity dropped to half its value after the membranes were subjected to 10 hours of testing (Sjoberg et al., 2013).

Modifications are required for viable industrial applications. Although reports have shown the possibilities of sub-micron membrane synthesis, this technique is yet to be extended to other types of membranes particularly those that have been demonstrated to have a high $CO_2$ separation performance in flue gas applications (Argrawal et al., 2015; Korelskiy et al., 2012; Sjoberg et al., 2013).

In membranes separation technology, $CO_2$ separation and capture from flue gas applications in the presence of impurities was found to be detrimental to the membranes. This statement was previously reported by Kapteijn and coworker (1995) who conducted a review on zeolite

membranes for $CO_2$ applications. Similar results were recently observed by Wu and coworkers (2015) who were using CHA zeolite membranes to separate $CO_2/N_2$ and $CO_2/CH_4$. In this study, propane was introduced in the separations process and there was a huge reduction in the flux as well as the separation performance. In order to apply the membranes in $CO_2$ separations, there need to study closely all the components within the gas mixtures to be separated. Currently, majority of lab scale studies only focus on separating binary mixtures and model them for potential industrial application. Moreover, a recent review by Ragnekar and coworkers (2015) highlighted other factors that limit applications of zeolite membranes industrially such factors include the effect of porous supports and sweep gas.

### 2.9 Applications of inorganic membrane in CO2 capture

Although various membranes have been studied for the separation and capture of carbon dioxide in flue gas, nanocomposite membranes have not been widely studied for the separation and capture of carbon dioxide from flue gas. For instance, Yang and coworkers (2008) discussed the feasibility of using inorganic membranes for the separation of carbon dioxide and nitrogen in flue gas. In this case, the thin selective membrane is coated on a porous ceramic support. The ceramic supports were found to increase the mechanical strength while minimizing the mass-transfer resistance (Yang *et al.*, 2008). Additionally, ceramic membranes have high separation energy efficiency and offer a high packing density for small plant installations (Bounaceur *et al.*, 2006).

In a study by Bernal and his coworkers (2004), ceramic supported MFI membranes for $CO_2/N_2$ separation from flue gas were explored. After varying the operating conditions, they concluded that ceramic MFI zeolite membranes separated $CO_2$ from the $CO_2/N_2$ mixture selectively (Bernal et al., 2004). The selectivity was highly influenced by the preferential adsorption of $CO_2$ in the pores of the zeolites which hinders the permeation of $N_2$ (Bernal et al., 2004; Yang et al., 2008). Although the membranes showed a high permeation flux and selectivity, they did not consider a comparison study with nanocomposite membranes.

On the other hand, SAPO-34 membranes have been intensively studied for light gas mixture separations by Li and his co-workers (2010; 2012). In their work, Li and Fan (2010) conducted a study on the preparation of high flux SAPO-34 membranes for $CO_2/N_2$ gas mixture separation.

In this study SAPO-34 membranes have been shown to be effective in the removal of $CO_2$ from natural gas (Li & Fan, 2010). Their study reported a desirable permeance and selectivity trade-off for $CO_2/N_2$ gas mixture separation through SAPO-34 membranes as compared to other reported membranes such as FAU/alumina disk (Gu *et al.*, 2005), FAU/alumina tube (Kusakabe *et al.*, 1997), silicalite-1/stainless steel net (Guo *et al.*, 2006), LTA/carbon Zhou *et al.*, 2007), Na-ZSM-5/alumina tube (Shin *et al.*, 2005) and DDR (van den Berg *et al.*, 2008) for $CO_2/N_2$ separation.

The results from the work of Li and his coworkers (2010) showed high potential of SAPO-34 membranes for the separation and capture of $CO_2$ in coal-fired power plant flue gas by SAPO-34 membranes (Li & Fan, 2010). However, this work followed the seeded hydrothermal synthesis approach for the preparation of the thin-layered membranes.

In the thin-film membranes, thermal expansion mismatch may occur at higher operating temperatures resulting in loss of membrane selectivity due to cracks formation. These drawbacks as well as abrasion associated with membrane handling and assembly may hinder potential industrial applications. These drawbacks associated with thin-film membranes can be overcome by using the pore-plugging hydrothermal synthesis technique to produce nanocomposite membranes.

### 2.10 Single gas permeation mechanisms

The transport through the zeolite by molecules is largely dependent on the affinity of the zeolite membrane towards the permeating molecules. Permeating molecules may have different kinetic diameters, different adsorption activation energies and more so the different zeolite membranes have different pore opening diameter as well (Sebastian et al., 2007). As a result, different permeation mechanisms have been reported.

Three main transport mechanisms have been extensively reported in literature for the permeation of molecules through microporous zeolite membranes, namely Knudsen diffusion, bulk diffusion and configurational (surface) diffusion (Algeiri et al., 2003; Ciavarella et al., 2000). Sommer and his co-worker (2003) stated that the most dominant transport mechanism in this case was reported to be the configurational diffusion.

Knudsen diffusion occurs mainly thorough the zeolite pores as well as the microspores which is often found in poor quality membranes as a form of grain boundaries. Knudsen flux was reported to be largely on the molecular weight of the permeating molecules (Choi et al., 2001). Hence, in essence light molecules often travel faster through the zeolite membranes under a similar concentration gradient.

Bulk diffusion is often referred to as the Poiseuille or viscous flow in literature (Algeiri et al., 2003). This particular mechanism is predominant in cases where the thin-film membrane has a high amount of defects and cracks in the membrane layer (Algeiri et al., 2003; Ciavarella et a., 2000). As a result, the viscous flow is experienced when membrane experiences a pore pressure difference (Choi et al., 2001).

The surface diffusion or better known as the configurational diffusion type of transport in zeolite membranes result from the interaction between the walls of the pores and the diffusing molecules (Xiao & Wei 1992). There has been two surface diffusion mechanisms reported in literature: (i) if the molecule is strongly adsorbed, then a strong zeolite-adsorbate interaction is experienced resulting in transport by the surface diffusion (Algeri et al., 2003; Ciavarella et al., 2000; Xiao & Wei, 1992). Provided that surface mobility is weaker than the attractive forces in the adsorption, interactions as described by Crittenden & Thomas (1998); (ii) in cases where by there is a weak adsorbate-zeolite interactions, the transport is governed by activated diffusion which is also referred to as gas translational diffusion (Xia & Wie, 1992).

The gas transport by surface diffusion zeolite membrane is exclusive to defect free membranes (Algeri et al., 2003; Ciavarella et al., 2000; Xiao & Wei, 1992). The key characteristic is the fact that the gas molecules keep their gaseous character as they overcome the energy barriers associated with the pores of the zeolite membranes (Algeri et al., 2003; Ciavarella et al., 2000; Crittenden & Thomas, 1998).

The polycrystalline nature in the structure of zeolite membranes implies that the membranes may also contain non-zeolite (intercrystalline) portions where diffusion takes place (Algeiri et al., 2003; Ciavarella et al., 2003; Sommer et al., 2003). Hence, the gas transport through the zeolite membranes often occurs via a combination of diffusion through the non-zeolite pores and filtration through the zeolite pores (Algeiri et al., 2003). Moreover, the capillary condensation

may also play and important role in the transport of gases through the zeolite membranes as well (Sommer et al., 2003).

It has been reported that the capillary condensation is favoured under the same conditions as those that favour the surface diffusion (Coronas and Santamaria, 1999). Often the two transport mechanisms may exist in the same system (Sommer et al., 2003).

Single gas permeation through zeolite membranes depends largely on the following factors: (i) the type of zeolite membranes and the characteristics of the permeating molecules i.e. whether the molecules strongly adsorbs on the zeolite membrane or not and (ii) the experimental conditions upon which the permeation tests are carried out, more especially the operating temperature and pressure as they affect the properties of the molecules.

As such, the as-synthesized membranes were all subjected to single gas nitrogen and carbon dioxide permeation experiments with a feed pressure of 1.2 bar and 1 bar permeation for 180 s at room temperature. No sweep gas was used as the sweep gas is known to change the system from a single gas to a more binary system as far as $CO_2$ permeation is concerned. A brief summary of the gas permeation mechanisms is detailed before the discussion of the single gas permeation results (Section 2.14.1).

### 2.10.1 Single gas permeation tests through the SAPO-34 membranes

The pure gas permeation tests were initially conducted with $N_2$ gas before calcination process to assess presence of unplugged pores. Plugged pores would not result in any permeance. This is as a result of the pore of the supports being blocked zeolites whose pores were blocked by the template. Thus, uncalcined membranes displayed lower permeance compared to the calcined counter parts.

Calcination unblocks the pores of the zeolite membrane by removing the template incorporated in the zeolite during the synthesis stage. Eight zeolite membranes (labelled M1-M8) were subjected to single gas permeation tests. In this study membrane M1 showed a high permeation for both $N_2$ and $CO_2$ which were 36.12 $x10^{-7}$ $mol.s^{-1}.m^2.Pa^{-1}$ and 37.56 $x10^{-7}$ $mol.s^{-1}.m^2.Pa^{-1}$ respectively with an ideal selectivity of 1.04. This results may be attributed to the smaller kinetic diameter of $CO_2$ (0.33 nm) passing through the pores of SAPO-34 membranes (0.38 nm) easily compared to the slightly bigger $N_2$ (0.36 nm).

In a study by Li and co-workers (2010; 2012), it was reported that SAPO-34 has a relatively higher affinity for $CO_2$ than $N_2$, resulting in preferential adsorption and diffusion of $CO_2$ through the membranes. Transports across porous SAPO-34 membranes can be described as either, molecular sieving, Knudsen diffusion or surface diffusion (Caro & Noack, 2012; Li et al., 2010).

The high permeance for $CO_2$ and $N_2$ observed in this study at ambient temperatures was expected for thin-film SAPO-34 membranes as reported by Li and Fan (2010). Thin-film membranes often result in poor quality when synthesized using the in situ hydrothermal synthesis and this was the case in this study (Miachon et al., 2007; 2008). Moreover, the short synthesis times may have resulted in poor interaction between the support surface and the zeolite membranes resulting in defect formation.

It was established that the short synthesis time may led to the formation of non-zeolite pores in thin-film membranes which resulted in the low $CO_2/N_2$ selectivity (Li & Fan; 2010). These defects were found to be minimised in the nanocomposite membranes (Bernal et al., 2012; Miachon et al., 2006; 2007; Daramola et al., 2008; 20012).

### 2.11 Applications of nanocomposite inorganic membrane in $CO_2$ capture

Alshebani and his coworkers (2008) explored the feasibility of using nanocomposite MFI membranes on ceramic hollow fibers for $CO_2$ capture. They found that the nanocomposite architecture of the membranes on the fibers offered relatively higher permeance; higher surface/volume ratios in similar operating conditions as compared to the ones in the study by Bernal and colleagues (2004) on tubular MFI membranes (Alshebani et al., 2008). The results found in this study showed high potential for high temperature industrial $CO_2$ separation by nanocomposite membranes. However, the nanocomposite architecture obtained in this study had grain boundaries that were found to limit the selectivity (Alshebani *et al.*, 2008). MFI membranes were found to have an average pore diameter of 0.55 nm while the kinetic diameter of $CO_2$ and $N_2$ are 0.33 nm and 0.36 nm, respectively (Alshebani *et al.*, 2008; Crawford, 2013). This presents drawbacks associated with the molecular sieving ability of the membranes. The pore opening diameter of membranes is large relative to the kinetic diameters of both gas molecules and thus reducing the selectivity.

Daramola and his co-workers (2016) explored the nanocomposite sodalite(HS)/ceramic membrane synthesized via the pore-plugging hydrothermal synthesis (PPH) protocol for pre-combustion $CO_2$ capture. In their study, the membranes had a high selectivity of $H_2$ which is essential for the IGCC system where by $H_2$ is used in the combustion process. However, for the post combustion $CO_2$ capture SAPO-34 zeolite membranes appear desirable due to their relatively smaller pore dimensions as well as a high adsorption affinity for $CO_2$. SAPO-34 illustrated in Figure 2.11 has an average pore dimension of 0.34 nm. Hence, the aim of this study is to explore the nanocomposite SAPO-34 membranes for post-combustion $CO_2$ capture.

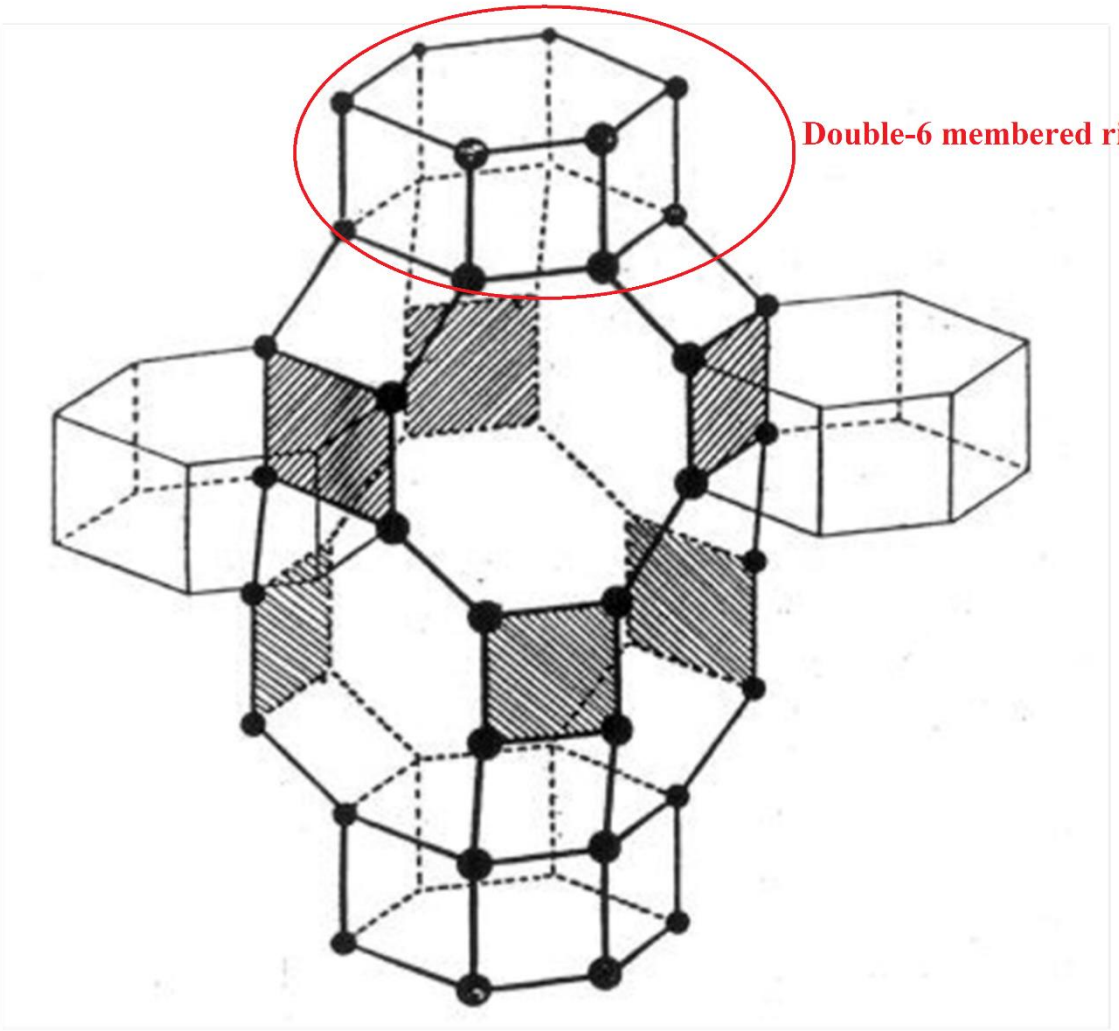


Figure 2.11 Crystal structure of SAPO-34 zeolite (adapted from Dent & Smith, 1958).

# Chapter Three

## Materials and Methodology

# 3 Experimental Procedures

## 3.1 Introduction

In this chapter, a short summary of the synthesis technique as well as materials required for the fabrication of SAPO-34 zeolite membranes is presented. The emphasis was placed on the experimental procedure that was followed in this study.

## 3.2 Synthesis of zeolite membranes

Various synthesis methods have been proposed for the fabrication of SAPO-34 zeolite membranes on porous α-alumina supports. This includes the single step hydrothermal synthesis and the two step secondary or seeded growth methods. The former method mainly consists of the application of previously synthesized seeds which are applied on the supports using various techniques. The supports are subjected to further hydrothermal synthesis whereby the growth of the zeolite crystals is governed by the previously applied seeds (heterogeneous catalysis). This has been the most widely applied synthesis method for the synthesis of zeolite membranes as it was found to have desirable reproducibility. Desirable advantages associated with this method include strict control of the zeolite formation. However, reproducibility remains a challenge as the synthesis in this case depends largely on the seeding techniques.

On the other hand, the simple hydrothermal synthesis of the membranes is performed by placing the support directly inside an autoclave containing the synthesis solution. The autoclave and its contents are then placed in a preheated oven and subjected to heating at a desired temperature for a certain period of time. The heating temperature and the synthesis times for this process have been reported to depend largely on the type of structure directing agents (SDAs) which are usually organic templates such as tetrapropylammoniumhydroxide (TPAOH) or morpholine.

Although this is a simple synthesis method, there are various drawbacks associated with this method. The drawbacks include the fact that the homogeneity of the membranes depends largely on the surface of the support. This is very difficult to control. Moreover, extended synthesis times may result in thick membranes. Thick membranes are known to have very low membrane flux due to large thickness that presents resistance to the transport.

### 3.3 The pore-plugging synthesis for nanocomposite membranes

The main objective of the synthesis methods is to generate reproducible thin-film, zeolite layers with little to no defects or grain boundaries. Considering this objective, Miachon and coworkers (2006) reported an alternative synthesis technique which results in nanocomposite zeolite membranes (Miachon et al., 2006). In this technique, the pores of the supports are "plugged" with zeolite crystals grown within the pores of the supports. In the end, the entire pores are blocked by the zeolite crystals hence the term "pore-plugging" hydrothermal method (Miachon et al., 2006 & 2008; Daramola et al., 2009). This method offers a wide range of desirable advantages when compared to other conventional thin-film membranes: (i) limitation of defect to the size of the support, (ii) reduced effects of thermal expansion mismatch between the supports and the membrane materials, and (iii) production of reproducible membranes. Moreover, the advantages of the nanocomposite zeolite membrane is not only limited to enhanced mechanical strength but extended to the protection of the membrane from abrasion during handling. It has also been reported that nanocomposite membranes have high separation performance (Daramola et al, 2009; 2010; 2011; van Dyk et al., 2005).

### 3.4 The support

The ceramic supports (Figure 3.1 and Figure 3.2) used in this study were microporous, asymmetrical α-alumina tubes (Franhoufer IKTS, Germany). The tubes were 15 cm in length, with an inner diameter of 7 mm, and an outer of 10 mm. These tubes were sealed for a length of 10 mm on both ends to create non-permeable endings. The effective permeation area for separation was 13 cm.

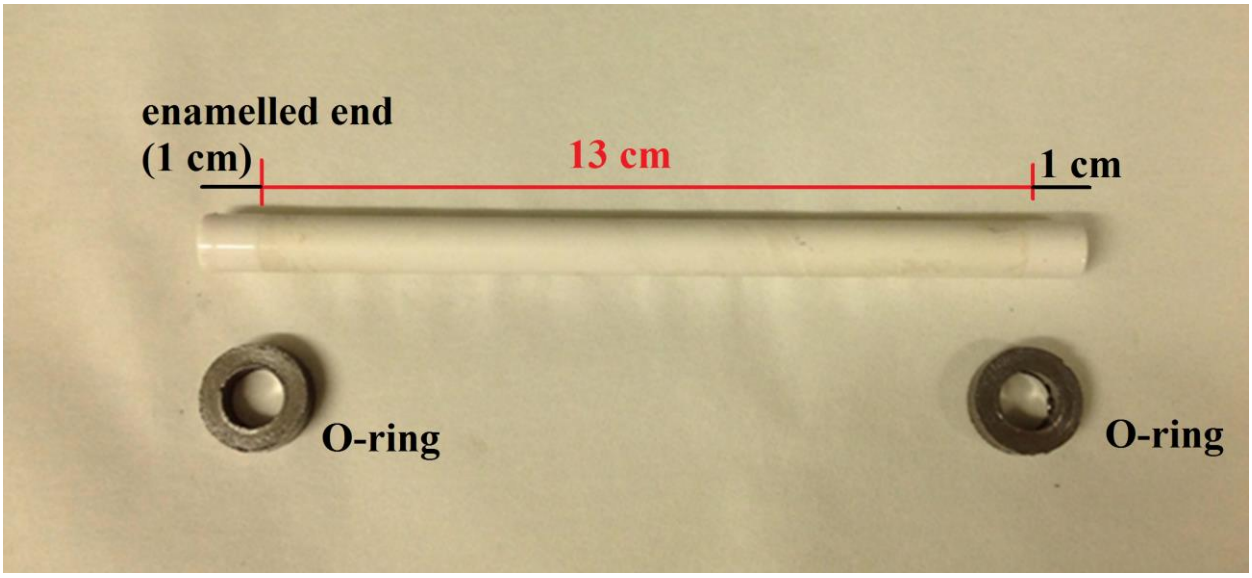


Figure 3.1 Ceramic membrane tube with graphite O-rings (note 10 mm sealed endings) (picture not to scale)

These tubes consisted of three layers with different incremental porosity from the inner to the outer layer of the tube (Figure 3.2).

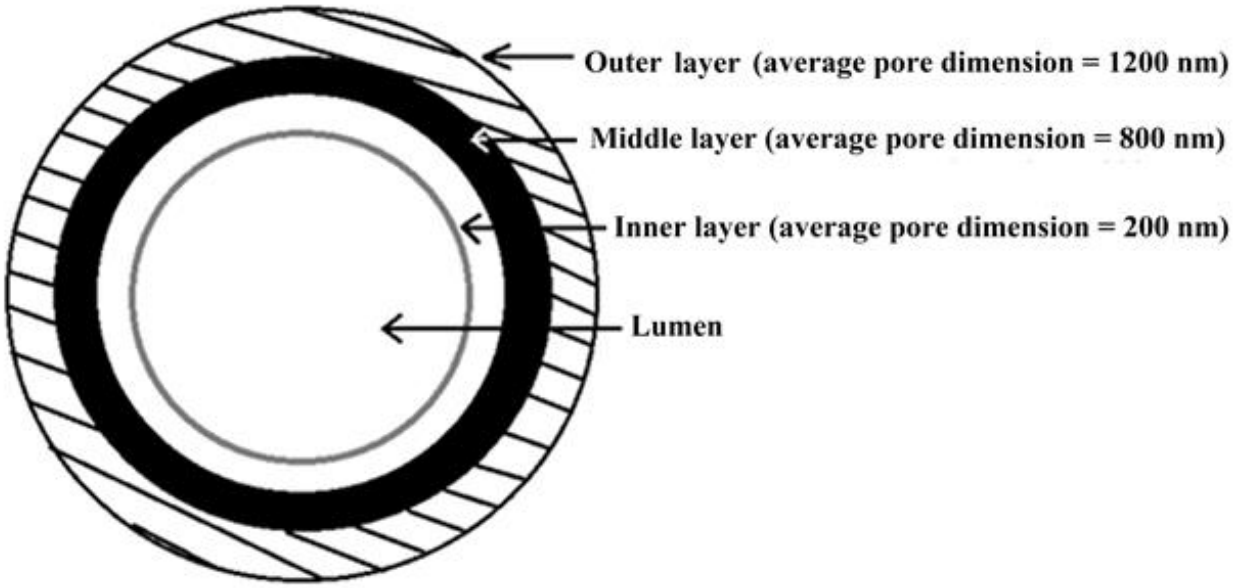


Figure 3.2 The cross-sectional view of the asymmetric ceramic support

### 3.5 Experimental methods

The experimental procedure that was followed in this work was divided into components shown in the Flow Chart 3.1.

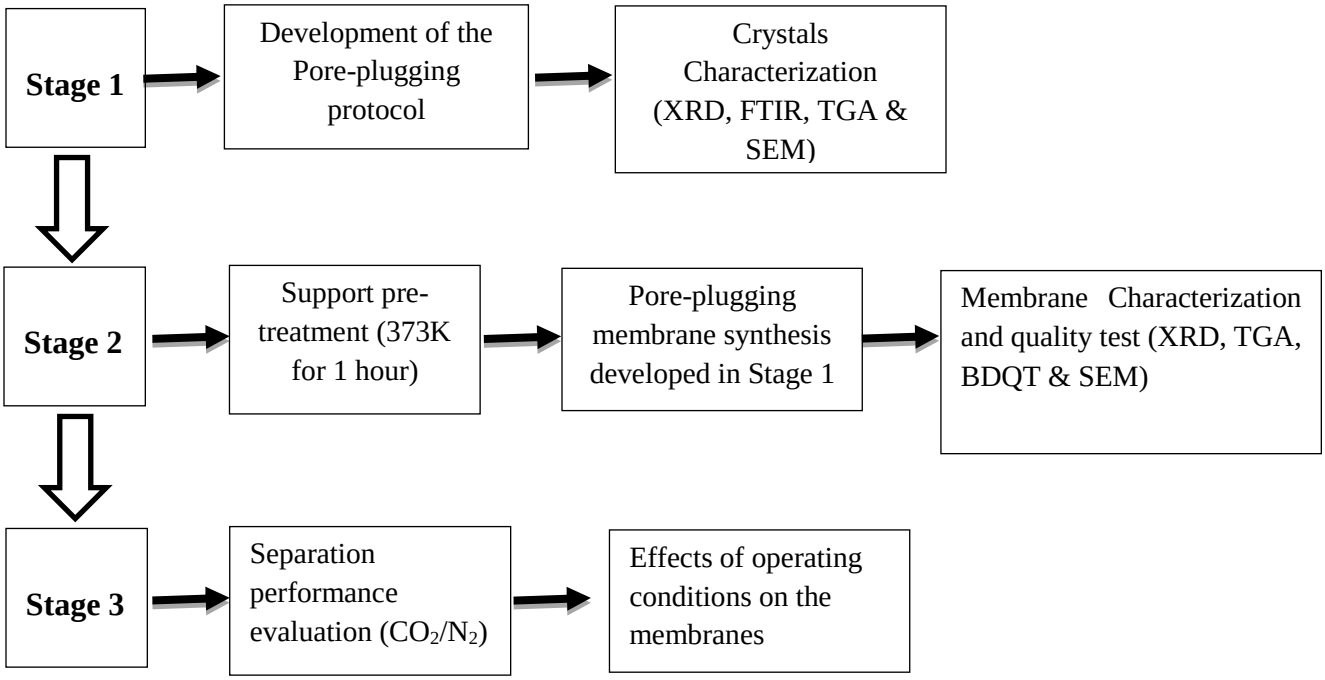


Flow chart 3.1 Experimental flow diagram illustrating the experimental procedure.

The SAPO-34 membranes used in this study was produced using an organic template which was used as a structure directing agent (SDA, 1 M tetrapropylammonium hydroxide, TPAOH), the silica source tertraethyl orthosilicate (TEOS), and the alumina source aluminium triisopyopylate (Al *i*-Pr) all supplied by Merk Millipore as well as the phosphorous source othorphosphoric acid ($H_3PO_4$) supplied by Sigma-Aldrich.

In a typical procedure, the alumina source was mixed with distilled water for half an hour to form a paste, then a dilute phosphoric acid was added dropwise to the solution with continuous stirring. The solution was stirred for an hour, then the silica source (TEOS) was added dropwise, and consequently the structure directing agent, TEOH was added under continuous stirring. The solution was further stirred at ambient temperature until a homogeneous solution was formed. Upon obtaining a homogenous precursor solution, the support was placed in a stainless-steel

Teflon-lined autoclave (Figure 3.5) and the resulting gel solution was carefully poured into an autoclave until the Teflon liner and the tube were covered up. The autoclave was then covered up and sealed with the 6 nuts and bolts. Finally, it was placed in a pre-heated oven at 150 °C. The autoclave remained in the oven using the temperature program depicted in Figure 3.6. Upon completion of the synthesis, the crystals were washed with distilled water and dried overnight at 373 K. The dried crystals were crashed and subjected to characterization.

### 3.5.2 Preparation of nanocomposite membranes

Upon obtaining pure SAPO-34 crystals in the previously mentioned synthesis protocol, then the nanocomposite membranes were prepared as depicted in Stage 2 in Figure 3.3. The ceramic supports were immersed in distilled water which was boiled for one hour to remove particles that might have been adsorbed on the pores of the supports. These supports were then placed in an oven and dried at 373 K for one hour. The ceramic supports employed in this study are illustrated in Figure 3.1 with the asymmetrical cross-section depicted in Figure 3.2. The dimensions of this asymmetrical layers are listed in Table 3.1.

### 3.5.3 Membrane synthesis

The procedure developed in section 3.3.1 was followed to obtain the homogeneous precursor solution. Figure 3.4 illustrates the experimental procedure for the nanocomposite membrane synthesis by the pore-plugging method. The as-synthesized membranes were subjected to membrane quality tests using single gas permeation tests. Low quality membranes were returned to the synthesis solution for a further multistage synthesis to improve the quality. The multistage membranes displaying high quality were used for further characterization.

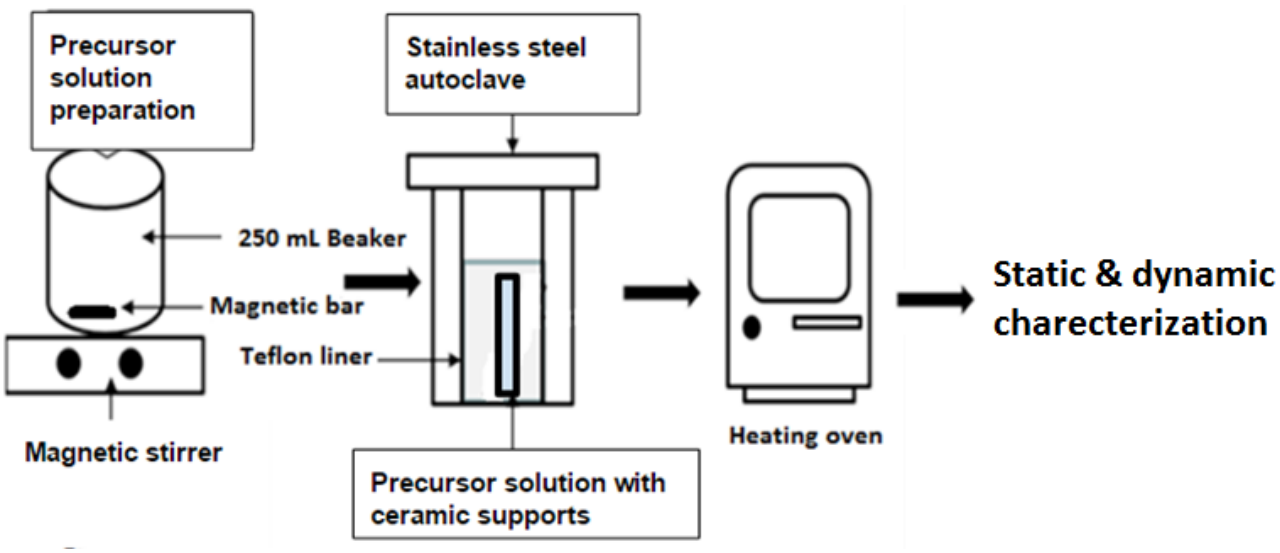


Figure 3.4 Experiment method for the synthesis of SAPO-34/ceramic membranes

About 240 ml of the solution was placed into a Teflon-lined stainless steel autoclave (Figure 3.5) and the pre-treated support was placed into the solution and sealed. For the desired nanocomposite architecture to be obtained, the autoclave was placed in a pre-heated oven at 423 K and subjected to an interrupted hydrothermal synthesis. The interruption is essential to ensure the diffusion of the synthesis solution into the pores of the supports, without it thin-film membranes are obtained.

Figure 3.5 A Teflon-lined stainless autoclave components used for the synthesis of SAPO-34

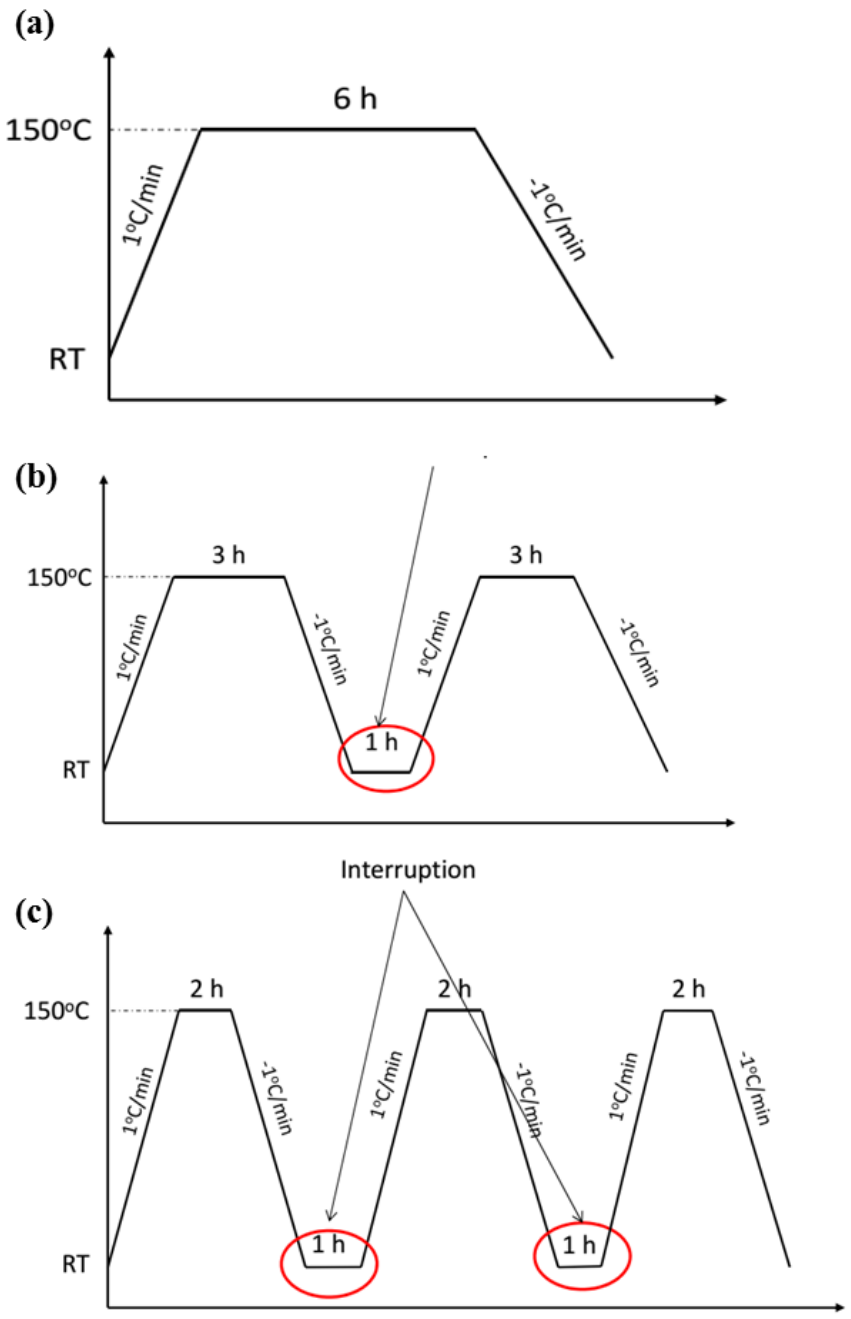


Figure 3.6 (a) Temperature programme employed for the synthesis of the thin-film SAPO-34/ceramic membrane (no interruption); (b) Temperature programme employed for the PPH synthesis of nanocomposite SAPO-34/ceramic membranes with one interruption; (b) Temperature programme employed for the synthesis of nanocomposite SAPO-34/ceramic membranes with 2 interruptions. RT: room temperature.

### 3.6 Static characterization techniques

The fabricated membranes were subjected to various physicochemical characterization techniques which have been used in previous reported studies for the characterization of crystalline zeolite membranes. These techniques include X-ray diffraction (XRD), scanning electron microscopy (SEM) and energy dispersive spectroscopy (EDS), Fourier transform infrared (FTIR) spectroscopy and thermogravimetric analysis (TGA). The membranes were further subjected to dynamic characterization techniques; these include the single gas permeation test to assess the presence of and defect.

#### 3.6.1 X-ray Diffraction

The technique is essential for the assessment of the crystallinity of the membranes by utilizing the diffraction angles of the X-rays by the crystalline phase of the membranes. These angles along with the specific radiation wavelength can then be related by Bragg's law to their characteristic lattice planes (HKL values).

In this study, the zeolite structure of the as-synthesized membranes was analyzed by using a Bruker D2 AXS phaser equipped with Scintillation counter, 1-dimensional LYNXEYE, detector and using a Cu-kα radiation (30 kV, 19 Ma) in the scan range was $10\ ^\circ \leq 2\theta \leq 90^\circ$. The resulting peaks were compared and decoupled with the PDF standards found on the Diffract EVA software.

#### 3.6.2 Scanning electron microscopy and EDS

The SEM was used to observe the morphology of the as-synthesised membranes. The SEM was also used to provide the particle sizes and shape of grains that might be present on the supported membranes. The analyses were done by breaking the membrane support and examining the membrane incorporation on a small part of the supports.

#### 3.6.3 Thermogravimetric analysis

The TGA analyses in this study which resulted with a derived curve of the weight loss measurements were conducted on a Perking Elmer STA 4000 analyser which was coupled with a auto sampler. A small (about 10 mg) amount of the membrane material was placed on a ceramic

pan which was then placed inside the instrument's furnace. The temperature was then increased from room temperature to 950 °C under a nitrogen gas.

The resulting TGA weight loss plot displayed the necessary data about the thermal stability of the membranes. The temperature was then monitored with a Pyris Software coupled to a computer. The weight lost was then expressed as a percentage as the temperature increased.

### 3.6.4 Fourier Transform Infrared Spectroscopy (FTIR)

The FTIR spectroscopy conducted on a Bruker Tensor 27 was used to analyse the surface chemistry of the synthesised zeolite membranes and the type of functional groups present. The FTIR spectra recorded was in the range of 550-4000 $cm^{-1}$.

## 3.7 Membrane calcination

The as-synthesized tubular membranes were then calcined at high temperature pre-treatment before use in gas permeation tests. This was essential to unblock the pores that might be blocked by the structure directing agents (TPAOH).

The membranes were placed in a stainless steel tubular membrane reactor module (Figure 3.7) and sealed with two graphite O-rings on both ends. The module was then put in a furnace which was used for the gas permeation tests as well as the Basic Desorption Quality Test to evaluate the quality of the membranes. Figure 3.8 depicts the cross-section of an assembled membrane reactor module.

Figure 3.7 Stainless steel membrane reactor module include the graphite ring and the membrane

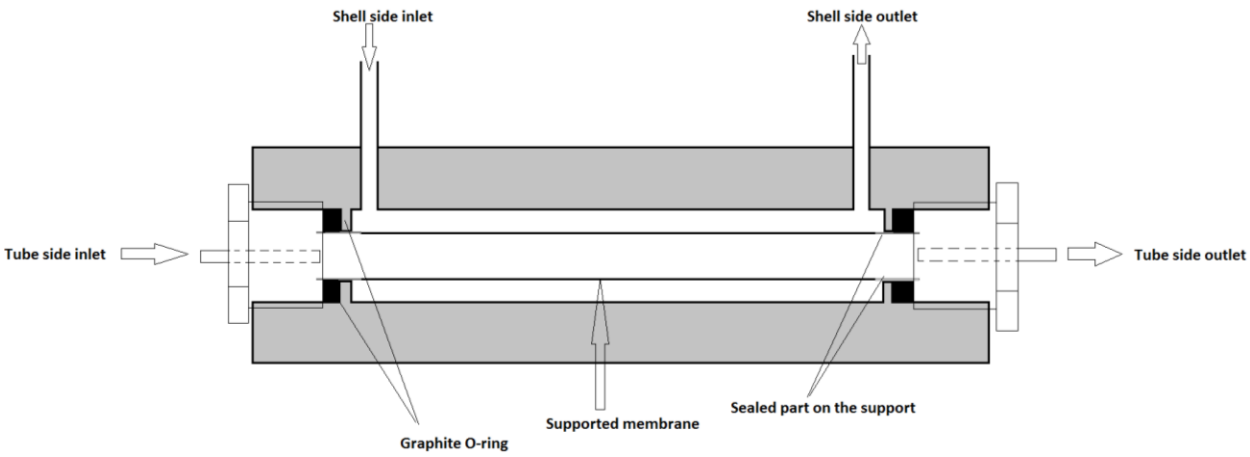


Figure 3.8 Cross-section view of the assembled membrane reactor module (not to scale)

The membrane was heated to 450 °C in the presence of nitrogen gas in an oven displayed in Figure 3.10. The membrane was left in the furnace (Figure 3.9) for 3 hours and only then the testing could commence. Further, this process also ensures that the water and or hydrocarbons that are likely to adsorb on the zeolite pores have been removed as well. It has been reported that water and hydrocarbons can be desorbed at 300 °C and 360 °C respectively (van Dyk, 2005). The furnace and the membrane module are then cooled to ambient temperature (Figure 3.10).

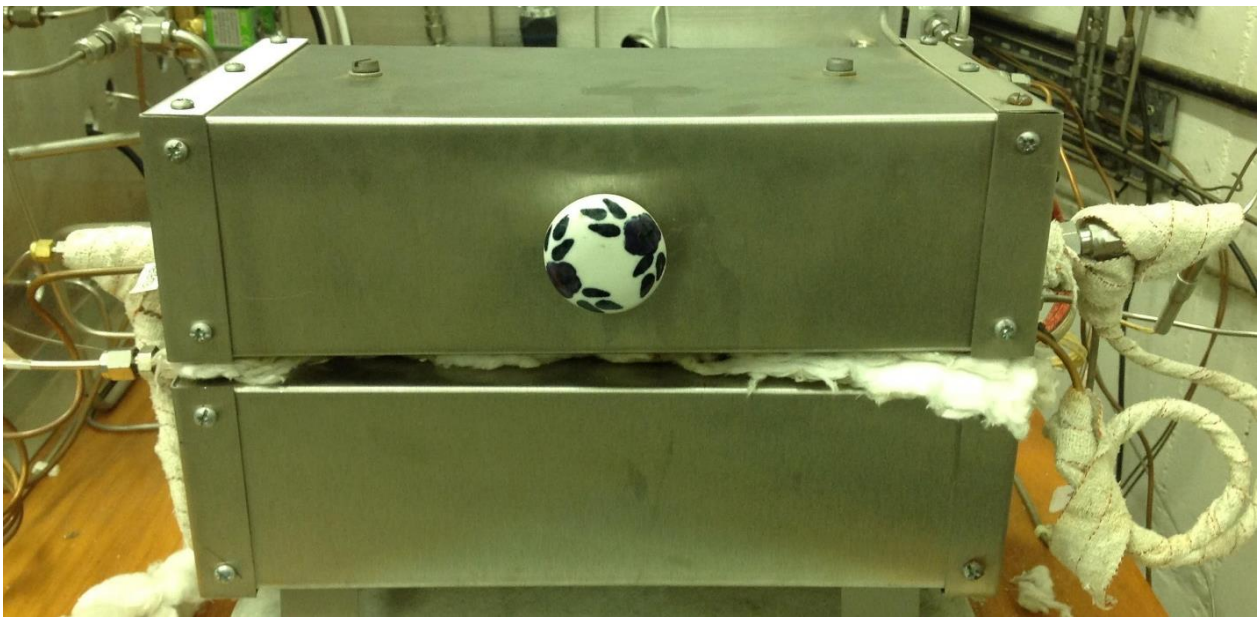

Figure 3.9 Heating furnace used for the calcination of the membranes under $N_2$ atmosphere

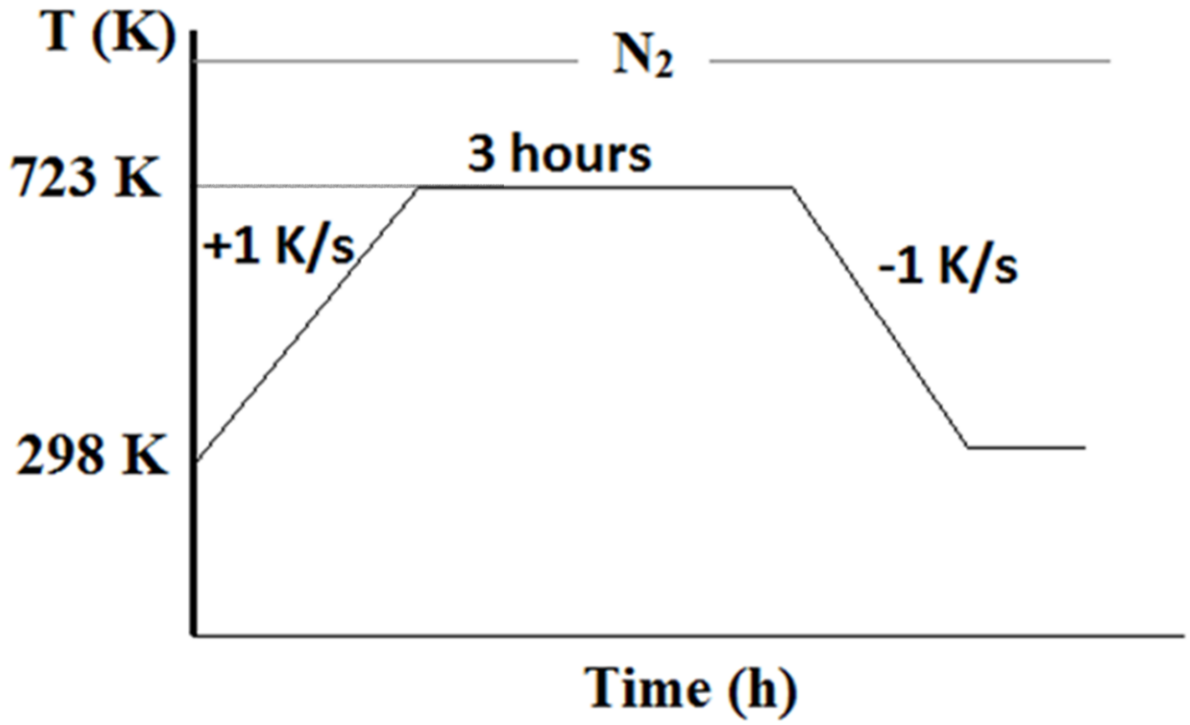


Figure 3.10 The temperature program for the calcination process

### 3.8 Dynamic characterization

To assess the quality of the as-synthesized membranes, the membranes were subjected to single gas permeation experiment as well as the Basic Desorption Quality Test.

#### 3.8.1 Single gas permeation before calcination

Upon completion of the pore-plugging hydrothermal synthesis, to assess the penetration of the support pores by the precursor solution, single gas permeation experiments were conducted with nitrogen gas. The structure directing agent (TPAOH) is known to occupy the pore of the zeolite membranes which in turn blocks the pore of the support, as a result, less to no gas permeation at ambient temperature.

### 3.8 Basic desorption quality test

The quality of the membranes is governed by the absence of defects, their adsorption characteristics as well as the properties of the mixture to be separated (Daramola et al., 2012). Hence, mixed gas permeation experiments can be used as a method to assess the quality of the membranes (Pachtová et al 2003). However, it has been reported that this technique requires

highly sophisticated equipment and is very difficult to control (Nakao, 1994; Pachtová et al 2003).

Nakao (1994) described an alternative technique called the permporometry technique which has been applied on microporous membranes. This technique involves a dynamic desorption of a strongly adsorbing gas (water or n-butane) which has been previously adsorbed on the membranes by a non-adsorbing gas (nitrogen of hydrogen). This process then provides valuable information about the structure of the membranes but often leads to unsatisfactory results (Pachtová et al 2003).

Other reported techniques include mercury porosimetry (Jareman et al., 2004) and bubble point technique (Jakobs and Koros, 1997). Although these techniques provided a clear indication of the presence of defects or lack thereof in the above-mentioned cases, they fall short when it comes to asymmetrical membranes (Daramola et al., 2010).

On the other hand, Pachtova and co-workers (2003) described a much easier adsorption-desorption technique for characterizing asymmetrical membranes. This technique involved saturating the membrane with an adsorbing gas such as water or n-butane, after the membranes were subjected to high temperature pre-treatment to remove the moisture, followed by dynamic desorption under a pressure difference of a non-adsorbing gas such as nitrogen or hydrogen.

According to Pachtova and co-workers (2003), during the adsorption process all the pores within the membranes are plugged for all sizes up to what is referred to as “critical dimeter”. Hence, it is at this stage that all the pores opening with the zeolite membranes blocked by the adsorbing gas. The remaining pore openings if present, are due to the intercrystallite defect or cracks within the membranes.

It has been reported that, during desorption processes, any defects that are larger than the “critical diameter” (which thus would not be plugged during the adsorption stage) would present the permeation of the non-adsorbing gas through the membranes (Daramola et al., 2010; Patchtova et al., 2003).

The permeation of the non-adsorbing gas is expected to increase with an increase in time due to desorption of the previously adsorbed gas. This is correlated with the presence of defects and the

quality of the membranes (Pachtova et al., 2003). Thus, poor quality membranes show a high initial permeation which is due to unplugged inter-crystalline pore openings. Ideally, low permeance are expected for high quality membranes.

The single gas permeation measurements, using equation 3.1 and the setup in Figure 3.11, which result from the dynamic adsorption-desorption technique can then provide relatively rapid analysis of the quality of the membranes (Pachtova et al., 2003). This study followed the quality test described by Pachtová et al (2003) to assess the quality of the as-synthesized supported membranes. The tests were conducted for selected membranes which were saturated with n-butane, a strongly adsorbing gas, at 14 KPa for 1 hour.

Desorption of n-butane was carried out under the conditions of nitrogen single gas permeation measurements with a transmembrane pressure of 20 KPa. The dynamic desorption thus observed were correlated to the quality of the membrane (Pachtová et al 2003).

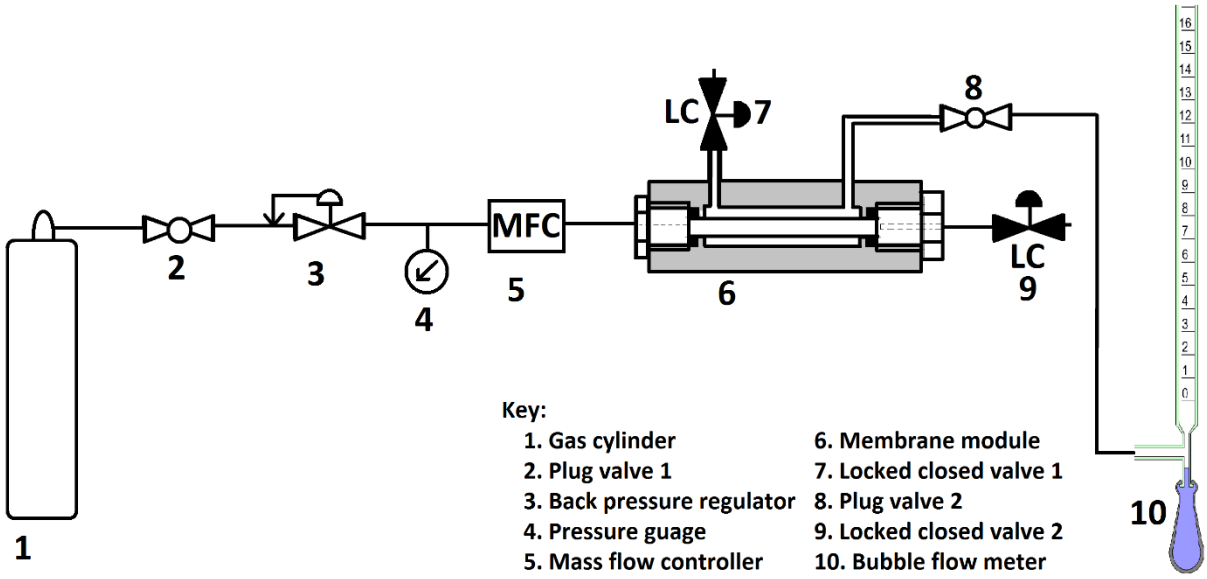


Figure 3.11 Schematic representation of the BDQT experimental setup

### 3.9 Single gas permeation tests

Prior to the pretreatment of the membranes, single gas permeation tests with nitrogen were done by closing all the exit of the membrane module including the sweep gas exit. Thus, the gas is then forced to go through the membrane at a certain pressure. This is done to ensure that the precursor solution plugged all the pores of the supports well.

A well plugged membrane would not have any nitrogen gas permeation since the porosity of the supports should be all occupied by the membranes whose pore would then be blocked by the structure directing agent (TPAOH) at this stage. This procedure is conducted to assess the presence of defects within the membrane. The presence of any defects will result in the permeation of the nitrogen gas. This test was conducted at a pressure of 1.2 bar the lower permeation correlated with a well plugged membrane.

During these tests the molar flux, $N_i$, was then obtained by the following equation:

$$N_i = \frac{V_i}{A} \tag{3.1}$$

Where by $V_i$ is the molar flow rate ($mol.s^{-1}$) and A is the area of the membrane ($m^2$) which is available for permeation.

The permeation was then calculated using the formula:

$$\prod_i = \frac{N_i}{\Delta P_i} \tag{3.2}$$

Where by $\prod_i$ is the pearmeance ($mol.m^{-2}.s^{-1}$), $\Delta P_i$ is the trans-membrane pressure difference (Pa) for a certain gas component *i*.

$$\Delta P_i = P_f - P_p \tag{3.3}$$

Where by $P_f$ is the feed pressure, and $P_p$ is the permeate pressure

**3.10 Gas separation performance**

The membrane separation performances of the membranes were conducted by single gas permeance using $CO_2$ and $N_2$ through the setup depicted in Figure 3.11. The ideal selectivity of the membranes was calculated with the ratio of the permeance of the single gas components. Thus, the selectivity is given by:

$$\prod_{i/j} = \frac{\prod_i}{\prod_j} \tag{3.4}$$

Where *i* is $CO_2$ and *j* is $N_2$.

# Chapter Four

## Nanocomposite SAPO-34/Ceramic Membranes: Synthesis and Characterization

# 4 Nanocomposite SAPO-34/Ceramic membranes: Synthesis, Static and Dynamic Characterization

## 4.1 Introduction

This chapter discusses the results obtained from the synthesis and characterization of the membranes developed in Chapter 3.

## 4.2 Nanocomposite membrane synthesis and characterization

The nanocomposite membranes were prepared by the hydrothermal synthesis method discussed in Chapter 3 (Section 3.3.2). The membranes were synthesised using a single-stage compared with other multi stage synthesis in order to obtain membranes with the highest quality. The as-synthesized crystals were collected from the bottom of the autoclave and characterized using SEM, FTIR spectroscopy, XRD and TGA as discussed in Chapter 3. Similarly, the supported zeolite membranes were also crushed and characterised.

## 4.3 Membrane quality evaluations

The Basic Desorption Quality Test has been reported as an ideal method used to evaluate the quality of the as-synthesized membranes (Pachtova, 2003). As discussed in Chapter 3, The BDQT was used in this study to evaluate the quality of the as-synthesised nanocomposite membranes.

## 4.4 Results and discussion

### 4.4.1 FTIR spectroscopy results

The Chabazite (CHA) cage type structure of SAPO-34 is made up of eight-membered rings and six-membered rings which are interconnected by units of four-membered rings as illustrated in Figure 2.10. The CHA related framework topology has been highly characterized by layers of double six-membered rings which stack in an ABC sequence (Bordiga et al., 2004). The structure has a single unique tetrahedral site with four different oxygen atoms in the asymmetric unit (Bordiga et al., 2004).

The FTIR spectrum illustrated in Figure 4.1 indicates the characteristic SAPO-34 framework vibration and bending peaks which are consistent with CHA related framework that were

reported in literature (Barot et al. 2015; Li et al. 2015). The as-synthesised SAPO-34 crystals showed a good agreement with the previously published data ( Barot et al., 2015; Li et al., 2015; Masoumi & Towfighi, 2015).

The FTIR spectroscopy data, summarised in Table 4.1, shows an absorption peak at 1500 – 1100 $cm^{-1}$ which is ascribed to the asymmetric stretch of T–O tetrahedral. Masoumi & Towfighi (2015) reported that the T-O bending tetrahedral at 1100 $cm^{-1}$ is specifically due to the asymmetric O-P-O. The peak observed a 730 $cm^{-1}$ corresponds to the symmetric stretch of T–O tetrahedral due to O-P-O (Masoumi & Towfigi, 2015). The peak at 680 $cm^{-1}$ is due to the bend vibration of the double 6-rings (D6R). The peaks from 600 – 550 $cm^{-1}$ are due to the bending vibration of the T–O tetrahedral attributed to $PO_4$, $AlO_4$ and $SiO_4$.

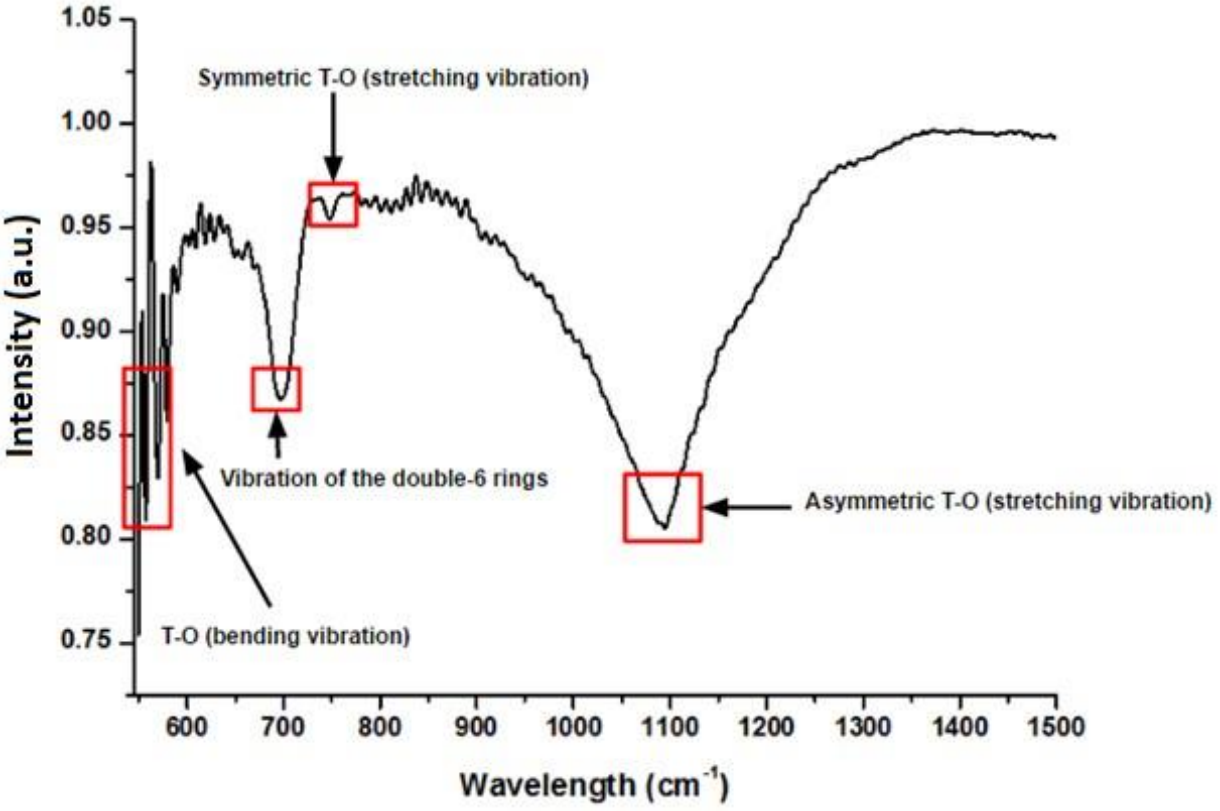


Figure 4.1 FTIR spectrum of the SAPO-34 crystals

Table 4.1 FTIR functional group identification and interpretation

| **Functional group** | **Wavelength** | **Attribute** |
|---|---|---|
| T-O (T=Al, Si, P) | 550-600 $cm^{-1}$ | Bending vibration T-O tetrahedral |
| D6R | 680 $cm^{-1}$ | Bending vibration of the Double 6-rings |
| T-O (T=Al, Si, P) | 730 $cm^{-1}$ | Symmetric stretching of T-O tetrahedral |
| T-O (T=Al, Si, P) | 1050-1100 $cm^{-1}$ | Asymmetric stretch of T-O tetrahedral |

### 4.4.2 TGA analysis

The TGA profile of the calcined crystals shown in Figure 4.2 displayed two major weight losses which were expected. The initial weight loss of 5 % below the 100 °C temperature region was due to the endothermic desorption of water/moisture which was adsorbed on the surface of the crystals. The second weight loss of about 6.5 % is attributed to the resistance of the structure to collapsing at high temperature. The high thermal stability is consistent with the profiles reported in open literature (Barot et. al. 2015; Das et. al. 2012).

However reported profiles show three major weight losses two of which are consistent with the one observed in the profile below. The third weight loss is due to the loss of the template or structure directing agent at temperatures above 350 – 500 °C. The third weight loss is not observed here as the template was removed by calcination prior to TGA analysis. Consequently, the as-synthesized crystals showed a high thermal stability.

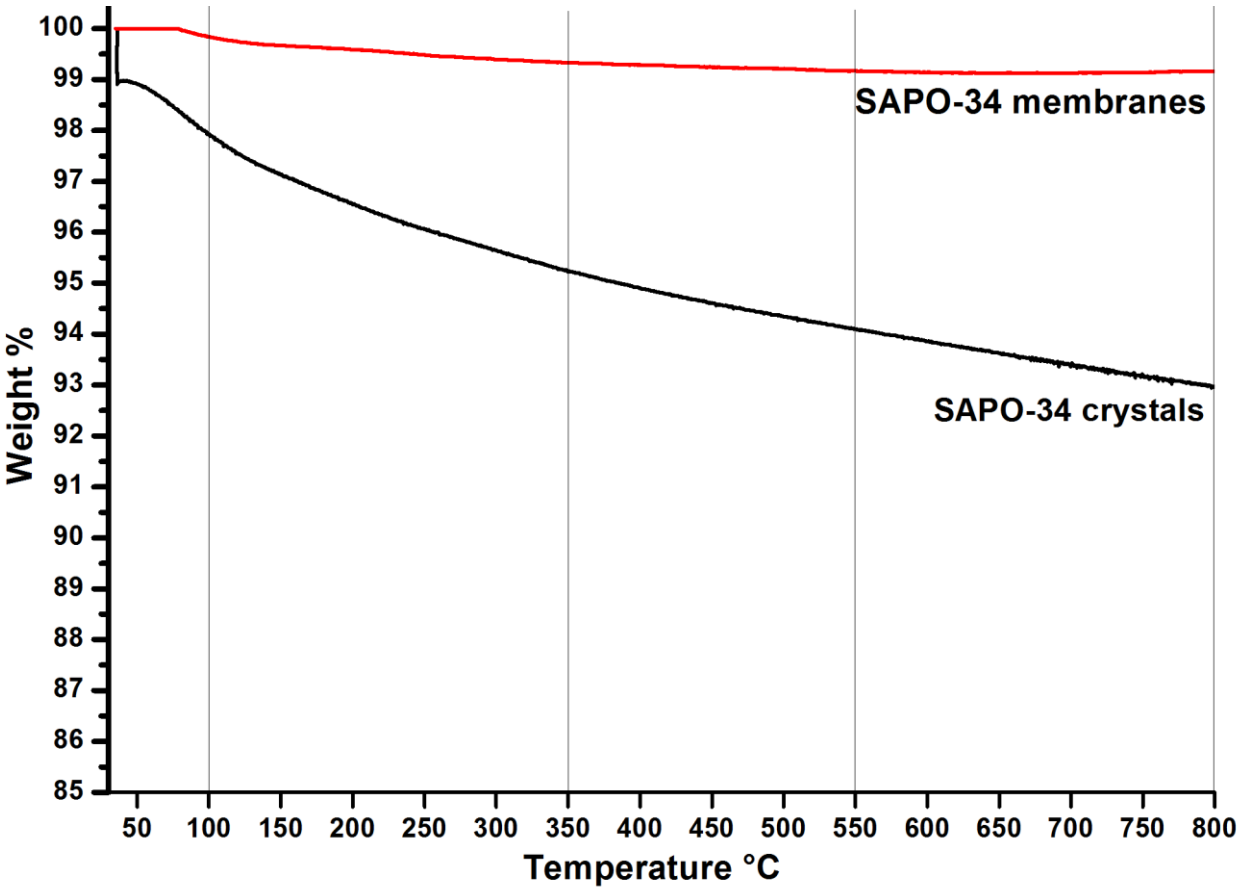


Figure 4.2 TGA profiles of the as-synthesized SAPO-34 crystals and membrane

### 4.4.3 XRD analysis

The XRD pattern of the SAPO-34 molecular sieves that were synthesised at 150 °C for 6 hours along with the international zeolite association (IZA) database reference pattern are shown in Figure 4.3. The XRD pattern of the crushed supported zeolite membrane was crushed and the XRD of the supported membranes is shown in Figure 4.4. In both Figure 4.3 and Figure 4.4 the XRD patterns for the SAPO-34 materials corresponds to the CHA-structure reported in the literature (Askari et al., 2016; Li et al., 2006; 2008; 2010; 2015; Prakash et al., 1994; 1999).

The XRD pattern of the as-synthesized crystals shown in Figure 4.4 displays the typical characteristic peaks corresponding to SAPO-34 with a CHA-structure. The 2θ = 20.6, 22.49, 25.9, 30.6 and 50 corresponds to the XRD peaks indexed by Charghand et al. (2014) to (1 2 -1), (1 0 4), (2 2 0), (4 0 1) and (0 1 8) respectively as phases of a rhombohedral phase of SAPO-34. The XRD pattern of the as-synthesized SAPO-34 had intense sharp peaks which indicated a

suitable degree of crystallinity of the as-synthesized SAPO-34 crystals. These particular peaks were consistent with the SAPO-34 peaks reported in literature (Barot et al., 2016; Li et al., 2006; 2008; 2010; 2015; Liu et al., 2008; Prakash et al., 1994).

However, the absence of other peaks below the 2θ value of 20.6 can be attributed to the short synthesis time as well as the relatively low synthesis temperature (Tian et al., 2011). In the study by Tian and co-workers who studied the effects of low synthesis time on the crystal structure, the missing peaks start to re-appear as time increases. The short synthesis time and the low temperature which were employed are essential in quest for energy efficient synthesis techniques.

Figure 4.4 shows the presence of the characteristic peaks of SAPO-34, revealing that SAPO-34 was successfully embedded in the alumina support. The intensities of the SAPO-34 are significantly lower than those of the alumina support which is likely due to the low amount of the SAPO-34 content in the support.

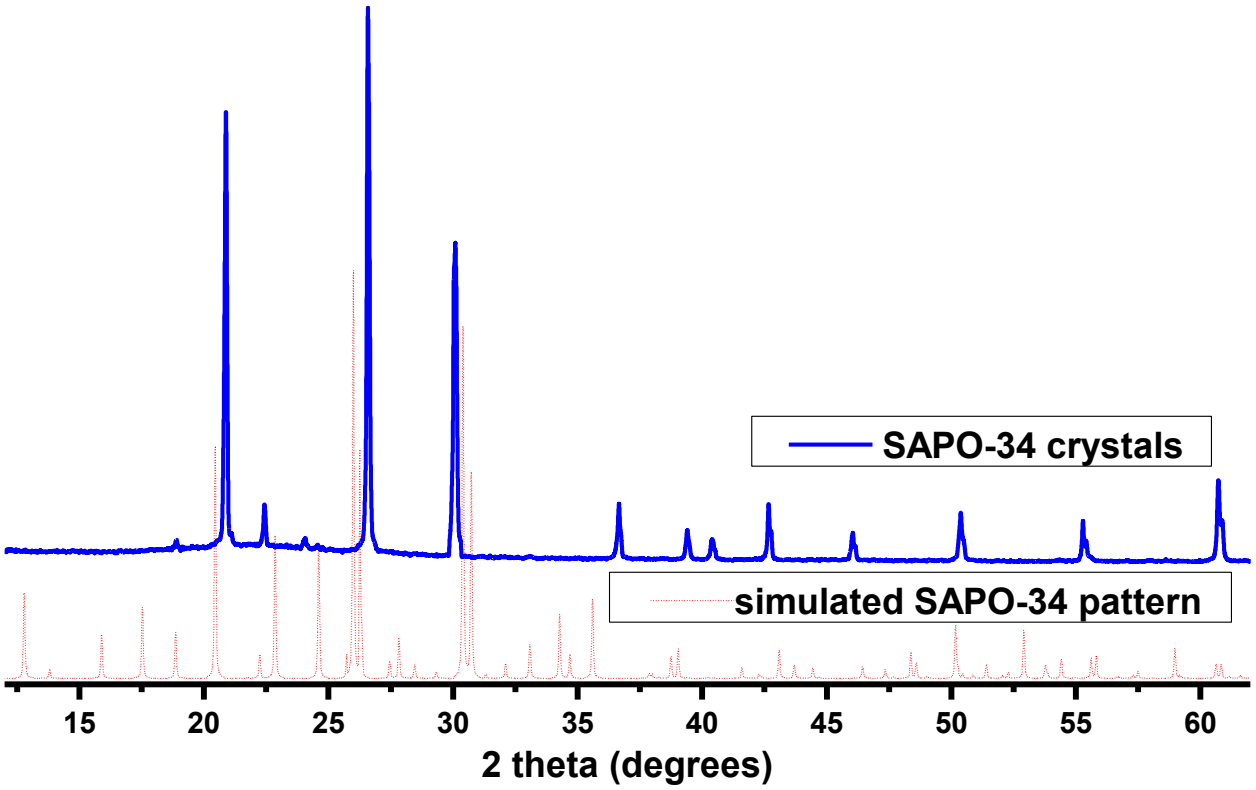


Figure 4.3 XRD patterns of the as-synthesized SAPO-34 compared with the simulated XRD pattern

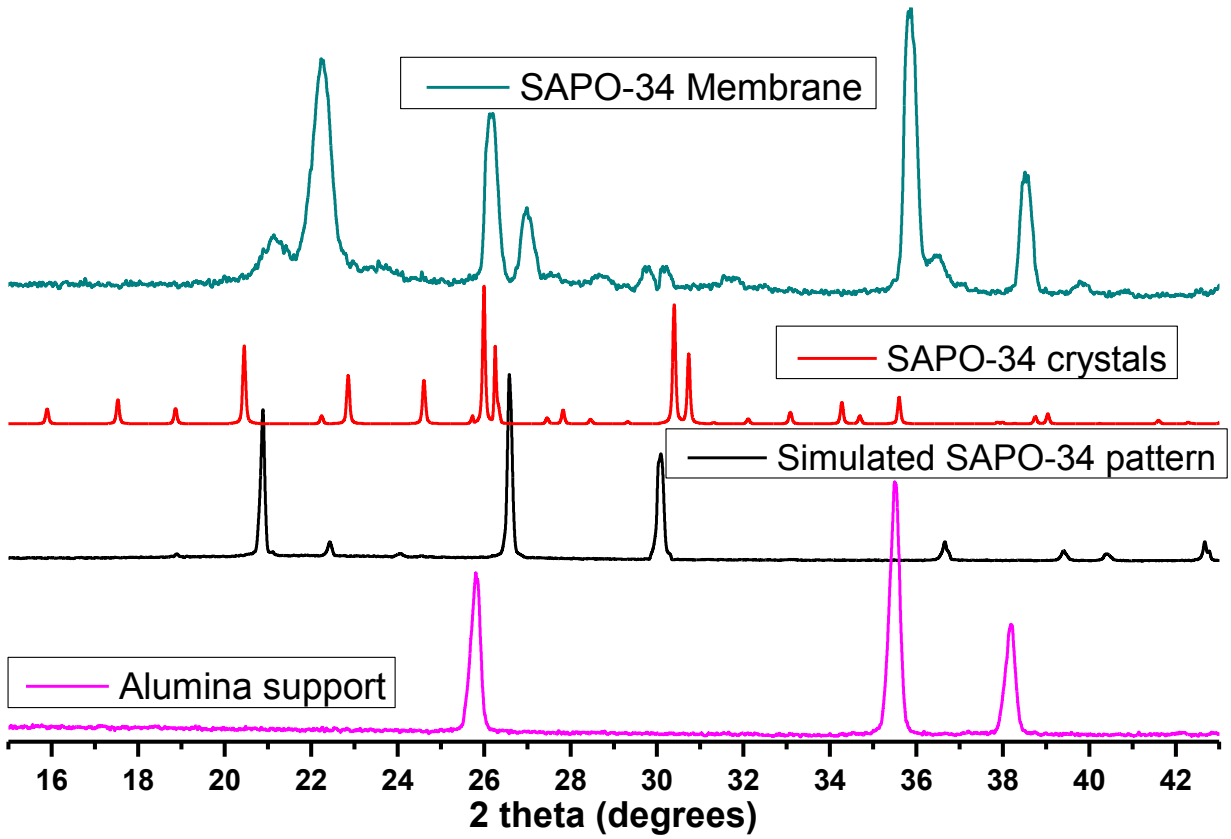


Figure 4.4 XRD patterns of the as-synthesized SAPO-34 crystals compared with the α-alumina support, supported zeolite membranes as well as the simulated XRD pattern.

### 4.4.5 SEM analysis

The SEM micrograph illustrated in Figure 4.5 shows a cubic structure of the SAPO-34 crystals. The expected crystal morphology expected was rhombohedral as per XRD crystal phase indices analysis. However, the cubic morphology is consistent with the micrographs reported in literature for a short synthesis time (Ghavipour et. al., 2016; Li et al., 2004; 2006; 2010; Najafi et al., 2014; Prakash et al., 1994; 1999). The SEM micrographs further confirms the formation of SAPO-34 crystals with an average crystalline size of approximately 2 μm from the 6 hour synthesis time.

It was initially reported by Prakash and co-workers (1994) that longer synthesis times and high temperatures result in an enhanced crystalline growth. In their study the synthesis time was varied to about 48 hours. However, they did not focus on lower synthesis temperatures. In this study, the smaller cubic morphology is ideal for the nanocomposite membranes within the pores of the supports.

Figures 4.6 shows the inner side of the thin-film membrane which was synthesized without any interruption time for comparison purposes. The morphology of the SAPO-34 observed in this case maintained the cubic structure. Figure 4.7 shows the typical EDS analysis of the surface crystals. The analysis were performed locally which resulted in an indication of elemental composition of the as-synthesized SAPO-34 crystals. The EDS results were consistent with the elemental percentages reported in literature (Charghand et al. 2014).

Figure 4.8 illustrates the SEM image of the cross-section from the nanocomposite membranes. From the image, it can be seen that the SAPO-34 membranes were grown throughout the three asymmetric layers of the supports. This further proves that the pore-plugging hydrothermal synthesis was successful. Figure 4.8 and Figure 4.9 illustrate the SEM images of the inner and the outer side of the nanocomposite membranes. From this images, it can be clearly established that there is a high presence of uniformly inter grown zeolite crystals covering the pores of the supports on both sides. Figures 4.10 – 4.13 shows an image of what appears to be zeolite crystals grown within 12 μm pore of the support. This further supports the success of the pore plugging hydrothermal synthesis.

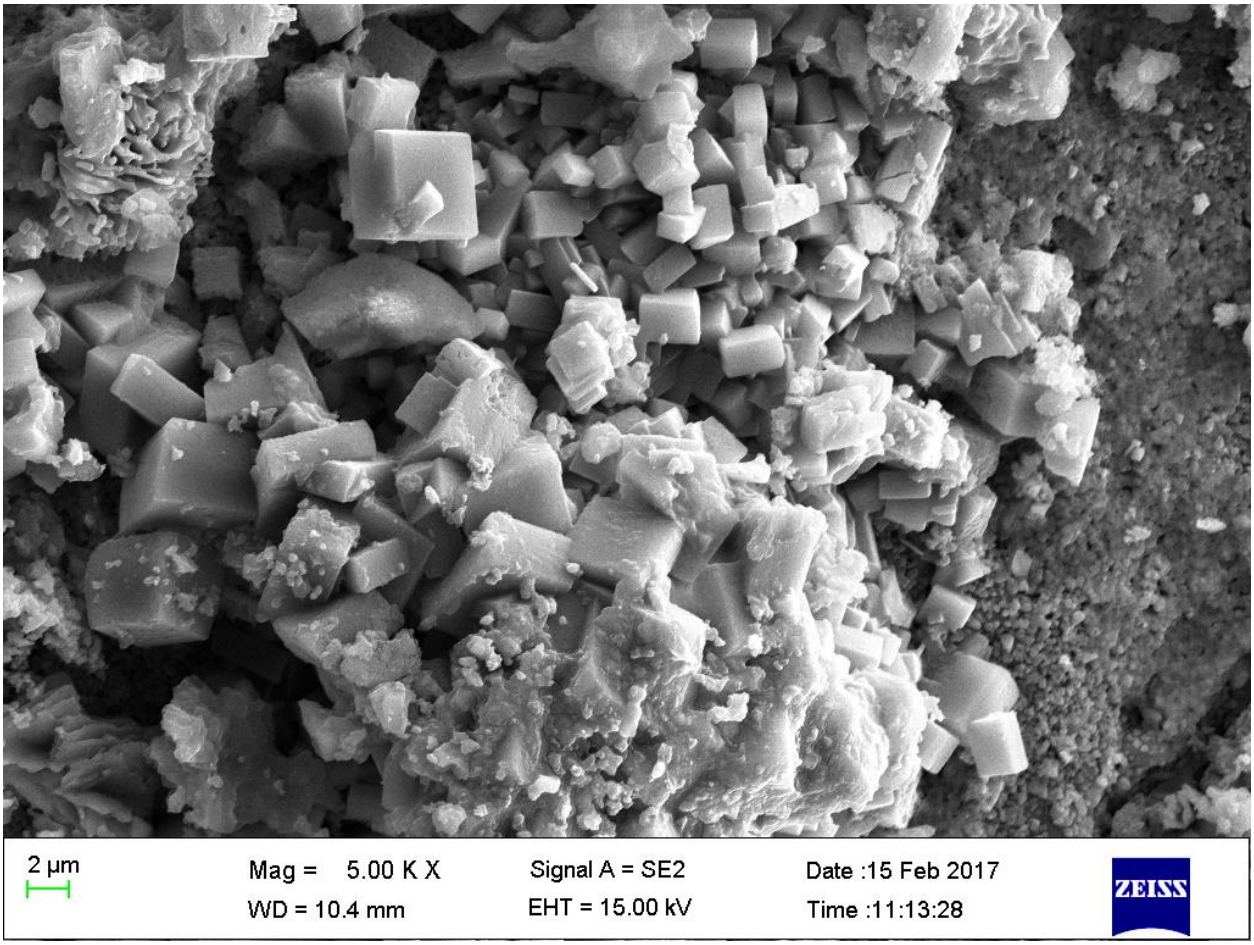


Figure 4.5 SEM image of the as-synthesized SAPO-34 crystals

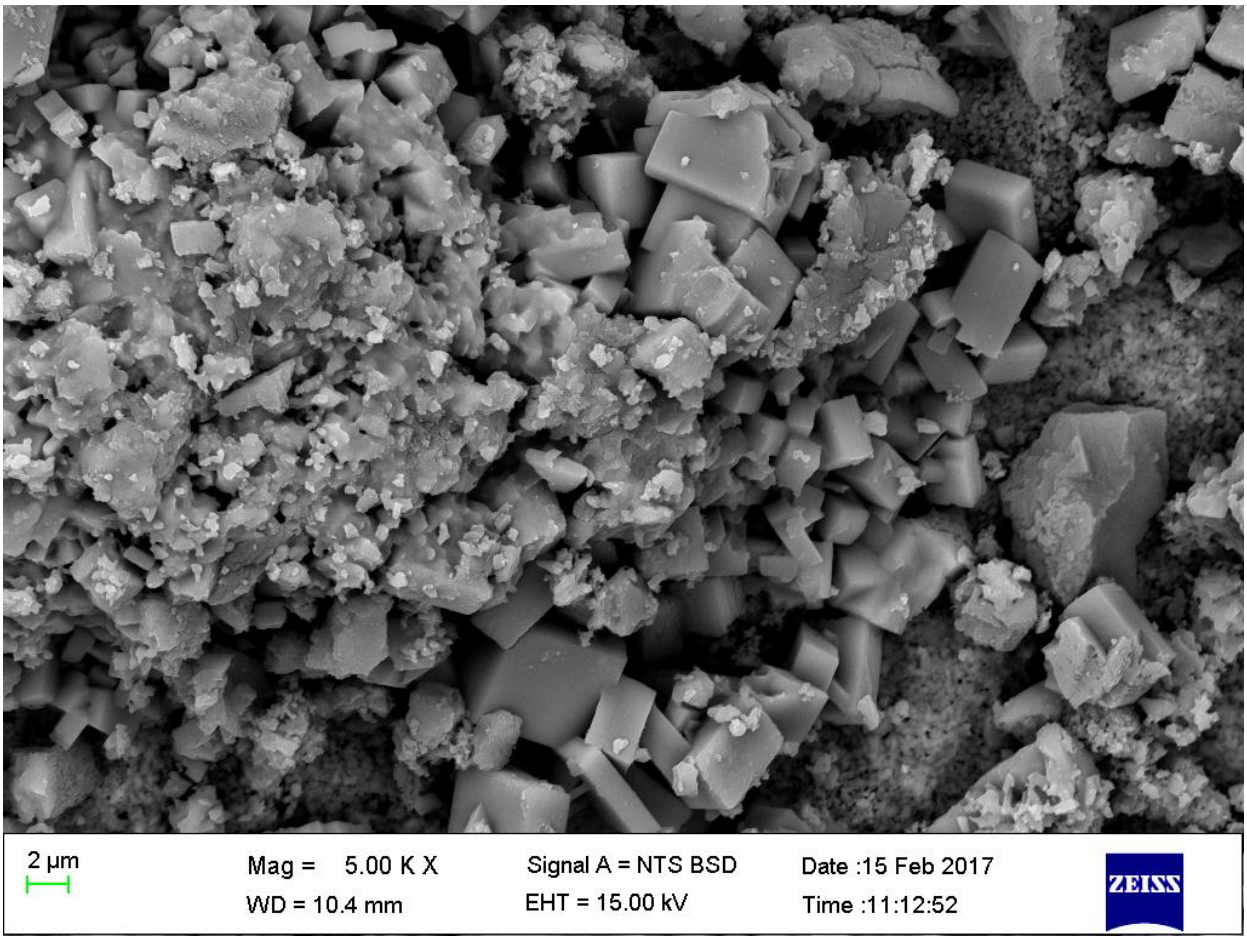


Figure 4.6 SEM image of the inner side of the thin-film membrane

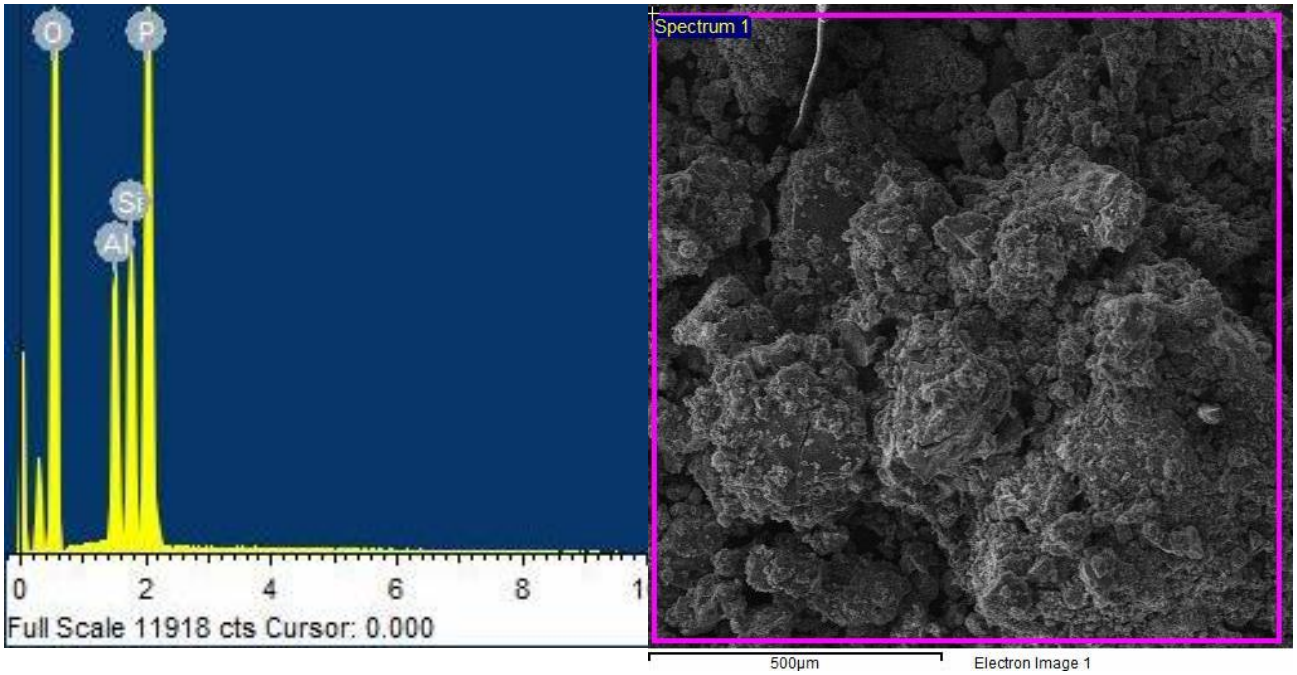

Figure 4.7 SEM-EDS spectrum of the as-synthesized SAPO-34 crystals

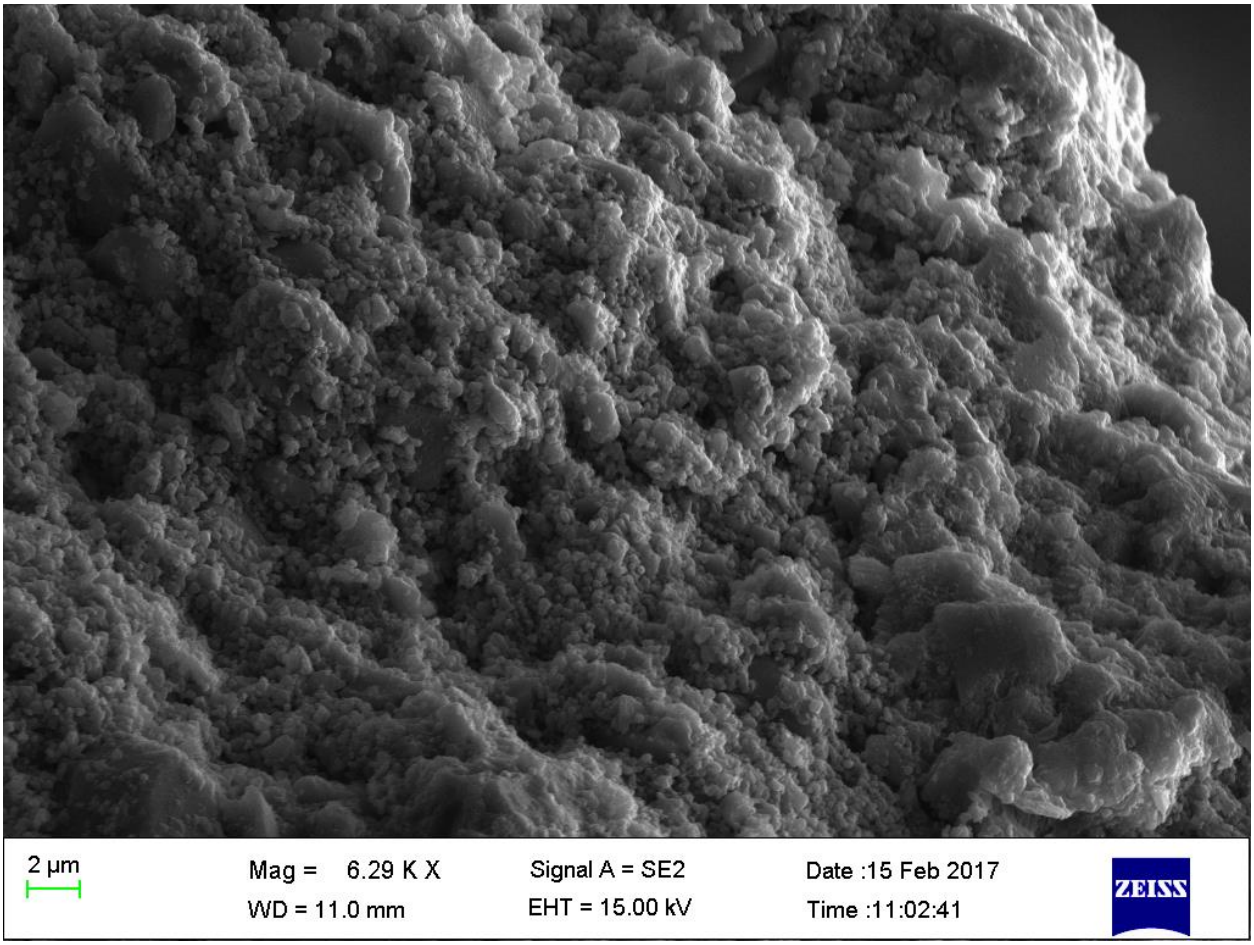

Figure 4.8 SEM image of the cross cut layers of the asymmetric support showing the presence of nanocomposite membranes within the support

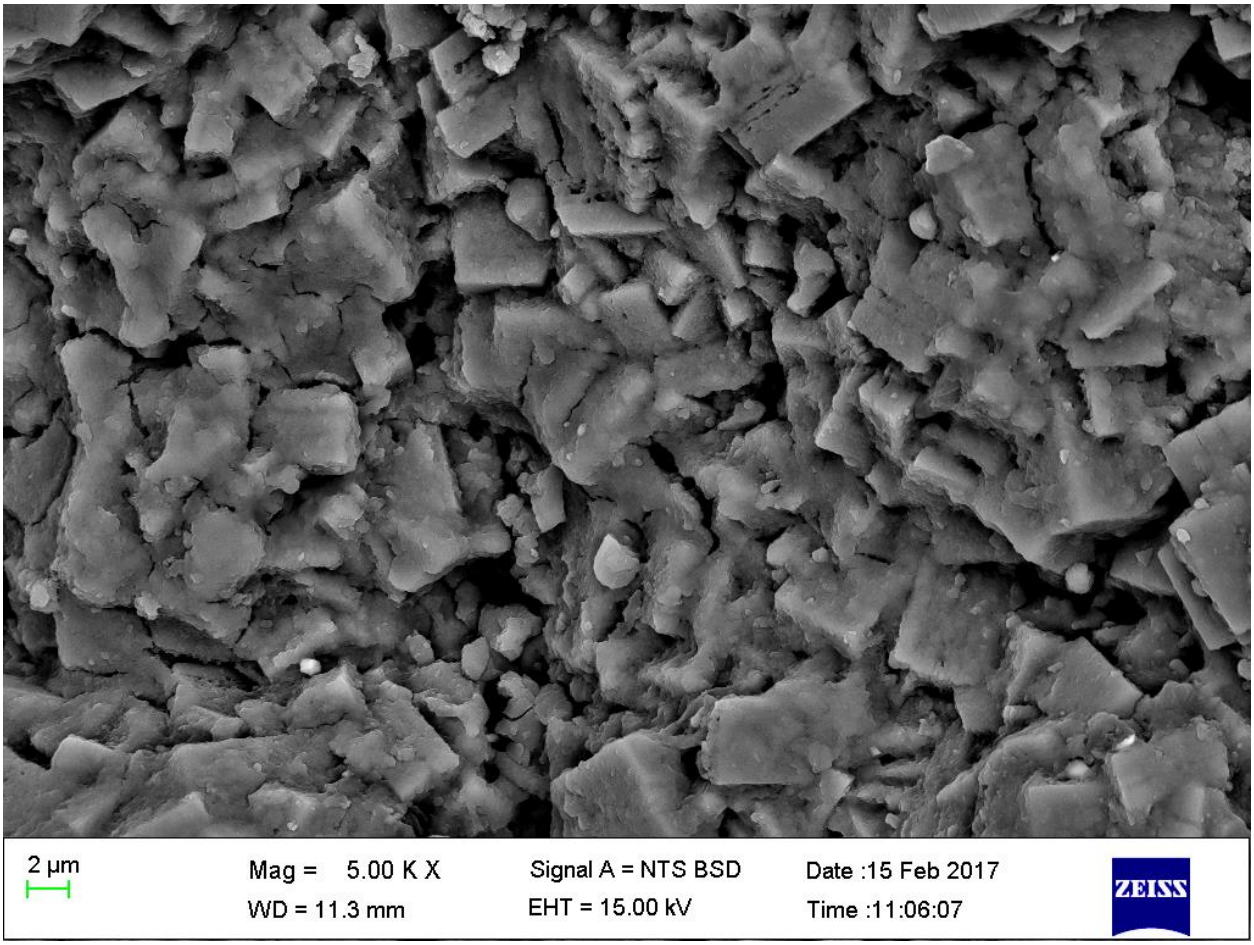

Figure 4.9 SEM micrograph of the outer layer of the nanocomposite support

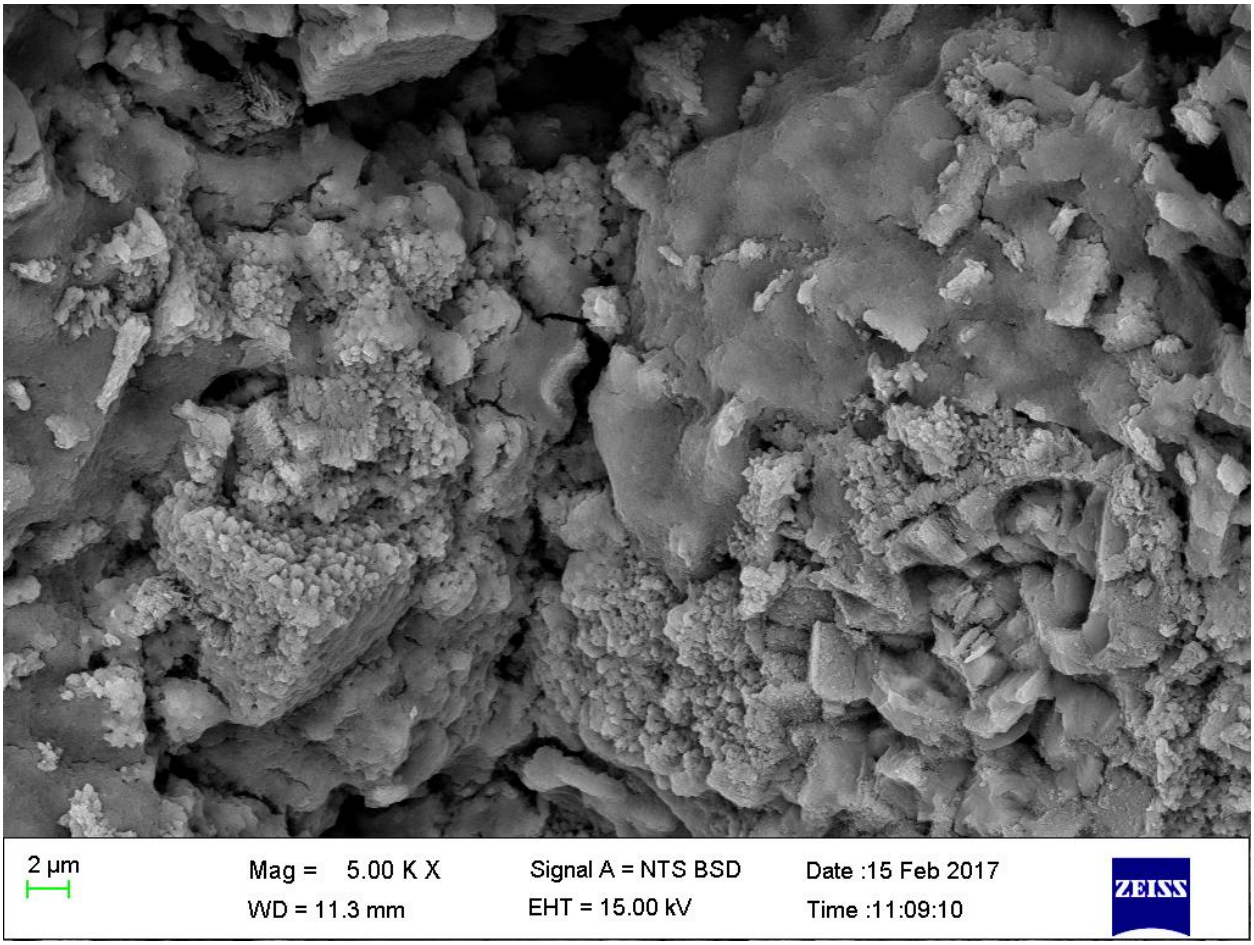

Figure 4.10 SEM image of the inner side of the tubular membrane

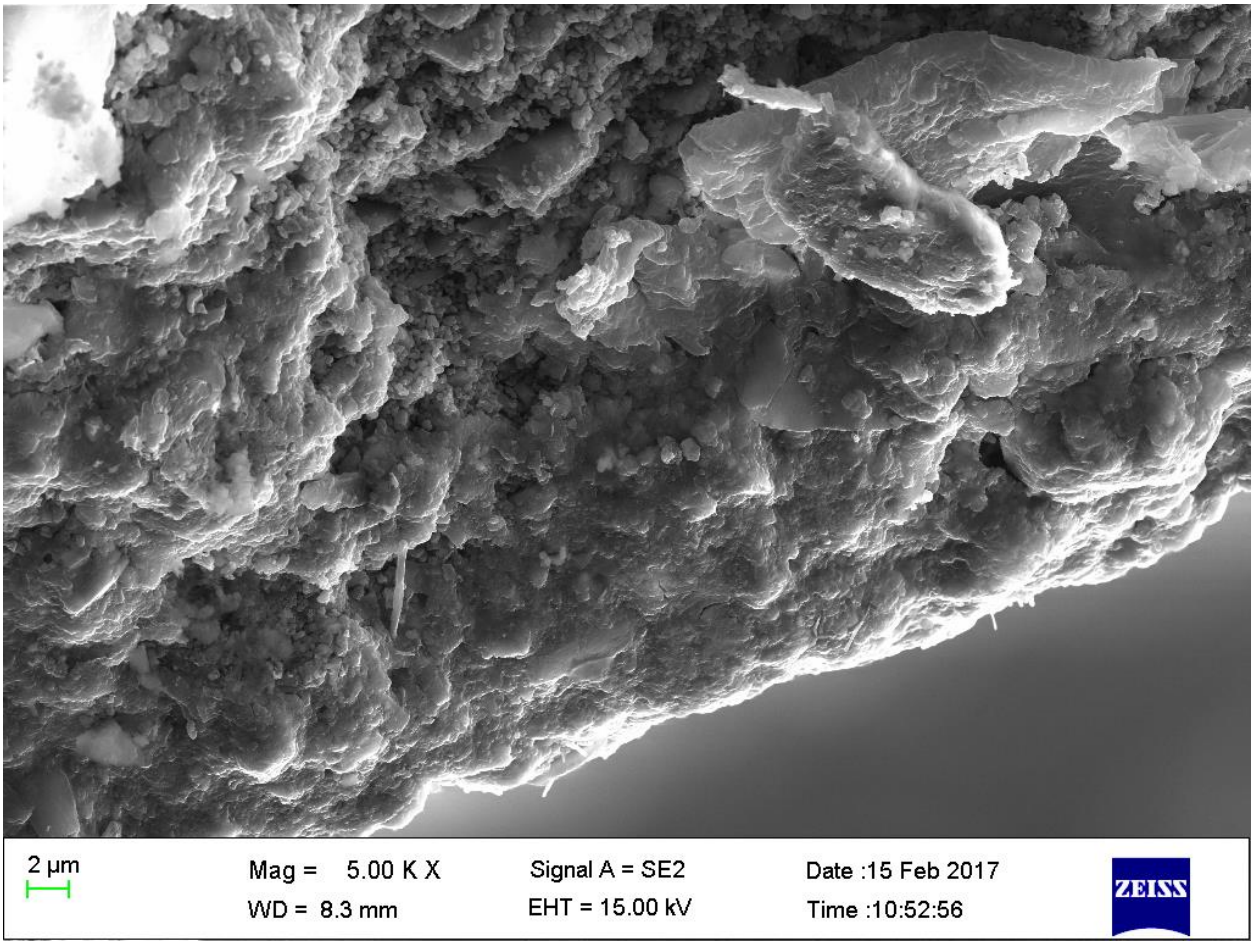

Figure 4.11 SEM image highlighting how the crystalline material grows into the support

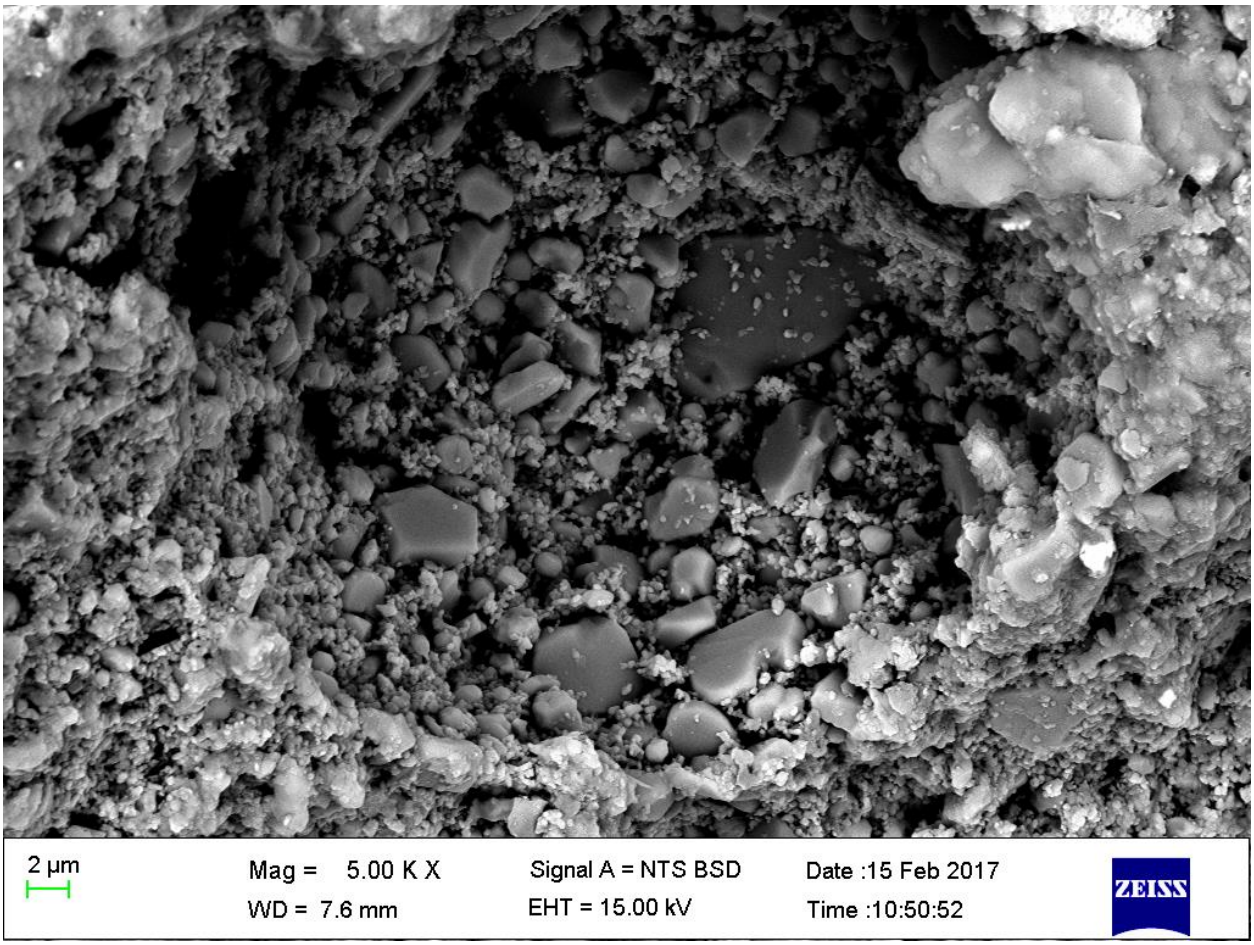

Figure 4.12 SEM image of the SAPO-34 crystals growing through the outer 1200 nm outer pores

### 4.5 Basic Desorption Quality Test

To assess the quality of the as-synthesized supported membranes, basic desorption quality tests (BDQT) were conducted as previously reported (Pachtová et al 2003). According to the procedure described by Pachtová and co-workers (2003), the BDQT tests were conducted for selected membranes which were saturated with n-butane, a strongly adsorbing gas, at 14 KPa for 1 hour. Desorption of n-butane was carried out under the conditions of nitrogen single gas permeation measurements with a transmembrane pressure of 20 KPa. The dynamic desorption thus observed were correlated to the quality of the membrane (Pachtová et al 2003).

For comparison purposes, the BDQT results from membranes that showed a high permeance (M1, M2, M3 and M4) are plotted in Figure 4.13. On the other hand the membranes that exhibited higher quality (M6, M7 and M8) demonstrated with low permittivity. M9 showed a

high permeance because it was a single stage synthesis with two interruptions. M9 has similar quality with M2 which had a single interruption. This shows that the two interruptions do not improve the quality of the membrane.

The thin-film membrane and nanocomposite membranes with fewer multistage synthesis (M2, M3 & M4) showed poor quality as compared to the pore-plugged nanocomposite membranes. The BDQT results of selected membranes showed repeating of the synthesis procedure results in membranes with a better quality.

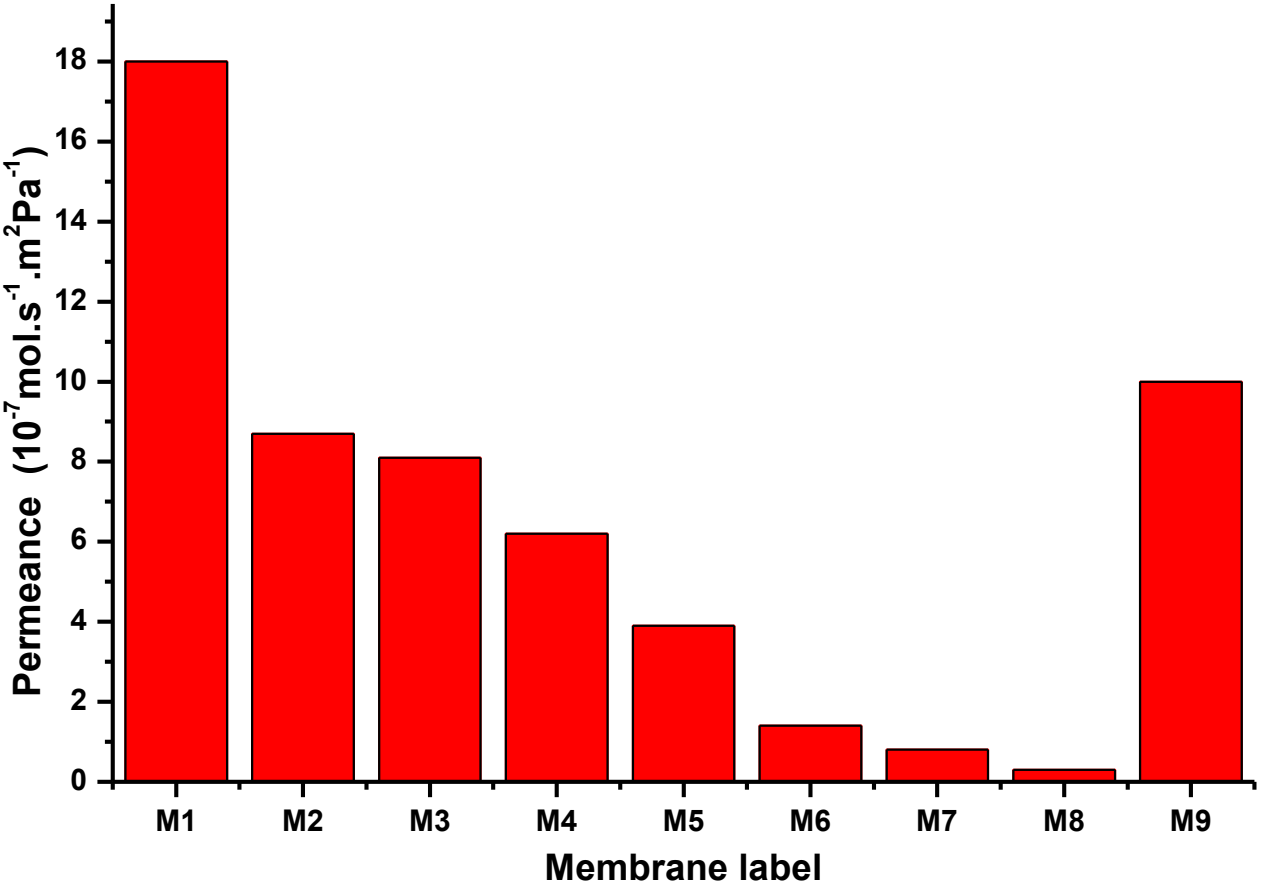


Figure 4.13 BDQT results of selected membranes (M1 - M9). Experimental conditions: Temperature: room-temperature; Transmembrane pressure (TMP): 20kPa; Permeation time: 5 minutes; Active permeation area: 26 $cm^2$

**4.6 Concluding remarks**

The synthesis and characterization of SAPO-34 crystals conducted by the pore-plugging hydrothermal synthesis. The static characterization techniques (FTIR spectroscopy, TGA, XRD and SEM-EDS) results revealed that SAPO-34 crystals were obtained at low temperatures (150 °C) with a short synthesis time (6 h). The cubic crystalline morphology were formed as a result

of the synthesis conditions which favour the very initial stages of the SAPO-34 crystal formation. The FTIR spectrum shows the formation of the D-6 rings which are essential in the complete formation of the CHA framework type SAPO-34 crystal structure. The XRD pattern confirmed the formation of the CHA framework with matching indexed crystal phases. In addition, the TGA analysis confirms a high thermal stability of the as-synthesised SAPO-34 crystals. The thermal stability is essential for high temperature applications such as the intended post combustion carbon capture. In addition, the BDQT revealed that the longer the time it takes for nitrogen to permeate through, the fewer the presence of intercrystallite defects and cracks in the membranes. Moreover, the multi stage synthesis was found to improve the quality of the membrane.

# Chapter Five

## $CO_2/N_2$ Separation Performance of Nanocomposite SAPO-34/Ceramic Membranes

# 5 Nanocomposite ceramic/SAPO-34 membranes: the effects of operating conditions on the separation performance

## 5.1 Introduction

This chapter discusses the results obtained from evaluating the effects of operating variables on the separation of $CO_2$ from $CO_2/N_2$ mixtures using the single gas permeation methods discussed in Chapter 3. However, only the membrane, M8, was used as it showed the highest quality compared to the other membranes. The separation analysis were conducted using the dead-end mode and the flow rate was measured using the bubble flow meter as illustrated in Figure 3.11. The resulting flux, permeance and ideal selectivity were calculated using Equations 3.1, 3.2 and 3.3 respectively.

## 5.2 Results and discussion

### 5.2.1 Error analysis in measured values

The reliability of the experimental results discussed in this chapter can be ensured by taking into consideration the accuracy and repeatability of the obtained and calculated experimental data. However, the data was prone to errors. For instance, the source of errors include and not limited to;

I. Reading of mass flow meters and pressure gauges,
II. Reading the flow rate on the bubble flow meter, and
III. Handling errors during the experimental procedure.

These errors associated with measuring values manually may have resulted in uncertainties in the calculated values which were permeance, ideal selectivity and flux in this case. Moreover, errors associated with the fluctuations in experimental conditions as well as changes in environmental condition were very difficult to quantify. These errors might account for up to 10% of the errors in the calculated values.

### 5.2.2 Single gas permeation tests through the SAPO-34 membranes

The pure gas permeation tests were initially conducted with $N_2$ gas before calcination process to assess presence of unplugged pores. Plugged pores would not result in any permeance. This is as a result of the pore of the supports being blocked zeolites whose pores were blocked by the

template. Thus, uncalcined membranes displayed lower permeance compared to the calcined counter parts.

Calcination unblocks the pores of the zeolite membrane by removing the template incorporated in the zeolite during the synthesis stage. Eight zeolite membranes (labelled M1-M8) were subjected to single gas permeation tests. In this study membrane M1 showed a high permeation for both $N_2$ and $CO_2$ which were 36.12 $x10^{-7}$ $mol.s^{-1}.m^2.Pa^{-1}$ and 37.56 $x10^{-7}$ $mol.s^{-1}.m^2.Pa^{-1}$ respectively with an ideal selectivity of 1.04. The results may be attributed to the smaller kinetic diameter of $CO_2$ (0.33 nm) passing through the pores of SAPO-34 membranes (0.38 nm) easily compared to the slightly bigger $N_2$ (0.36 nm).

In a study by Li and co-workers (2010; 2012), it was reported that SAPO-34 has a relatively higher affinity for $CO_2$ than $N_2$, resulting in preferential adsorption and diffusion of $CO_2$ through the membranes. Transports across porous SAPO-34 membranes has can described as either, molecular sieving, Knudsen diffusion or surface diffusion (Caro & Noack, 2012; Li et al., 2010).

The high permeance for $CO_2$ and $N_2$ observed in this study at ambient temperatures was expected for thin-film SAPO-34 membranes as reported by Li and Fan (2010). Thin-film membranes often result in poor quality when synthesized using the in-situ hydrothermal synthesis as which was the case in this study (Miachon et al., 2007; 2008). Moreover, the short synthesis time may have resulted in poor interaction between the support surface and the zeolite membranes resulting in defect formation.

It was established that the short synthesis time may led to the formation of non-zeolite pores in Thin-film membranes which resulted in the low $CO_2/N_2$ selectivity (Li & Fan; 2010). These defects where found to be minimised in the nanocomposite membranes (Bernal et al., 2012; Miachon et al., 2006; 2007; Daramola et al., 2008; 20012).

The single stage pore-plugging synthesis conducted on membranes M2 did not significantly improve both the single gas permeance and the selectivity. The permeance was reduced slightly to 10.73 $x10^{-7}$ $mol.s^{-1}.m^2.Pa^{-1}$ for $N_2$ and 12.85 $x10^{-7}$ $mol.s^{-1}.m^2$. $Pa^{-1}$ for $CO_2$ with an ideal selectivity increasing slightly to 1.20. This was due to the pores of the supports being plugged to a minor extent. Thus, multi stage synthesis were required in order to obtain desired permeation and selectivity for the short synthesis time used in this study. Figure 5.1 illustrates the relation

between an increase in the number of synthesis stages and a decrease in permeance of both $CO_2$ and $N_2$. This may be due to the improvement of the pore-plugging protocol which results in more pores being plugged.

Table 5.1 shows that at ambient temperatures $CO_2$ has a high permeation across all the membranes. This is attributed to the smaller kinetic diameter resulting in faster diffusion (Li & Fan; 2010). Appreciable permittivity which resulted in acceptable selectivity was obtain from membranes after the seventh synthesis stage. The permeance for $N_2$ and $CO_2$ then dropped significantly to 0.31 $x10^{-7}mol.s^{-1}.m^2.Pa^{-1}$ and 2.44 $x10^{-7}$ $mol.s^{-1}.m^2.Pa^{-1}$ respectively. The resulting improvements in the single gas permeances led to the ideal selectivity being increased to 8. The observation comes as a result of less presence of defects in the nanocomposite membranes.

The non-zeolite openings experienced previously were now all covered up with the zeolite membranes. Thus, the gases were passing through mostly the small zeolite pores. Figure 5.1, Figure 5.2 and Figure 5.3 illustrate how the improvement in the pore-plugging protocol by multiple synthesis stages resulted in an improvement of the single gas permeance, lower flux and higher ideal selectivity, respectively.

Table 5.1 Room temperature single gas permeation properties

| **Membrane** | **No. of synthesis stages** | **Permeance [$10^{-7}$ $mol.s^{-1}.m^2Pa^{-1}$]** | | | **$CO_2/N_2$ selectivity $\alpha_{i/N2}$** |
|---|---|---|---|---|---|
| | | $N_2$ before calcination | $N_2$ after calcination | $CO_2$ after calcination | |
| M1 | 1 (thin-film) | 21.46 | 36.12 | 37.56 | **1.04** |
| M2 | 1 | 8.94 | 10.73 | 12.85 | **1.20** |
| M3 | 2 | 7.25 | 8.01 | 12.09 | **1.51** |
| M4 | 3 | 6.92 | 7.4 | 14.578 | **1.97** |
| M5 | 1 (2*interruptions) | 9.2 | 12.65 | 13.18 | **1.042** |
| M4 | 4 | 6.92 | 5.4 | 12.42 | **2.3** |
| M6 | 5 | 0.94 | 1.63 | 4.564 | **2.8** |
| M7 | 6 | 0.57 | 0.829 | 2.36 | **4.05** |
| M8 | 7 | 0.011 | 0.31 | 2.44 | **7.87** |

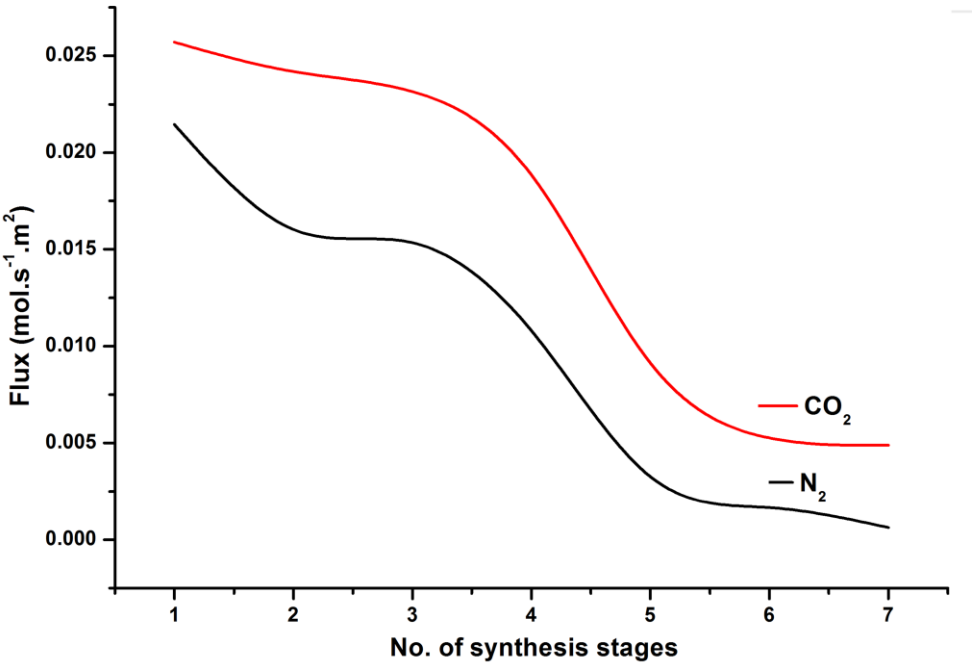


Figure 5.1 Membrane flux variation as a function of no. of synthesis stages. Experimental conditions: Temperature: room-temperature; Transmembrane pressure (TMP): 20kPa; Active permeation area: 26 $cm^2$

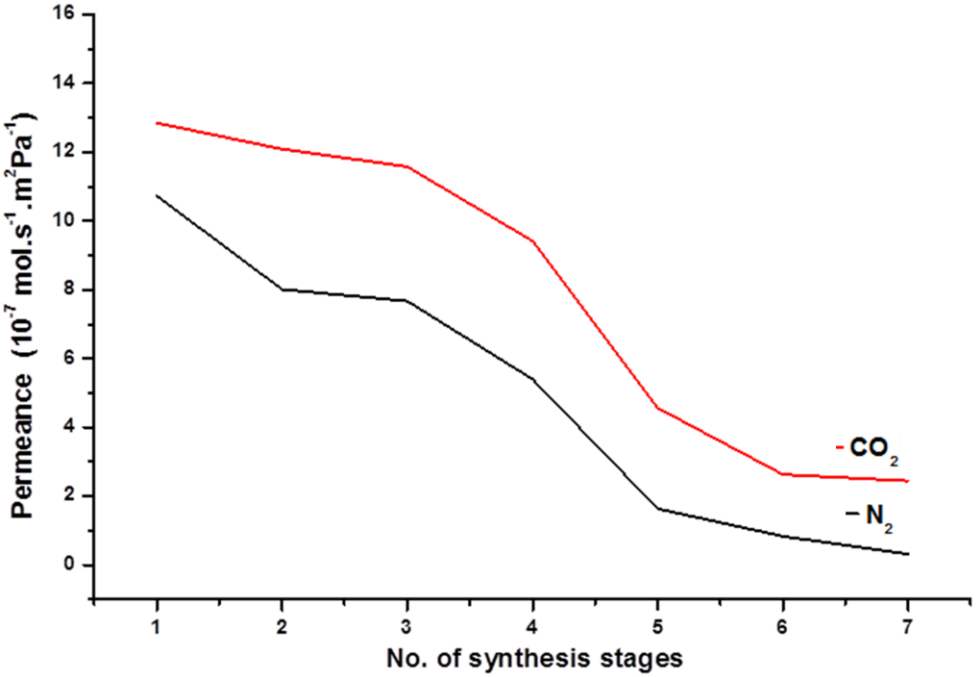


Figure 5.2 Single gas permeance as function of number of synthesis stages. Experimental conditions: Temperature: room-temperature; Transmembrane pressure (TMP): 20kPa; Active permeation area: 26 $cm^2$

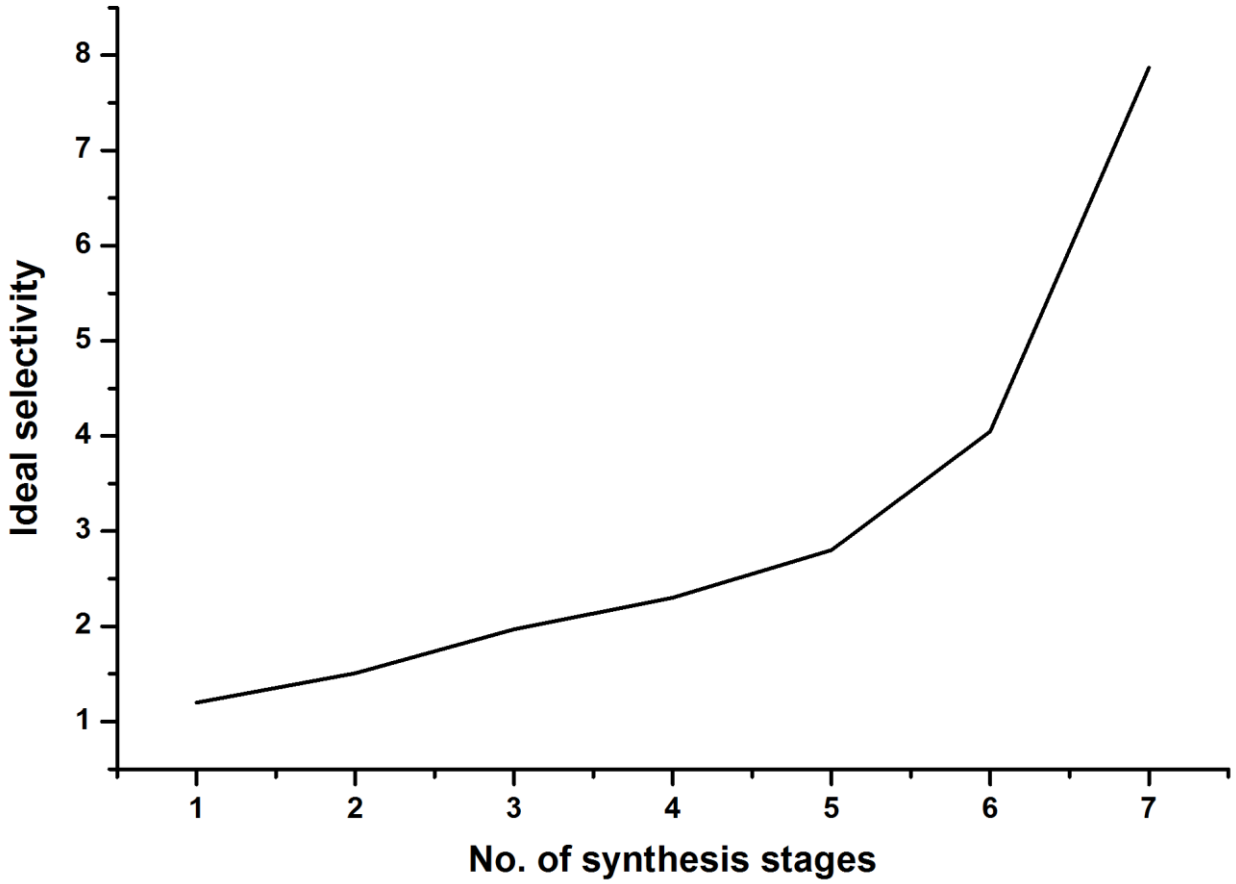


Figure 5.3 Ideal selectivity as a function of no. of synthesis stages. Experimental conditions: Temperature: room-temperature; Transmembrane pressure (TMP): 20kPa; Active permeation area: 26 $cm^2$

**5.3 Comparison of obtained results to selected zeolite membranes reported in literature**

Various type of zeolite membranes classified either as small-pore, medium-pore and large-pore have been reported for $CO_2/N_2$ gas separation studies (Li et al., 2010, Miachon et al., 2006; 2007; Yang et al., 2008). Table 5.2 provides a summary of the comparison of $CO_2$ permeance and ideal selectivity from this study with the results reported in the literature. Kusakape and his co-workers (1997) studied the separation of $CO_2$ and $N_2$ using FAU/alumina tube membranes (0.74 nm pore opening diameter).

The $CO_2$ permeance reported in this study was 0.4 - 3 $x10^{-7}$ $mol.m^{-2}.s^{-1}.Pa^{-1}$ and the selectivity was 20 at 30 °C for a 1:1 $CO_2/N_2$ mixture separation. Although the pore opening diameter for FAU (0.74 nm) zeolite membranes is significantly higher than that of SAPO-34 (0.38 nm), the $CO_2$ permeance are in a similar range.

Gou and his co-workers (2006) reported a permeance of 7.0 $x10^{-7}$ $mol.m^{-2}.s^{-1}.Pa^{-1}$ and a selectivity of 68 using ZSM-5 (MFI type structure, 0.55 nm pore opening diameter) membranes at room temperature. In these cases, $CO_2$ and $N_2$ are significantly smaller than the pore opening diameters of the membranes. Thus, separation in these membranes was achieved by competitive adsorption and not by the common molecular sieving methods (Li & Fan, 2010).

In cases such as the above mentioned ones whereby the pore opening diameter and the kinetic diameters of $CO_2$ and $N_2$ had a considerable difference, the Monte Carlo model was one of the simulation used to predict the $CO_2/N_2$ separations (Li & Fan, 2010; Ohtaa et al., 2007). It was found that zeolite membranes with smaller pore diameters had larger adsorption sites as well as a high connectivity of the pores resulting in higher $CO_2/N_2$ selectivity (Li & Fan, 2010; Ohtaa et al., 2007). However, these findings contradicted with the study by Zhou and co-workers (2007) who reported a selectivity of 6.0 for NaA membranes (0.42 nm pore opening diameter). Moreover, in this study an ideal selectivity of 7.86 was observed using SAPO-34 membranes which have a much smaller pore opening diameter of 0.38 nm. As a result the Monte Carlo simulation model was not the ideal method for interpreting the trend in the selectivity as compared to the pore opening diameter of zeolite membranes.

The highest selectivity of 107 (Table 5.2) that was reported by Ciu and his co-workers (2004) on the T-type zeolite membrane (0.41 pore opening diameter) was enhanced by using a vacuum on the permeate side. The vacuum was found to be the contributing factor to the high selectivity (Li & Fan, 2010). From Table 5.2, the SAPO-34 membranes obtained in this study showed a high potential for $CO_2$ capture from flue gas although it showed slightly lower selectivity compared to the thin-film membranes reported by Li & Fan (2010). In another study, Fan and his co-workers (2013) studied MFI (0.55 nm pore dimension) membranes fabricate using in-situ hydrothermal synthetic method on $\alpha$-$Al_2O_3$ hollow ceramic fibres. The $CO_2$ separation properties of the as-prepared MFI membrane had an ideal selectivity of 9.2 for $CO_2/N_2$.

The secondary seed growth synthesis has been a widely preferred membrane synthesis method. However, this method results in irreproducible membranes. Moreover, the quality of the membranes depends on the quality of the seeds and the seeding technique applied which in most cases results in non-uniform seed leading to cracks in the membranes. Hence, Deng and his co-workers (2010) studied nanocomposite membranes grown in the pore alumina fibre tube which

had comparable permeances and selectivity observed in this study. In their study they reported a $CO_2$ permeance of 10.6 $x10^{-7}$ $mol.m^{-2}s^{-1}Pa^{-1}$ and a selectivity of 6 through MFI membranes (0.55 nm pore opening diameter). However, hollow fibres reported in this study presents limitations associated with grain boundaries.

Table 5.2 Comparison of $CO_2/N_2$ separations through selected zeolite membranes

| Membrane/support | Synthesis Type | No. of Synthesis stages | Type of membrane | Pore dimensions (nm) | T(°C) | Permeance ($10^{-7}$ mol.m$^{-2}$.s$^{-1}$.Pa$^{-1}$) | | Ideal selectivity $\frac{\Pi_{CO2}}{\Pi_{N2}}$ | References |
|---|---|---|---|---|---|---|---|---|---|
| | | | | | | $N_2$ | $CO_2$ | | |
| SAPO-34/alumina tube | Pore-plugging (short time) | 7 | Nanocomposite | 0.38 | 23 | 0.31 | 2.44 | 7.9 | This study |
| SAPO-34/alumina tube | Secondary Seeded growth (short time) | 1 | Thin-film | 0.38 | 22 | 0.57-0.19 | 12 – 15 | 21 – 32 | Li & Fan, 2010 |
| FAU/alumina tube | Secondary seeded growth | 1 | Thin-film | 0.74 | 30 | 0.11 – 0.2 | 0.4 – 3 | 20 – 100 | Kusakabe et al, 1997 |
| Silicalite-1/stainless steel net | Secondary seeded growth | 1 | Thin-film | 0.55 | 20 | 0.102 | 7 | 68 | Guo et al., 2006 |
| Na-ZSM-5/alumina tube | In situ (single step) synthesis | 1 | Thin-film | 0.55 | 35 | 0.025 | 1 | 40 | Shin et al., 2005 |
| NaA/carbon | In situ (single step) synthesis | 1 | Thin-film | 0.42 | 22 | 0.567 | 3.4 | 6.0 | Zhou et al., 2007 |
| T-type/mullite tube | Secondary Seeded growth | 6 | Thin-film | 0.41 | 35 | 0.016 | 0.239 | 14 | Cui et al., 2004 |
| MFI/alumina fibre | In situ (single step) synthesis | 1 | Thin-film | 0.55 | 25 | 0.33 | 3 | 9.2 | Fan et al., 2013 |
| MFI/alumina fibre | Pore-plugging | 1 | Nanocomposite | 0.55 | 25 | 1.78 | 10.6 | 6 | Deng et al., 2010 |

### 5.4 Maxwell-Stefan modelling for the SAPO-34 membranes

The Maxwell-Stefan (M-S) diffusion model describes the diffusion for multicomponent systems. The equation (5.1) describes the transport mechanism through the fluids and solids via the adsorption diffusion. There have been reported to be a useful approach to modelling the separation performance of zeolite membranes (Kapteijn et al., 2000; Krishna & van Baten, 2010; Miachon et al., 2007).

In the M-S modelling, data for single gas component adsorption and diffusion is used as an input to the model to predict the permeance in the zeolite membranes. As a result, the pure gas permeation can be fitted into a model based only on the M-S approach, in that it takes into account exclusively adsorption coefficients. This results in alteration of the flux in equation (5.1) shown below;

$$N = \frac{C_{sat}\rho\varepsilon D_0^{\infty}}{\tau L\left\{\ln\left[1+\left(\frac{P_R}{P_0}\right)\exp\left(\left(\frac{\Delta S°ads}{R}\right)-\left(\frac{\Delta H°ads}{RT}\right)\right)1+\left(\frac{P_P}{P_0}\right)\exp\left(\left(\frac{\Delta S°ads}{R}\right)-\left(\frac{\Delta H°ads}{RT}\right)\right)\right]\exp\left[-\frac{E_D}{RT}\right]\right\}} \quad (1)$$

The parameters for this equation were taken from the study reported by Li and co-workers.[13] Where R is the ideal gas constant (8.314 $J.mol^{-1}.K^{-1}$). $C_{sat}$ is the saturated concentration of the gas SAPO-34 crystals (4.52 $mol.kg^{-1}$). ρ is the density of SAPO-34 (2260 $kg.m^{-3}$). ε is the porosity of the material (0.55) obtained by the product of support and SAPO-34 porosity values. $D_0^{\infty}$ is the Maxwell-Stefan diffusivity (0.8 $x10^{-7}$ $m^2$ $.s^{-1}$, fitted parameter). τ is the tortuosity (2.5) as indicated by the support provider. $P_R$ is the retentate pressure (Pa). $P_p$ is the permeate pressure (Pa). $P_0$ is the reference atmospheric pressure (101,325 Pa). $\Delta S_{ads}°$ is the adsorption entropy (213.79 $J.mol^{-1}.K^{-1}$). $\Delta H_{ads}°$ is the adsorption enthalpy (32 000 $J.mol^{-1}$). $E_D$ is the diffusion activation energy (8.2 $x10^3$ $J.mol^{-1}$). L is membrane equivalent thickness which was arbitrarily obtained in this study (0.096 $x10^{-6}$ m)

The membrane effective thickness, L = 73, 2 μm, was obtained by comparing different gas permeances at various temperatures from the experimental result with the permeance obtained using equation (5.1) in a modelling software (MATLAB plot), while taking into

consideration the variation in diffusivity data. The adsorption data ($\Delta S_{ads}°$ and $\Delta H_{ads}°$) for $CO_2$ were obtained from literature. As a result the Figure 5.4 is plotted by the modelling software.

The experimental data fitted with the M-S diffusion model for $CO_2$ showed an acceptable correlation. The permeance as a function of temperature plot in Figure 5.4 showed a slight deviation. Grahn and Hudlund (2014) reported that the shortfall of the M-S model is the fact that most reports do not take into account the flow-through defects in the zeolite membranes as well as the pressure drop in the supports.

The pressure drops may results in a relatively higher flux the membranes which result in a variation in permeances between the model and the experimental data as displayed in at 298 K on Figure 5.4 (Grahn & Hudlun, 2014).

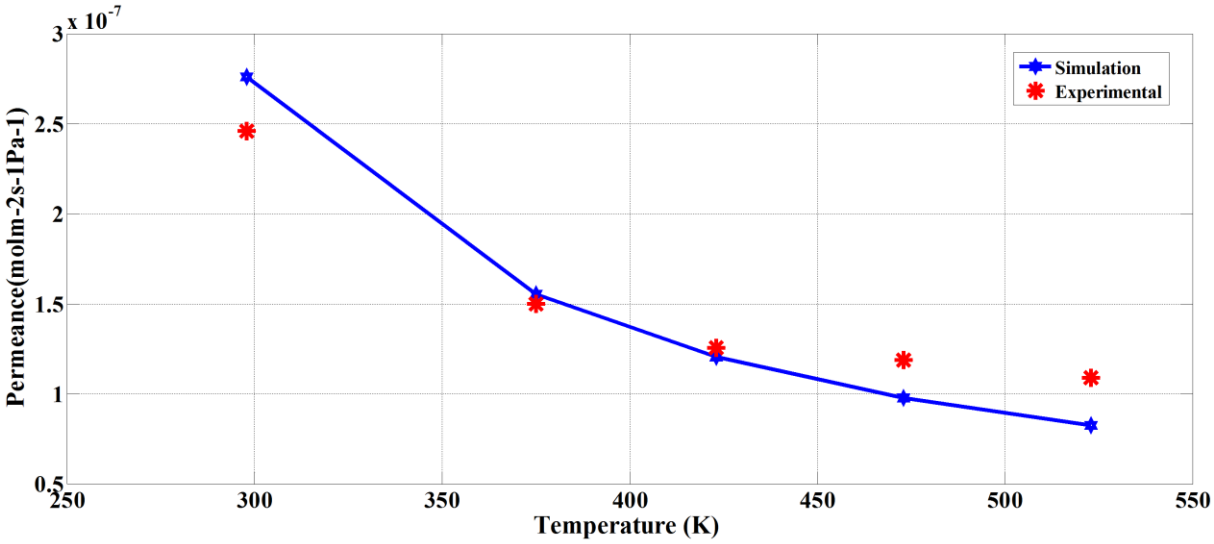


Figure 5.4 Maxwell-Stefan model fitted against the results obtained from membrane M8. Experimental conditions: Transmembrane pressure (TMP): 20kPa; Active permeation area: 26 $cm^2$

### 5.5 The effect of temperature on the separation performance

The transport mechanism of single gases through the pores of zeolite membranes is mainly governed by selective adsorption and diffusion (Daramola et al., 2010; Miachon et al., 2006; 2007). At ambient temperatures, depending on the adsorption coefficient of a particular gas on the zeolite membrane surface the permeance is quite high (Figure 5.5). The initial

permeance of $CO_2$ at room temperature was 2.44 $x10^{-7}$ $mol^{-1}.s^{-2}.m^2.P^{-1}$ while the $N_2$ had a permeance of 0.31 $x10^{-7}$ $mol^{-1}.s^{-2}.m^2.P^{-1}$.

The permeance of $CO_2$ through the membrane decreased significantly with an increase in temperature. On the other hand, the $N_2$ permeance only varied slightly due to a much less preferential adsorption of $N_2$ across the entire temperature range. As temperature increases, the amount of time the gas takes to pass through the pore reduces significantly due to reduced amount of adsorption taking place. Miachon and his co-workers (2007) reported that, at high temperature the transport mechanism is governed mostly by the molecular sieving techniques. As a result, a significant drop in the $CO_2$ permeance is observed which was in agreement with the report by Li & Fan (2010).

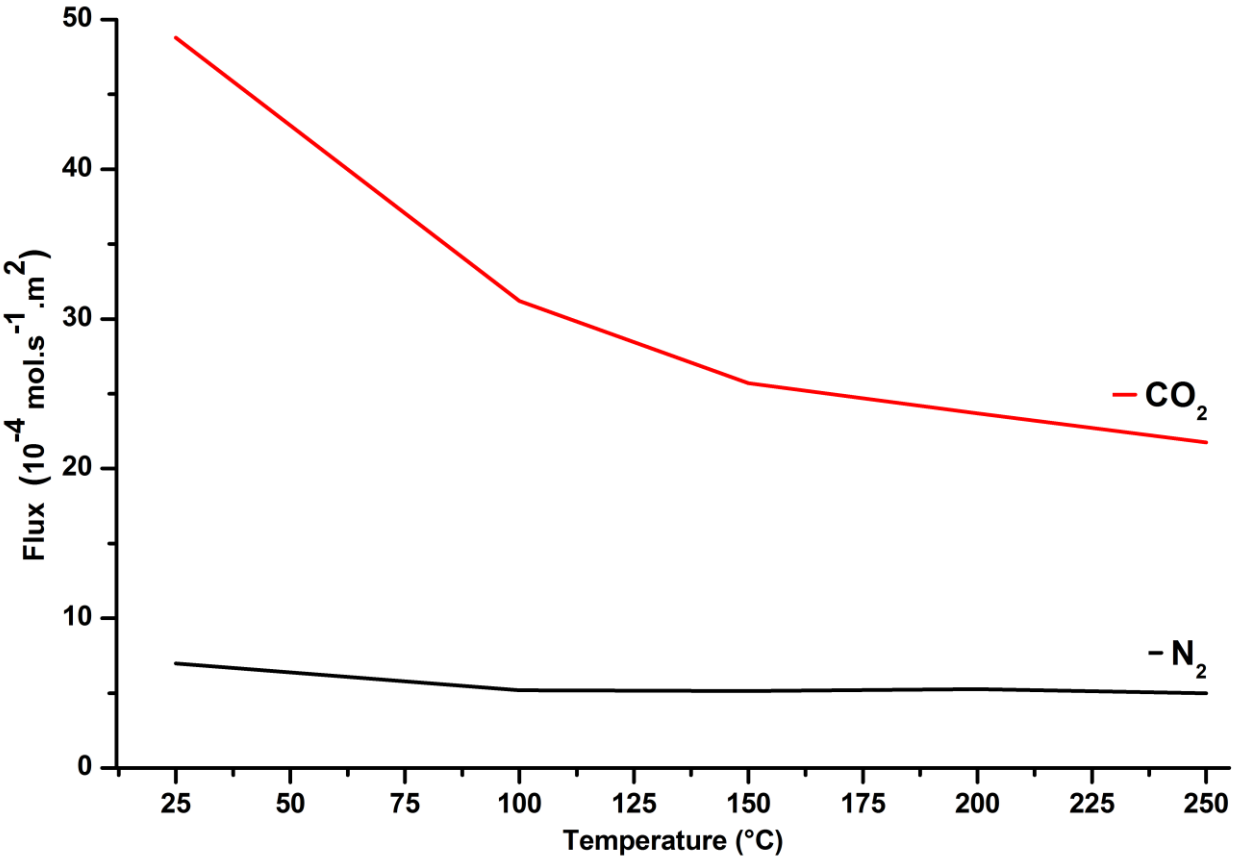


Figure 5.5 Membrane flux variation as temperature increases. Experimental conditions: Transmembrane pressure (TMP): 20kPa; Active permeation area: 26 $cm^2$

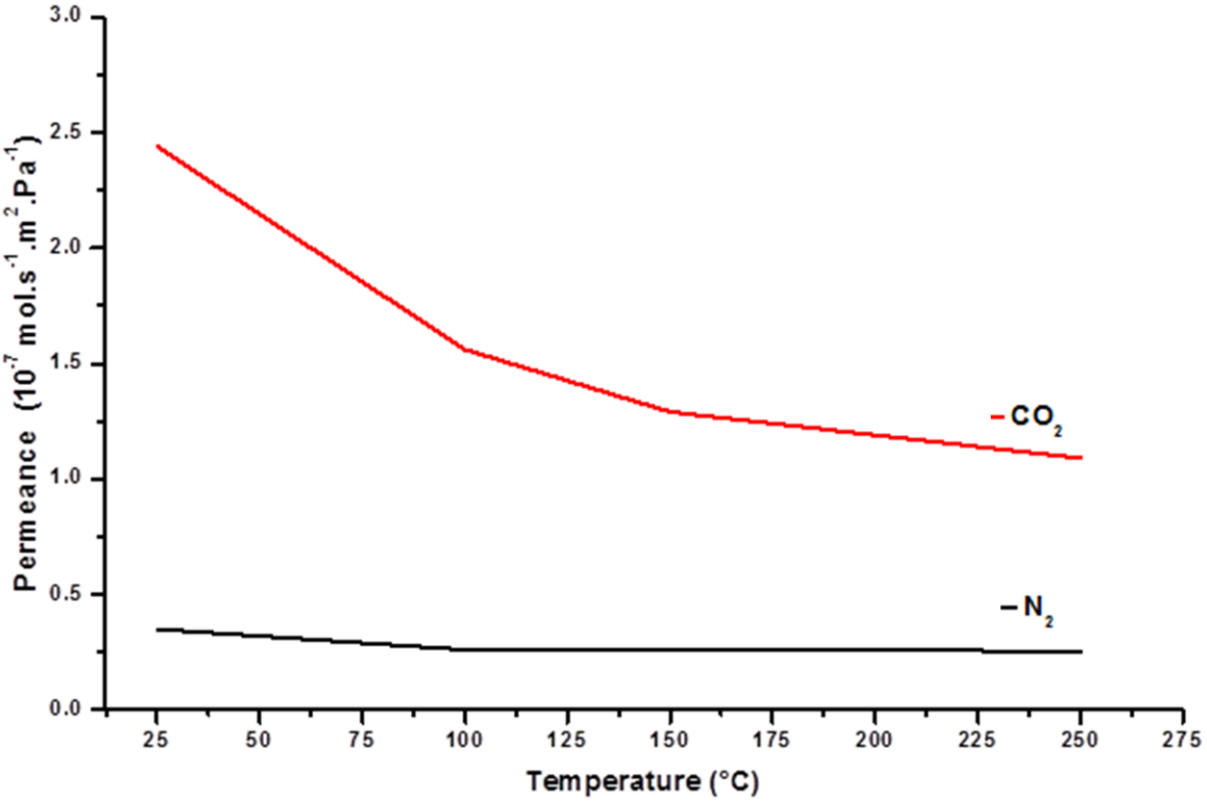


Figure 5.6 The membrane permeance variation as temperature increases. Experimental conditions: Transmembrane pressure (TMP): 20kPa; Active permeation area: 26 $cm^2$

The significant drop in the $CO_2$ permeance in Figure 5.6 resulted in a loss in $CO_2/N_2$ ideal selectivity which was calculated using the single gas permeances. Figure 5.7 illustrates the drop in ideal selectivity as the temperature increases. The ideal selectivity dropped from 7.8 at room temperature to 4 at 350 °C. Similarly, changes in flux which were calculated from the permeance observed per unit pressure difference dropped as observed in Figure 5.5.

The flux for $CO_2$ across membrane at room temperature was 48.8 $x10^{-4}$ $mol^{-1}.s^{-1}.m^2$ which was relatively low compared to reported studies in literature (Li et al., 2006; 2008; Li & Fan 2010). This low flux is attributed to plugged pores of the supports in the nanocomposite architecture. The low flux has been reported as one of the limitations of the nanocomposite membranes (Daramola et al., 2010; 2012; Miachon et al., 2006; 2007). In our study, the $CO_2$ flux from 48.8 $x10^{-4}$ $mol^{-1}.s^{-1}.m^2$ at room temperature to 21.75 $x10^{-4}$ $mol^{-1}.s^{-1}.m^2$ at 350 °C. There was around 50 % drop in flux at higher temperature which was comparable with a study by Chew & Ahmad (2016).

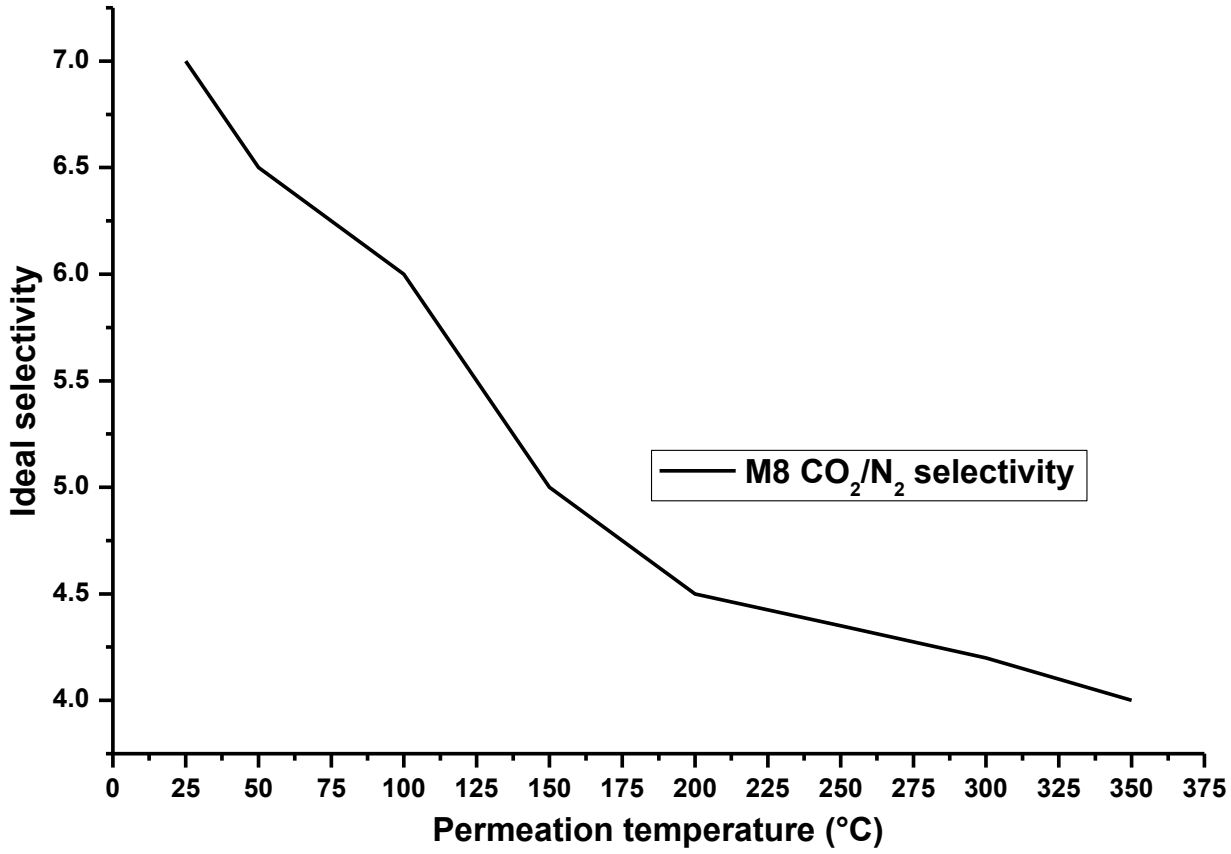


Figure 5.7 Ideal selectivity as a function of temperature increase Experimental conditions: Transmembrane pressure (TMP): 20kPa; Active permeation area: 26 $cm^2$

### 5.5.1 The effect of pressure on the separation performance

The effect of operating pressure on the SAPO-34 membranes were explored using single gas ($CO_2$ or $N_2$) permeation tests. In these experiments the feed pressure was increased while keeping the permeate pressure at atmospheric pressure. Figure 5.8 illustrates the effect of pressure on the permeance of $CO_2$ and $N_2$.

At atmospheric pressure the permeance of the adsorbing gas $CO_2$ at 2.44 x10 $^{-7}mol^{-1}.s^{-1}.m^2.Pa^{-1}$ was higher than that of the non-adsorbing gas $N_2$ which was 0.31 $x10^{-7}mol^{-1}.s^{-1}.m^2.Pa^{-1}$. It was reported by Li and his co-workers (2011) that the high permeance difference at low pressure is associated with a narrow pore size distribution as well a less presence of defects. Li and his co-workers (2010; 2011) previously reported that at low pressures, there is a surface adsorption by the adsorbing gas which then decreases as the pressure increase after

saturation was reached. As a result the permeance of $CO_2$ at 4 Bar (400 KPa) was 0.56 x$10^{-7}$mol$^{-1}$.s$^{-1}$.m$^2$.Pa$^{-1}$ while the permeance of $N_2$ was 0.10 x$10^{-7}$mol$^{-1}$.s$^{-1}$.m$^2$.Pa$^{-1}$.

The dependency of the permeance on the pressure is attributed to surface diffusion mechanism (Li et al., 2011). This is seen on Figure 5.8, whereby the permeance of the less absorbable gas ($N_2$) decreases slightly with an increase in pressure. The permeance for $CO_2$ decreased more because the adsorption capacity of $CO_2$ is far from saturation as compared to $N_2$ (Li et al., 2011).

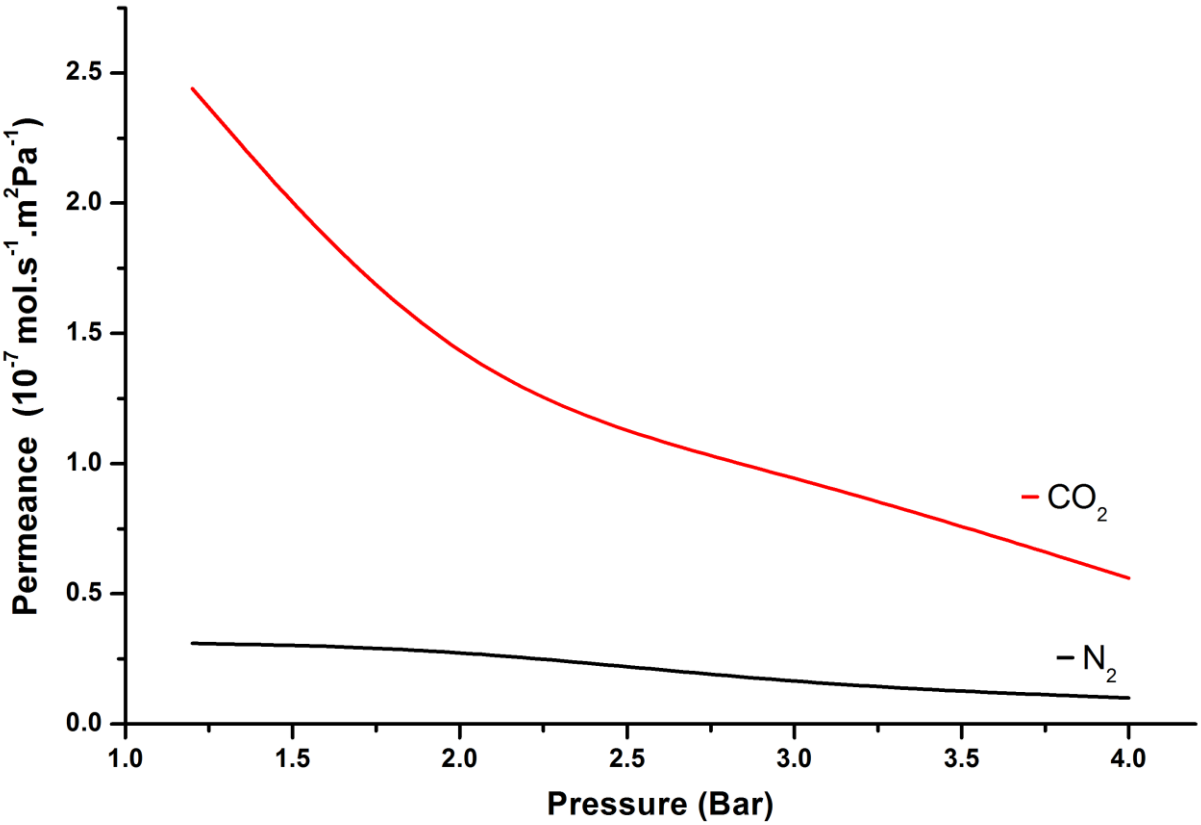


Figure 5.8 Permeance as a function of feed pressure. Experimental conditions: Temperature: room-temperature; Active permeation area: 26 cm$^2$

The flux (Figure 5.9) increased significantly with an increase in feed pressure because of the increased transmembrane pressure required for the calculations. The higher pressures are known to overcome the low flux limitation associated with nanocomposite membranes (Miachon et al., 2006; 2007). This was expected in terms of the weakly adsorbing $N_2$ which experienced the transport though the membrane by Knudsen diffusion and/or gas translational diffusion as reported in literature (Li et al., 2010; Xiao & Wei, 1992). As a result, higher

pressures often lead to higher selectivity. The resulting ideal selectivity showed a sudden sharp increase as displayed in Figure 5.10. It is clear that this selectivity is due to the surface diffusion of the gases.

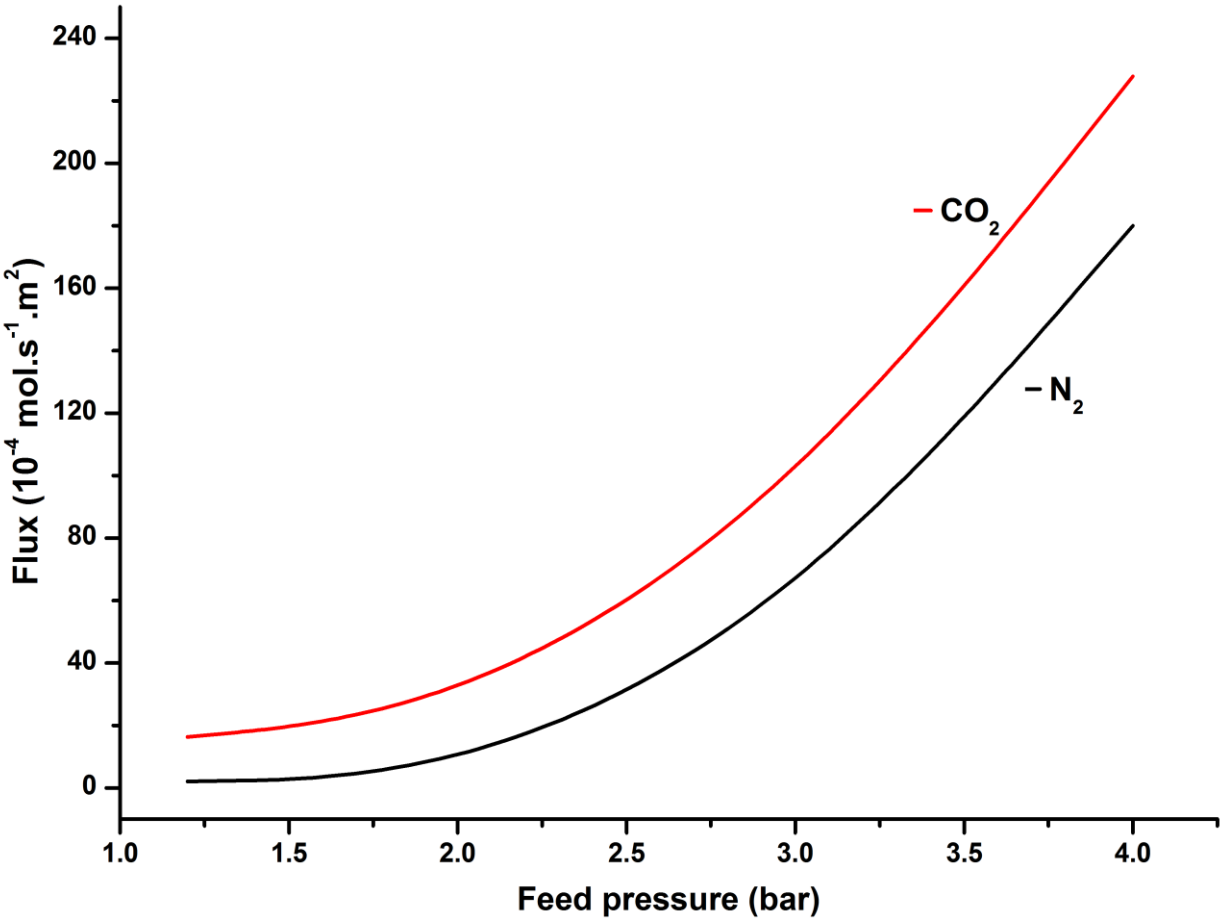


Figure 5.9 The effect of feed pressure on the calculated flux. Experimental conditions: Temperature: room-temperature; Active permeation area: 26 $cm^2$

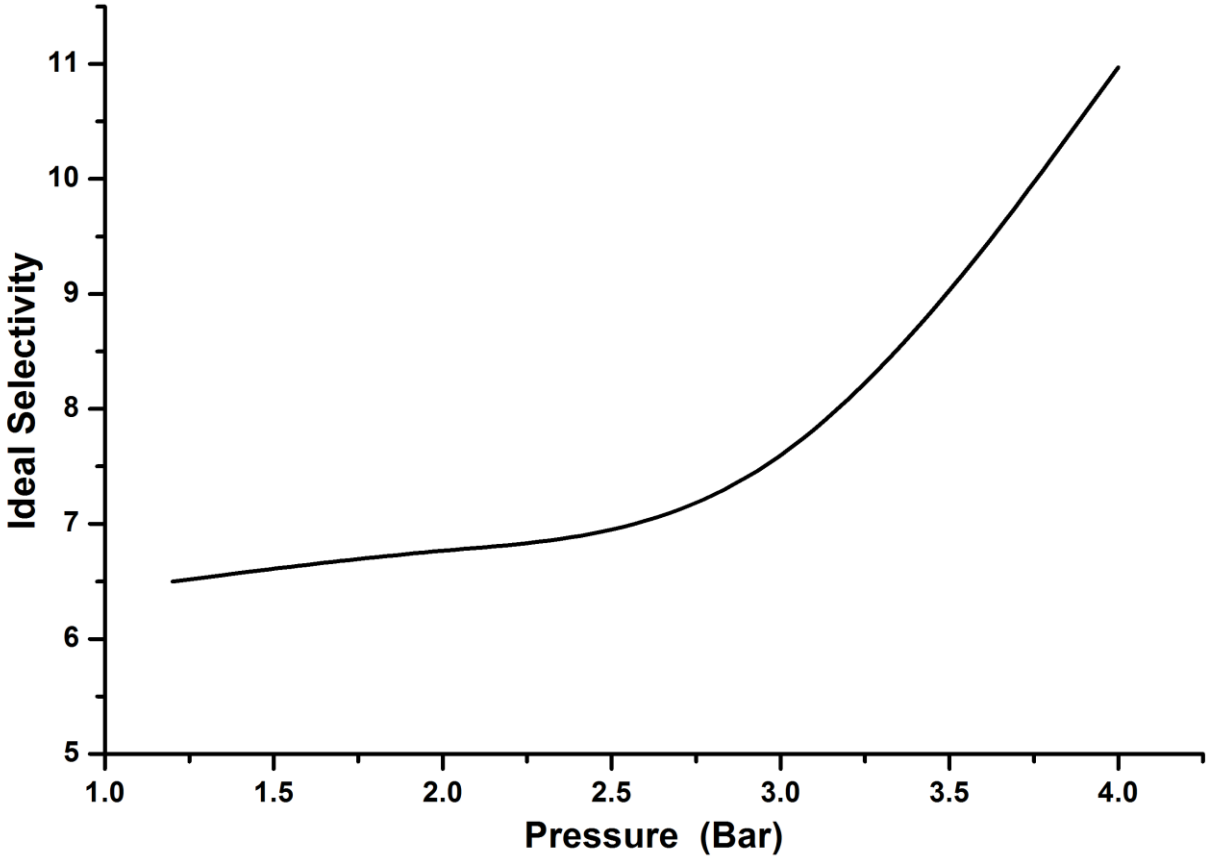


Figure 5.10 The effect of pressure on the ideal selectivity. Experimental conditions: Temperature: room-temperature; Active permeation area: 26 $cm^2$

### 5.5.2 The effect of flow rate on the separation performance

The effect of flow rate on the high driving force results in a high flux as displayed in Figure 5.11 and the effect of flow rate on the permeance plotted on Figure 5.12 shows a small increment gradient up to about 25 $x10^{-3}$ mol. $s^{-1}$ and then there seem to be a sharp increase from 30 $x10^{-3}$ $mol.s^{-1}$. The main explanation for this trend may be due to the high increase in the partial pressure as the flow rate increases. This comes as a result of the flow rates which are conducted at pressures where by the membrane is saturated with the gases. In terms of $CO_2$ at this pressures, less $CO_2$ would be adsorbed on the zeolite membrane.

As the feed flow rate increases the permeance is not expected to increase as the saturation is expected to be reached. However, beyond the saturation point, the gases are expected to permeate through the membrane without any adsorption being involved. This phenomenon explains the sharp increase in the permeance illustrated in Figure 5.12.

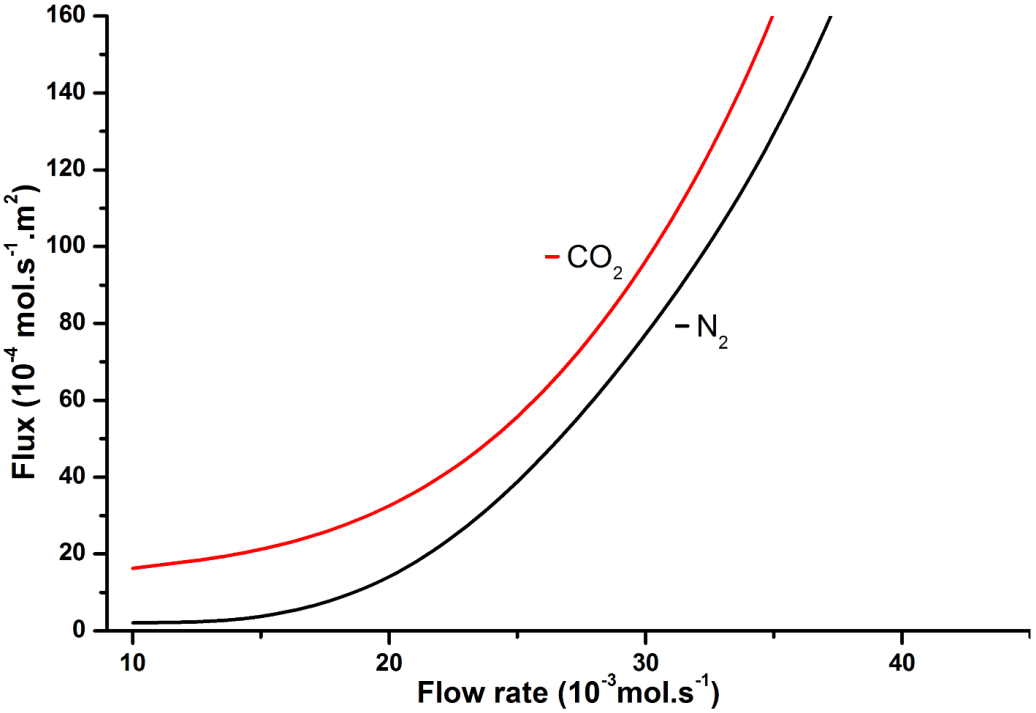


Figure 5.11 Flux as a function of feed flow rate. Experimental conditions: Temperature: room-temperature; Active permeation area: 26 $cm^2$

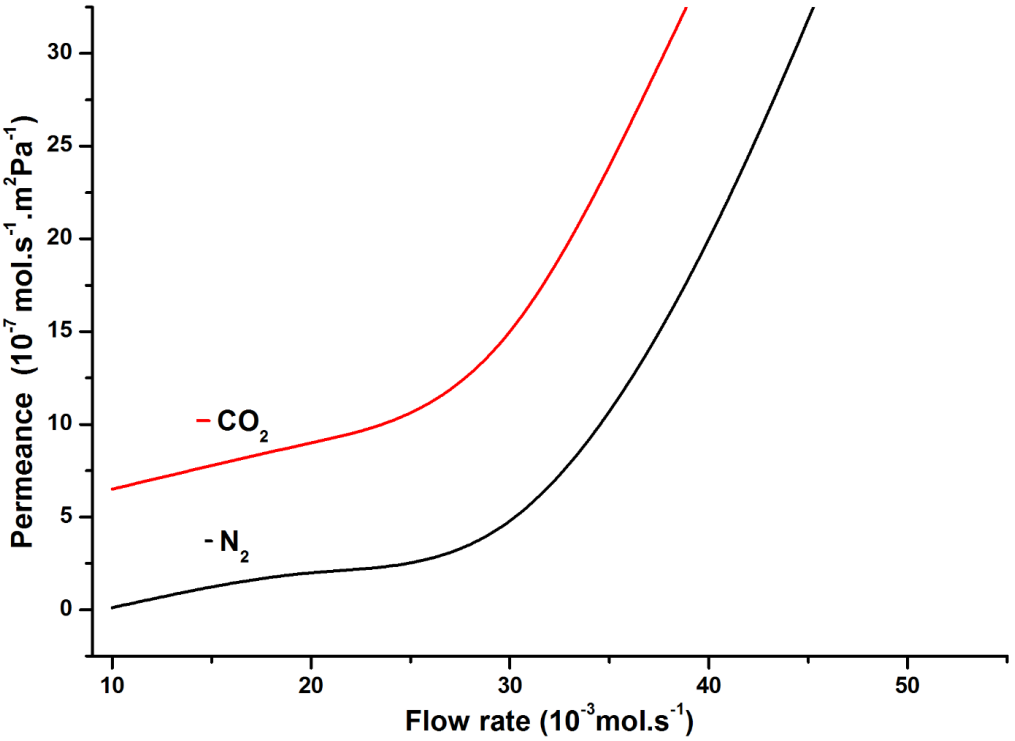


Figure 5.12 Permeance as a function of feed flow rate. Experimental conditions: Temperature: room-temperature; Active permeation area: 26 $cm^2$

The ideal selectivity of the nanocomposite membrane illustrated in Figure 5.13 shows a decrease in selectivity as the feed pressure increases from 7 to below 1. The resulting drop in the selectivity is due to the increase in the driving force of the gases which leads to more gas molecules passing through the membrane. The membrane cannot selectively adsorb the $CO_2$ as it does at low pressure since the saturation is reached quite quickly.

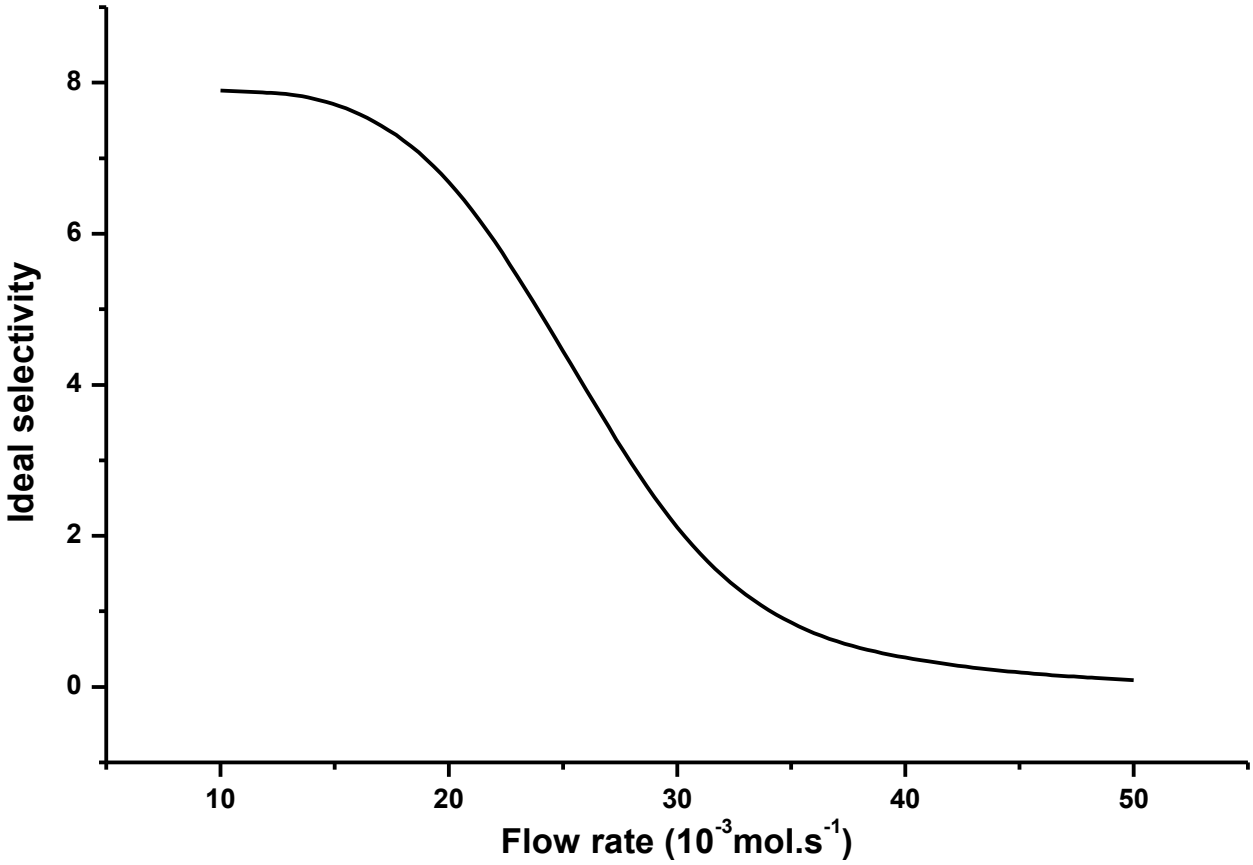


Figure 5.13 Ideal selectivity as a function of feed flow rate. Experimental conditions: Temperature: room-temperature; Active permeation area: 26 $cm^2$

## 5.6 Concluding remarks

The membrane, M8, demonstrated good separation performance characteristics. The single gas permeance depended largely on the adsorption interaction between the gas and the zeolite membrane. As a result, $CO_2$ exhibited high permeance in most cases during the test compared

to $N_2$ due to the high affinity of the membrane to $CO_2$. The separation of the single gases through the membrane was highly governed by the Knudsen diffusion mechanism.

However, the ideal selectivity depended largely on the pressure, temperature and the feed flow rate. Hence, highlighting that other transport mechanism such as the configurational diffusion might be responsible for transport in the membranes. For instance, capillary condensation may occur under low temperature and high pressure where by a significant adsorption of the strongly adsorbing gas might be experienced (Bakker et al., 1996 & 1997; Bernal et al., 2002). This means the Knudsen diffusion could occur at the same time as the capillary diffusion (Bernal et al., 2002).

# Chapter Six

## General Conclusions and Recommendations

## 6 Conclusions and general outlook

This chapter summarises the general conclusions drawn from all the previously discussed chapters in this dissertation by highlighting the overall conclusions and suggested future work.

### 6.1 Conclusions

The synthesis, characterization and performance evaluation of tubular SAPO-34 membranes for the separation of $CO_2$ and $N_2$ has been extensively explored in this work. It has been established and highlighted in this study that understanding the gas transport mechanisms of separation of the gases as well as obtaining reliable experimental data with less errors are of the essence in the successful application of SAPO-34 membranes in the post combustion capture of $CO_2$.

Single gas permeation tests were conducted in this study in order to thoroughly understand the quality of the membranes as well as the transport mechanisms of the single gases through the membranes. The effects of operating conditions (temperature, feed flow rate, pressure etc.) have been experimentally explored and as a result. Optimum operating conditions were determined.

Moreover, the Maxwell-Stefan model was fitted against the experimental data to determine the thickness of the as-synthesized membranes as well as to assess the reliability of the experimental data obtained.

The key findings from this study includes the following:

- The static characterization techniques confirmed the synthesis of nanocomposite SAPO-34 supported membranes.
- The lower temperature and shorter synthesis time showed key characteristics of the CHA type structure SAPO-34 membranes.
- The quality of the as-synthesized zeolite membranes improved as the layers of the active material increased.
- The single gas permeance results obtained showed that the $CO_2$ (MW = 46 $g.mol^{-1}$) permeance was higher due to the preferential adsorption as it is higher than that of the less adsorbing gas $N_2$ (MW = 28 $g.mol^{-1}$). This went against the notion that lighter gases permeate faster through the porous membrane than heavier gases.

- It was observed in this study that the overall gas transport mechanism through the porous membranes was through both the zeolite pores as well as the non-zeolite pores.
- The permeance, flux and ideal selectivity depends significantly on the operating conditions.
- $CO_2$ was preferentially adsorbed on the SAPO-34 membranes while $N_2$ was weakly absorbed through the membranes, as a result the transport of the gases through the membranes was configurational diffusion. The ideal selectivity as a result was at around 8 for the membrane with the best quality.
- The Maxwell-Stefan model closely correlated with the experimentally obtained data highlighting the dependence of the permeance on the operating temperature.
- The permeation test results confirm that the as-synthesised nanocomposite SAPO-34 can indeed be good candidates for the post combustion separation and capture of $CO_2$.

This research will therefore pave way for the selective membrane separation systems to be applied in the separation and capture of $CO_2$ from the post combustion power plant flue gas. Moreover, this could be to the application of membranes technologies in other industries as well. As it stands. The membranes therefore produced in this work will be suitable for separation in cases where selectivity is preferred more that the permeance and the flux.

### 6.2 Recommendations

This study has led to number of interesting questions and observations. We would like to propose the following as interesting future directions from this work:

- Enhancing the pore-plugging synthesis to produce more defect free SAPO-34 membranes as well permeation experiments under power plant flue gas conditions in order to justify further application in industrial processes.
- Gas mixture permeation tests as well as multi-component isotherms are needed to be conducted.
- It has been found that adsorption properties of the gases may vary in the presence of other gases found in flue gas; therefore, further tests are required to subject the membranes to the flue gas environments.

# References

## 7.1 References

Abolhosseini, S., Heshmati, A., Altmann, J., (2014), A Review of Renewable Energy Supply and Energy Efficiency Technologies, Discussion Paper No. 8145.

Akpınar, A., Kömürcü, M. İ., & Kankal, M. (2011). Development of hydropower energy in Turkey: The case of Çoruh river basin. Renewable and Sustainable Energy Reviews, 15(2), 1201-1209.

Algieri, C., Bernardo, P., Golemme, G., Barbieri, G. & Drioli, E. (2003) Permeation properties of a thin silicalite-1 (MFI) membrane. Journal of Membrane Science, 222, 181-190.

Alimov, V., Busnyuk, A., Notkin, M., Livshits, A. (2014) Pd–V–Pd composite membranes: Hydrogen transport in a wide pressure range and mechanical stability. Journal of Membrane Science, 457, 103-112.

Allen, D. T., Torres, V. M., Thomas, J., Sullivan, D. W., Harrison, M., Hendler, A., & Lamb, B. K. (2013). Measurements of methane emissions at natural gas production sites in the United States. Proceedings of the National Academy of Sciences, 110(44), 17768-17773.

Al-Mufachi, N., Rees, N., Steinberger-Wilkens, R. (2015) Hydrogen selective membranes: A review of palladium-based dense metal membranes. Renewable and Sustainable Energy Reviews, 47, 540-551.

Alshebani, A., Pera-Titus, M., Landrivon, E., Schiestel, Th., Miachon, S., & Dalmon, J-A. (2008), Nanocomposite MFI-Ceramic hollow fibres: Prospects for $CO_2$ separation. Micropor. Mesopor. Mater. 115, 197-205.

Anastas, P. T., & Warner, J. C. (1998). Principles of green chemistry. Green chemistry: Theory and practice, 29-56.

Anderson, S., & Newell, R. (2004). Prospects for carbon capture and storage technologies. Annu. Rev. Environ. Resour., 29, 109-142.

Aoki, K., Kusakabe, K. & Morooka, S. (1998) Gas permeation properties of A-type zeolite membrane formed on porous substrate by hydrothermal synthesis. Journal of Membrane Science, 141, 197-205.

Aoki, K., Tuan, V. A., Falconer, J. L. & Noble, R. D. (2000) Gas permeation properties of ion-exchanged ZSM-5 zeolite membranes. Microporous and Mesoporous Materials, 39, 485-492.

Armstead, H. C. H. (1978). Geothermal energy: its past, present and future contributions to the energy needs of man.

Au, L. T. Y. & Yeung, K. L. (2001) An investigation of the relationship between microstructure and permeation properties of ZSM-5 membranes. Journal of Membrane Science, 194, 33-55.

Ayral, A., Julbe, A., Roussac,V., Roualdes,S., Durand, J. (2008) Microporous silica membranes: Basic principles and recent advances. Membrane Science and Technology, 13, 33-79.

Azar, C., Lindgren, K., Larson, E., & Möllersten, K. (2006). Carbon capture and storage from fossil fuels and biomass–Costs and potential role in stabilizing the atmosphere. Climatic Change, 74(1-3), 47-79.

Azar, C., Lindgren, K., Obersteiner, M., Riahi, K., van Vuuren, D. P., den Elzen, K. M. G., ... & Larson, E. D. (2010). The feasibility of low $CO_2$ concentration targets and the role of bio-energy with carbon capture and storage (BECCS). Climatic Change, 100(1), 195-202.

Babu, P., Kumar, R., & Linga, P. (2013). A new porous material to enhance the kinetics of clathrate process: application to precombustion carbon dioxide capture. Environmental science & technology, 47(22), 13191-13198.

Babu, P., Linga, P., Kumar, R., & Englezos, P. (2015). A review of the hydrate based gas separation (HBGS) process for carbon dioxide pre-combustion capture. Energy, 85, 261-279.

Babu, P., Yao, M., Datta, S., Kumar, R., & Linga, P. (2014). Thermodynamic and kinetic verification of tetra-n-butyl ammonium nitrate (TBANO3) as a promoter for the clathrate process applicable to precombustion carbon dioxide capture. Environmental science & technology, 48(6), 3550-3558.

Baetens, Ruben, Bjørn Petter Jelle, & Arild Gustavsen. (2010). Properties, requirements and possibilities of smart windows for dynamic daylight and solar energy control in buildings: A state-of-the-art review." Solar Energy Materials and Solar Cells 94.2 (2010): 87-105.

Baker, R.W. (2002), Future directions of membrane gas separation technology. Ind. Eng. Res., 41, 1393-1411.

Bakker, W. J. W., Kapteijn, F., Poppe, J. & Moulijn, J. A. (1996) Permeation characteristics of a metal-supported silicalite-1 zeolite membrane. Journal of Membrane Science, 117, 57-78.

Bakker, W. J. W., Van Den Broeke, L. J. P., Kapteijn, F. & Moulijn, J. A. (1997) Temperature dependence of one-component permeation through a silicalite-1 membrane, AIChE Journal, 43, 22034-2214.

Barbier, E. (2002). Geothermal energy technology and current status: an overview. Renewable and Sustainable Energy Reviews, 6(1), 3-65.

Barbieri, G., Marigliano, G., Golemme, G. & Drioli, E. (2002) Simulation of CO2 hydrogenation with CH3OH removal in a zeolite membrane reactor. Chemical Engineering Journal, 85, 53-59.

Barrer, R. M. (1990) Porous Crystal Membranes. Journal of the Chemical Society. Faraday Transactions, 86, 1123-1130.

Basu, A., Akhtar, J., Rahman, M. H. & Islam, M. R. (2004) A review of separation of gases using membrane systems, Petroleum Science and Technology. 22, 1343-1368.

Benson, S. M., Bennaceur, K., Cook, P., Davison, J., Coninck, H. D., Farhat, K., ... & Wright, I. (2012). Carbon capture and storage.

Bernado, P., Clarizia, G. (2013) 30 years of membrane technology for gas separation. Chemical Engineering Transactions,32,1999-2004.

Bernal, M. P., Coronas, J., Menendez, M. & Santamaria, J. (2002) Characterization of Zeolite Membranes by Measurement of Permeation Fluxes in the Presence of Adsorbable Species. Industrial & Engineering Chemistry Research, 41, 5071-5078.

Bernal, M. P., Coronas, J., Menendez, M. & Santamaria, J. (2003) On the effect of morphological features on the properties of MFI zeolite membranes. Microporous and Mesoporous Materials, 60, 99-110.

Bonhomme, F., Welk, M. E. & Nenoff, T. M. (2003) CO2 selectivity and lifetimes of high silica ZSM-5 membranes. Microporous and Mesoporous Materials, 66, 181-188.

Bonilla, G., Vlachos, D.G., & Tsapatsis, M. (2001), Simulations and experiments on the growth and microstructure of zeolite MFI films and membranes made by secondary growth. Micropor. Mesopor. Mater., 42, 191–203.

Boot-Handford, M. E., Abanades, J. C., Anthony, E. J., Blunt, M. J., Brandani, S., Mac Dowell, N., ... & Haszeldine, R. S. (2014). Carbon capture and storage update. Energy & Environmental Science, 7(1), 130-189.

Boudreau, L.C.; Kuck, J.A.; Tsapatsis, M. (1999), Deposition of oriented zeolite a films: In situ and secondary growth. J. Membr. Sci., 152, 41–59.

Bounaceur, R., Lape, N., Roizard, D., Vallieres, C., & Favre, E. (2006), Membrane processes for post-combustion carbon dioxide capture: A parametric study. Energy, 31, 2556-2570

Bowen, T.C., Noble, R.D., Falconer, J.L. (2004) Fundamentals and applications of pervaporation through zeolite membranes. Journal of Membrane Science, 245, 1-33.

Brandt, A. R., Heath, G. A., Kort, E. A., O'Sullivan, F., Pétron, G., Jordaan, S. M., ... & Wofsy, S. (2014). Methane leaks from North American natural gas systems. Science, 343(6172), 733-735.

Camus, O., Perera, S., Crittenden, B., Van Delft, Y. C., Meyer, D. F., Pex, P., Kumakiri, I., Miachon, S., Dalmon, J. A., Tennison, S. & Chanaud, P. (2006) Ceramic membranes for ammonia recovery. Aiche Journal, 52, 2055-2065.

Caro, J. (2011). Are MOF membranes better in gas separation than those made of zeolites? Current Opinion in Chemical Engineering [Online]. 1, 77-83 Available from: www.sciencedirect.com. [10th January 2017].

Caro, J., & Noack, M. (2000), Zeolite membranes – State of their development and perspective. Micropor. Mesopor. Mater., 38(1), 3-24.

Caro, J., & Noack, M. (2008), Zeolite membranes – Recent development and progess. Micropor. Mesopor. Mater., 115 215-233.

Caro, J., Noack, M. & Kolsch, P. (2005) Zeolite Membranes: From the Laboratory Scale to Technical Applications. Adsorption, 11, 215-227.

Caro, J., Noack, M., Kolsch, P. & Schafer, R. (2000) Zeolite membranes - state of their development and perspective. Microporous and Mesoporous Materials, 38, 3-24.

Carreon, M. A., Li, S., Falconer, J. L., & Noble, R. D. (2008), Alumina supported SAPO-34 membranes for CO2/CH4 separations. J. Am. Chem. Soc., 130, 5412.

Carreon, M. A., Li, S., Falconer, J. L., & Noble, R. D. (2008), SAPO-34 seeds and membranes prepared using multiple structure directing agents. AdV. Mater., 20, 729.

Chau, J.L.H.; Tellez, C.; Yeung, K.L. (2000), Ho, K. The role of surface chemistry in zeolite membrane formation. J. Membr. Sci., 164, 257–275.

Chiang, A. S. T. & Chao, K.-J. (2001) Membranes and films of zeolite and zeolite-like materials. Journal of Physics and Chemistry of Solids, 62, 1899-1910.

Choi, J., Jeong, H., Snyder, M., Stoeger, J., Masel, R., Tsapatsis, M. (2009) Grain Boundary Defect Elimination in a Zeolite Membrane by Rapid Thermal Processing. Science, 325, 590-593.

Choi, J.G., Do, D.D., Do, H.D. (2001) Surface diffusion of adsorbed molecules in porous media: monolayer, multilayer, and capillary condensation regimes. Industrial & Engineering Chemistry Research, 40, 4005-4031.

Ciavarella, P., Casanave, D., Moueddeb, H., Miachon, S., Fiaty, K., & Dalmon, J. (2001), Isobutane dehydrogenation in a membrane reactor. Influence of the operating conditions on the performance. Catal. Today, 67, 177

Ciavarella, P., Moueddeb, H., Miachon, S., Fiaty, K. & Dalmon, J.-A. (2000) Experimental study and numerical simulation of hydrogen/isobutane permeation and separation using MFI-zeolite membrane reactor. Catalysis Today. 56, 253-264.

Coronas, J. & Santamaria, J. (1999) Separations using zeolite membranes. Separation and Purification Methods, 28, 127-177.

Coronas, J., Falconer, J. L. & Noble, R. D. (1997) Characterization and permeation properties of ZSM-5 tubular membranes. AIChE Journal. 43, 1797-1812.

Coronas, J., Noble, R. D. & Falconer, J. L. (1998) Separations of C4 and C6 isomers in ZSM-5 tubular membranes. Industrial & Engineering Chemistry Research, 37, 166-176.

Crawford, P. (2013), Zeolite membranes for the separation of krypton and xenon from spent nuclear fuel reprocessing off-gas. MSc Thesis, Georgia Institute of Technology.

Crittenden, B.D. & Thomas, W.I., 1998, Adsorption Technology and Design, Butterworth-Henemann, Oxford.

Crutzen, P. J., Mosier, A. R., Smith, K. A., & Winiwarter, W. (2008). N 2 O release from agro-biofuel production negates global warming reduction by replacing fossil fuels. Atmospheric chemistry and physics, 8(2), 389-395.

Cui, Y., Kita, H. & Okamoto, K. (2004) Preparation and gas separation performance of zeolite T membrane. Journal of Materials Chemistry, 14, 924-932.

Daramola, M. O., Dinat, A., & Hasrod, S. (2015). Synthesis and Characterization of Nanocomposite Hydroxy-Sodalite/Ceramic Membrane via Pore-Plugging Hydrothermal Synthesis Technique. J. Membr. and Separ. Tech., 4(1), 1-7.

Daramola, M.O., Aranisola, E.F., & Ojamu, T.V. (2012), Potential applications of zeolite membranes in reaction coupling separation processes. Mater. ,5, 2101-2136. Doi:10.3390/ma5112101.

Daramola, M.O., Burger, A.J. & Giroir-Fendler, A. (2011), Modelling and sensitivity analysis of a nanocomposite MFI-alumina based extractor-type zeolite catalytic membrane reactor for m-Xylene isomerization over Pt-HZSM-5 catalyst. Chem Eng. J, 171(2), 618-627

Daramola, M.O., Burger, A.J., Pera-Titus, M., Giroir-Fendler, A., Miachon, S, Lorenzena, L., & Dalmon, J-A. (2009), Nanocomposite MFI–ceramic hollow fibre membranes via pore-plugging synthesis: Prospects for xylene isomer separation. J. Membr. Sci. 337(1-2) 106-112.

Daramola, M.O., Deng, Z., Pera-Titus, M., Giroir-Fendler, A, Miachon, S., Burger, A.J. Lorenzena, L., & Guoc, L. (2010), Nanocomposite MFI–alumina membranes prepared via pore-pugging synthesis: Application as packed-bed membrane reactors for m-xylene isomerization over a Pt-HZSM-5 catalyst. Catal. Today ,156(3-4), 261-267

Davis, B.H.; Singh, K.S.W. (2002), Handbook of Porous Solids; Schüth, F., Singh, K.S.W., Weitkamp, J., Eds.; Wiley-VCH: Weinheim, Germany

Davis, S. P., Borgstedt, E. V. R. & Suib, S. L. (1990) Growth of zeolite crystallites and coatings on metal-surfaces. Chemistry of Materials, 2, 712-719.

del Rio, M. S., Gibbins, J., & Lucquiaud, M. (2016). On the retrofitting and repowering of coal power plants with post-combustion carbon capture: An advanced integration option with a gas turbine windbox. International Journal of Greenhouse Gas Control.

Demirbaş, A. (2002). Sustainable developments of hydropower energy in Turkey. Energy Sources, 24(1), 27-40.

Deng, Z.; Nicolas, C.; Daramola, M.; Sublet, J.; Schiestel, T.; Burger, A.; Guo, Y.; Giroir-Fendler, A.; Pera-Titus, M. (2010) Nanocomposite MFI-alumina hollow fiber membranes prepared via pore-plugging synthesis: Influence of the porous structure of hollow fibers on the gas/vapour separation performance. Journal of Membrane Science, 364, 1-8.

Dent, L.S. & Smith, J.V., (1958). Crystal Structure of Chabazite, A molecular sieve., Nature, 181, 1794-1796

Dicks, A. L. (1996). Hydrogen generation from natural gas for the fuel cell systems of tomorrow. Journal of power sources, 61(1), 113-124.

Doshi, K. J. (1978) Recovery of hydrogen and nitrogen from ammonia plant purge gas Union Carbide Corporation (New York, NY)

Duke, M. C., Da Costa, J. C. D., Lu, G. Q. & Gray, P. G. (2006) Modeling hydrogen separation in high temperature silica membrane systems. AIChE Journal, 52, 1729-1735.

Duval, J. M., Folkers, B., Mulder, M. H. V., Desgrandchamps, G. & Smolders, C. A. (1993) Adsorbent filled membranes for gas separation. Part 1. Improvement of the gas separation properties of polymeric membranes by incorporation of microporous adsorbents. Journal of Membrane Science, 80, 189-198.

Figueroa, J. (2016). US DOE carbon capture program: Advancing multiple generations of carbon capture solutions laboratory to pilot scale development.

Figueroa, J.D., Fout, T., Plasynki, S., Mcllvried, H., & Srivastava, R.D. (2008), Advances in CO2 capture technology – US Department of Energy's Carbon Sequestration Program. Int. J. GHG. Contr., 2, 9-20

Freemantle, M. (2005) Membranes for gas separation. Chemical & Engineering News[Online], 43, 49-57. Available from: http://pubs.acs.org/cen/coverstory/83/8340membranes.html [17 February 2017].

Fuertes, A. B. & Centeno, T. A. (1998) Carbon molecular sieve membranes from polyetherimide. Microporous and Mesoporous Materials, 26, 23-26.

Fuertes, A. B. (2000) Adsorption-selective carbon membrane for gas separation. Journal of Membrane Science, 177, 9-16.

Gardner, T. Q., Flores, A. I., Noble, R. D. & Falconer, J. L. (2002) Transient measurements of adsorption and diffusion in H-ZSM-5 membranes, AIChE Journal. 48, 1155-1167.

Gardner, T., Martinek, J., Falconer, J., Noble, R. (2007) Enhanced flux through double-sided zeolite membranes. Journal of Membrane Science, 304, 112-117.

Gavalas, G. R., Megiris, C. E. & Nam, S. W. (1989) Deposition of H2 permselective SiO2 films. Chemical Engineering Science, 44, 1829.

Gibbins, J., & Chalmers, H. (2008). Carbon capture and storage. Energy Policy, 36(12), 4317-4322.

Gouzinis, A., & Tsapatsis, M. (1998), On the Preferred Orientation and Microstructural Manipulation of Molecular Sieve Films Prepared by Secondary Growth. Chem. Mater., 10(9), 2497-2504.

Granqvist, C. G. (2007). Transparent conductors as solar energy materials: A panoramic review. Solar energy materials and solar cells, 91(17), 1529-1598.

Gu, X.; Dong, J.; Nenoff, T. M. (2005) Synthesis of defect-free FAU-type zeolite membranes and separation for dry and moist CO2/N2 mixtures. Ind. Eng. Chem. Res., 44, 937

Gump, C. J., Lin, X., Falconer, J. L. & Noble, R. D. (2000) Experimental configuration and adsorption effects on the permeation of C4 isomers through ZSM-5 zeolite membranes. Journal of Membrane Science, 173, 35-52.

Gump, C. J., Noble, R. D. & Falconer, J. L. (1999) Separation of Hexane Isomers through Nonzeolite Pores in ZSM-5 Zeolite Membranes. Industrial & Engineering Chemistry Research, 38, 2775-2781.

Guo, H.; Zhu, G.; Li, H.; Zou, X.; Yin, X.; Yang, W.; Qiu, S.; Xu, R. (2006) Hierarchical growth of large-scale ordered zeolite silicalite-1 membranes with high permeability and selectivity for recycling CO2. Angew. Chem., Int. Ed., 45, 7053

H.Z. Chen, P. Li, T.S. Chung, PVDF/ionic liquid polymer blends with superior separation performance for removing CO2 from hydrogen and flue gas, Int. J. Hydrogen Energy 37 (2012) 11796–11804.

Haszeldine, R. S. (2009). Carbon capture and storage: how green can black be?. Science, 325(5948), 1647-1652.

Hedlund, J., Noack, M., Kolsch, P., Creaser, D., Caro, J. & Sterte, J. (1999) ZSM-5 membranes synthesized without organic templates using a seeding technique. Journal of Membrane Science, 159, 263-273.

Hedlund, J., Sterte, J., Anthonis, M., Bons, A. J., Carstensen, B., Corcoran, N., Cox, D., Deckman, H., De Gijnst, W., De Moor, P. P., Lai, F., Mchenry, J., Mortier, W. & Reinoso, J. (2002) High-flux MFI membranes. Microporous and Mesoporous Materials, 52, 179-189.

Hennenberg, K. J., Dragisic, C., Haye, S., Hewson, J., Semroc, B., Savy, C., ... & Fritsche, U. R. (2010). The Power of Bioenergy-Related Standards to Protect Biodiversity. Conservation Biology, 24(2), 412-423.

Herzog, H., & Golomb, D. (2004). Carbon capture and storage from fossil fuel use. Encyclopedia of energy, 1, 1-11.

Hester, R. E., & Harrison, R. M. (2010). Carbon capture and storage. Royal Society of Chemistry.

Hong, M., Falconer, J., Noble, R. (2005) Modification of zeolite membranes for H 2 separation by catalytic cracking of methyldiethoxysilane. Industrial & Engineering Chemistry Research, 44, 4035-4041.

Hong, M., Li, S., Falconer, J.L., & Noble, R.D. (2008), Hydrogen purification using SAPO-34 membrane. J. Membr. Sci., 307, 277-283.

Hong, M., Li., S., Funke, H.F., Falconer, J.L., & Noble, R.D. (2007), Ion-exchanged SAPO-34 membrane for light gas separations. Micropor. Mesopor. Mater., 106, 140-146.

Hong, Z., Sun, F., Chen, D., Zhang, C., Gu, X., Xu, N. (2013) Improvement of hydrogen-separating performance by on-stream catalytic cracking of silane over 273 hollow fiber MFI zeolite membrane. International Journal of Hydrogen Energy, 38, 8409-8414.

Hong, Z., Zhang, C., Gu, X., Jin, W., Xu, N.(2011) A simple method for healing nonzeolitic pores of MFI membranes by hydrolysis of silanes. Journal of Membrane Science, 366, 427-435.

Howarth, R. W., Santoro, R., & Ingraffea, A. (2011). Methane and the greenhouse-gas footprint of natural gas from shale formations. Climatic Change, 106(4), 679-690. J. Chin. Chem. Soc 61, 719–730.

Ismail, A. F. & David, L. I. B. (2001) A review on the latest development of carbon membranes for gas separation. Journal of Membrane Science, 193, 1-18.

Ismail, A. F. & Lai, P. Y. (2003) Effects of phase inversion and rheological factors on formation of defect-free and ultrathin-skinned asymmetric polysulfone membranes for gas separation. Separation and Purification Technology, 33, 127-143.

Ismail, A. F., Ridzuan, N. & Rahman, A. (2002) Latest development on the membrane formation for gas separation. Songklanakarin Journal of Science and Technology, 24, 1025-1042.

J.-S. Kim, S. Lee, S.-B. Lee, M.-J. Choi, K.-W. Lee, Catal. Today, 115 (2006), pp. 228–234

Jansen, D., Dijkstra, J.W., van den Brink, R.W., Peters, T.A., Stange, M., Bredesen, R., Goldbach, A., Xu, H.Y., Gottschalk, A., & Doukelis, A. (2009), Hydrogen membrane reactor for CO2 capture, Energy Procedia, 1, 253-260.

Jia, M., Peinemann, K.-V. & Behling, R.-D. (1991) Molecular sieving effect of the zeolite-filled silicone rubber membranes in gas permeation. Journal of Membrane Science, 57, 289-292.

Jia, M.-D., Chen, B., Noble, R. D. & Falconer, J. L. (1994) Ceramic-zeolite composite membranes and their application for separation of vapor/gas mixtures. Journal of Membrane Science, 90, 1-10.

Jia, M.-D., Pleinemann, K.-V. & Behling, R.-D. (1992) Preparation and characterization of thin-film zeolite-PDMS composite membranes. Journal of Membrane Science, 73, 119-128.

Jia, W. & Murad, S. (2005) Separation of gas mixtures using a range of zeolite membranes: A molecular-dynamics study. The Journal Of Chemical Physics, 122, 234708-1 - 234708-11.

Kapteijn, F., Bakker, W. J. W., Zheng, G., Poppe, J. & Moulijn, J. A. (1995) Permeation and separation of light hydrocarbons through a silicalite-1 membrane: Application of the generalized Maxwell-Stefan equations. The Chemical Engineering Journal and the Biochemical Engineering Journal, 57, 145-153.

Keizer, K., Burggraff, A. J., Vroon, Z. A. E. P. & Verwiej, H. (1998) Two component permeation through thin zeolite MFI membranes. Journal of Membrane Science, 147, 159-172.

Keizer, K., Verwiej, H. (1996) Progress in inorganic membranes. Chemtech, 37.

Khajavi, S.; Jansen, J.C.; Kapteijn, F. (2010), Performance of hydroxy sodalite membranes as absolute water selective materials under acidic and basic conditions. J. Membr. Sci. 2010, 356, 1–6.

Kim, Y. K., Lee, J. M., Park, H. B. & Lee, Y. M. (2004) The gas separation properties of carbon molecular sieve membranes derived from polyimides having carboxylic acid groups. Journal of Membrane Science, 235, 139-146.

Kim, Y. S., Kusakabe, K., Morooka, S. & Yang, S. M. (2001) Preparation of microporous silica membranes for gas separation. Korean Journal of Chemical Engineering, 18, 106-112.

Koros, W. J. & Mahajan, R. (2000) Pushing the limits on possibilities for large scale gas separation: which strategies? Journal of Membrane Science, 175, 181-196.

Koros, W. J. (2002) Gas separation membranes: Needs for combined materials science and processing approaches. Macromolecular Symposia, 188, 13-22.

Koros, W.J. (2004), Evolving Beyond the Thermal Age of Separation Processes: Membranes Can Lead the Way. AIChE J. 50 2326.

Krishna, R. & Baur, R. (2003) Modelling issues in zeolite based separation processes. Separation and Purification Technology, 33, 213-254.

Krishna, R. & Paschek, D. (2000) Permeation of hexane isomers across ZSM-5 zeolite membranes. Industrial & Engineering Chemistry Research, 39, 2618-2622.

Krishna, R. & Van Den Broeke, L. J. P. (1995) The Maxwell-Stefan description of mass transport across zeolite membranes. The Chemical Engineering Journal and the Biochemical Engineering Journal, 57, 155-162.

Krishna, R. (1990) Multicomponent surface diffusion of adsorbed species: a description based on the generalized Maxwell--Stefan equations. Chemical Engineering Science, 45, 1779-1791.

Krishna, R. (1993) Problems and pitfalls in the use of the fick formulation for intraparticle diffusion. Chemical Engineering Science, 48, 845-861.

Krishna, R., Paschek, D. & Baur, R. (2004) Modeling the occupancy dependence of diffusivities in zeolites. Microporous and Mesoporous Materials, 76, 233-246.

Kusakabe, K., Kuroda, T. & Morooka, S. (1998) Separation of carbon dioxide from nitrogen using ion-exchanged faujasite-type zeolite membranes formed on porous support tubes. Industrial and Engineering Chemistry Research, 36, 649-655.

Kusakabe, K., Kuroda, T., Murata, A., Morooka, S. (1997), Formation of a Y-type zeolite membrane on a porous R-alumina tube for gas separation. Ind. Eng. Chem. Res., 36, 649

Kusakabe, K., Yoneshige, S., Murata, A. & Morooka, S. (1996) Morphology and gas permeance of ZSM-5-type zeolite membrane formed on a porous [alpha]-alumina support tube. Journal of Membrane Science, 116, 39-46.

Lai, Z.; Bonilla, G.; Diaz, I.; Nery, J.G.; Sujaoti, K.; Amat, M.A.; Kokkoli, E.; Terasak, O. (2003), Thompson, R.W.; Tsapatsis, M.; Vlachos, D.G. Microstructural optimization of a zeolite membrane for organic vapour separation. Science, 300, 456–460.

Larkum, A. W. D. (2010). Limitations and prospects of natural photosynthesis for bioenergy production. Current opinion in biotechnology, 21(3), 271-276.

Lassinantti, M., Hedlund, J., & Sterte, J. (2000), Faujasite-type films synthesized by seeding. Micropor. Mesopor. Mater., 38, 25.

Leo, A., Liu, S., & da Costa, J. C. D. (2009). Development of mixed conducting membranes for clean coal energy delivery. International Journal of Greenhouse Gas Control, 3(4), 357-367.

Li, S., & Fan, C.Q. (2010), High-Flux SAPO-34 Membrane for CO2/N2 separation. Ind. Eng. Chem. Res.,49, 4399-4404.

Li, S., Alvarado, G., Noble, R.D., & Falconer, J.L. (2005), Effects of impurities on CO2/CH4 separations through SAPO-34 membranes. J. Membr. Sci., 251, 59-66.

Li, S., Falconer, J. L., & Noble, R. D. (2006), Improved SAPO-34 membranes for CO2/CH4 separations. AdV. Mater., 18, 2601.

Li, S., Falconer, J. L., & Noble, R. D. (2007), Krishna , Modeling permeation of CO2/CH4, CO2/N2, and N2/CH4 mixtures across SAPO-34 membrane with the Maxwell-Stefan equations. Ind. Eng. Chem. Res., 46, 3904

Li, S., Falconer, J. L., Noble, R. D. & Krishna, R. (2007), Interpreting unary, binary, and ternary mixture permeation across a SAPO-34 membrane with loading-dependent Maxwell-Stefan diffusivities. J. Phys. Chem.,111, 5075.

Li, S., Falconer, J.L., & Noble, R.D. (2008), SAPO-34 membranes for CO2/CH4 separations: Effect of Si/Al ratio. Micropor. Mesopor. Mater., 110, 310-317.

Li, S., Martinek, J., Falconer, J. L., Noble, R. D., & Gardner, T. Q. (2005), High-pressure CO2/CH4 separation using SAPO-34 membranes. Ind. Eng. Chem. Res., 44, 3220.

Li, Y., Pera-Titus, M., Xiong, G., Yang, W., Landdrivon, E., Miachon, S., & Dalmon, J. (2008), Nanocomposite MFI-alumina membranes via pore-plugging synthesis: Genesis of the zeolite material. J. Membr. Sci., 325, 973-981.

Liang, Z. H., Rongwong, W., Liu, H., Fu, K., Gao, H., Cao, F., & Nath, D. (2015). Recent progress and new developments in post-combustion carbon-capture technology with amine based solvents. International Journal of Greenhouse Gas Control, 40, 26-54.

Lin Hao , Pei Li , Tingxu Yang , Tai-Shung Chung, Room temperature ionic liquid/ZIF-8 mixed-matrix membranes for natural gas sweetening and post-combustion CO2 capture, Journal of Membrane Science 436 (2013) 221–231

Lin, H. & Freeman, B. D. (2005) Materials selection guidelines for membranes that remove CO2 from gas mixtures. Journal of Molecular Structure, 739, 57-74.

Lin, X., Falconer, J. L. & Noble, R. D. (1998) Parallel Pathways for Transport in ZSM-5 Zeolite Membranes. Chemistry of Materials, 10, 3716-3723.

Lin, Y. S. (2001) Microporous and dense inorganic membranes: Current status and prospective. Separation and Purification Technology, 25, 39-55.

Lin, Y. S., Kumakiri, I., Nair, B. N. & Alsyouri, H. (2002) Microporous inorganic membranes. Separation and Purification Methods, 31, 229-379.

Lin, Y.S. (2000), Microporous and dense inorganic membranes: current status and prospective. Separation and Purification Technology, 25(1-3), 39-55.

Loiola, A.R., Andrade, J.C.R.A., Sasaki, J.M., & da Silva, L.R.D. (2012), Structural analysis of zeolite NaA synthesized by a cost-effective hydrothermal method using kaolin and its use as water softener. Journal of Colloid and Interface Science, 367, 34–39

Longwell, J. P., Rubin, E. S., & Wilson, J. (1995). Coal: Energy for the future. Progress in Energy and Combustion Science, 21(4), 269-360.

Lund, J. W., & Freeston, D. H. (2001). World-wide direct uses of geothermal energy 2000. Geothermics, 30(1), 29-68.

Luque, S., Gòmez, D., Alvarez, J.R. (2008) Industrial applications of porous ceramic membranes (Pressure driven processes). Membrane Science and Technology, 13, 177-216.

Lüthje, Mikael. "Carbon capture and storage." (2010).

Mason, J. A., McDonald, T. M., Bae, T. H., Bachman, J. E., Sumida, K., Dutton, J. J., ... & Long, J. R. (2015). Application of a high-throughput analyzer in evaluating solid adsorbents for post-combustion carbon capture via multicomponent adsorption of CO2, N2, and H2O. Journal of the American Chemical Society, 137(14), 4787-4803.

Matsufuji, T., Nishiyama, N., Matsukata, M., & Ueyama, K. (2000), Separation of butane and xylene isomers with MFI-type zeolitic membrane synthesized by vapour phase transport method. J. Membr. Sci., 178, 25–34.

Matsukata, M.; Nishiyama, N.; Ueyama, K. (1993), Synthesis of zeolites under vapour atmosphere. Effect of synthetic conditions on zeolite structure. Micropor. Mater., 1, 219–222.

Matsukata, M.; Nishiyama, N.; Ueyama, K. (1994), Zeolitic membrane synthesized on a porous alumina support. Chem. Commun., 3, 339–340.

Mccarley, K. C. & Way, J. D. (2001) Development of a model surface flow membrane by modification of porous [gamma]-alumina with octadecyltrichlorosilane. Separation and Purification Technology, 25, 195-210.

McCoy, S. T., & Rubin, E. S. (2008). An engineering-economic model of pipeline transport of CO 2 with application to carbon capture and storage. International journal of greenhouse gas control, 2(2), 219-229.

Mcleary, E. E., Jansen, J. C. & Kapteijn, F. (2006) Zeolite based films, membranes and membrane reactors: Progress and prospects. Microporous and Mesoporous Materials, 90, 198-220.

Meinema, H. A., Dirrix, R. W. J., Brinkman, H. W., Terpstra, R. A., Jekerle, J. & Kosters, P. H. (2005) Ceramic Membranes for Gas Separation - Recent Developments and State of the Art. Interceram, 54, 86-91.

Merkel, T.; Lin, H.; Wei, X.; He, J.; Firat, B.; Amo, K.; Daniels, R.; Baker, R. A (2009) membrane process to capture CO2 from coal-fired power plant flue gas, NETL review meeting, March 24-26.

Merkel, T.C., Lin, H., Wei, X., & Baker, R. (2010), Power plant post-combustion carbon dioxide capture: An opportunity for membranes. J. Membr. Sci., 359, 126-139.

Miachon, S., & Dalmon, J. (2004), Catalysis in membrane reactors: what about the catalyst. Top. Catal., 29, 59

Miachon, S., Ciavarella, P., van Dyk, L., Kumakiri, I., Fiaty, K., Schuurman, Y., & Dalmon, J. (2007), Nanocomposite MFI-alumina membranes via pore-plugging synthesis: Specific transport and separation properties. J. Membr. Sci., 298, 71-79.

Miachon, S., Landrivon, E., Aouine, M., Sun, Y., Kumakiri, I., Li, Y., Pachtova Prokova, O., Guilhaume, N., Giroir-Fendler, A., Mozzanega, & H., Dalmon, J. (2006), Nanocomposite MFI-alumina membranes via pore-plugging synthesis Preparation and morphological characterization. J. Membr. Sci., 281, 228-238.

Miachon, S., Mazuy, A., Dalmon, J.A. (2000) Catalysis of palladium salt reduction in a gas-liquid membrane reactor. Studies in Surface Science and Catalysis, 130, 2693-2698.

Miachon, S., Syakaev, V.V., Rakhmatullin, A., Pera-Titus, M., Caldarelli, S., & Dalmon, J. (2008), Higher gas solubility in nanoliquids?. Chem. Phys. Chem., 11 (1), 78-82

Miller, B. G. (2004). Coal energy systems. Academic Press.

Milora, S. L., & Tester, J. W. (1976). Geothermal energy as a source of electric power. Thermodynamic and economic design criteria.

Mor, G. K., Varghese, O. K., Paulose, M., Shankar, K., & Grimes, C. A. (2006). A review on highly ordered, vertically oriented TiO 2 nanotube arrays: fabrication, material properties, and solar energy applications. Solar Energy Materials and Solar Cells, 90(14), 2011-2075.

Muffler, L. P. (1979). Assessment of geothermal resources of the United States, 1978 (No. USGS-CIRC-790). Geological Survey, Reston, VA (USA). Geologic Div.

Mulder, M. (Ed.) (1996) Basic principles of membrane technology. Kluwer Academic Publishers: Netherlands.

Noack, M., Kolsch, P., Schafer, R., Toussaint, P. & Caro, J. (2002) Molecular sieve membranes for industrial application: Problems, progress, solutions (Reprinted from Chem. Ing. Tech., vol 73, pg 958-967, 2001). Chemical Engineering & Technology, 25, 221-230.

Noack, M., Kolsch, P., Schafer, R., Toussaint, P., Sieber, I. & Caro, J. (2001) Preparation of MFI membranes of enlarged area with high reproducibility. Microporous and Mesoporous Materials, 49, 25-37.

Noack, M., Kolsch, P., Seefeld, V., Toussaint, P., Georgi, G. & Caro, J. (2005a) Influence of the Si/Al-ratio on the permeation properties of MFI-membranes. Microporous and Mesoporous Materials, 79, 329-337.

Noack, M., Mabande, G. T. P., Caro, J., Georgi, G., Schwieger, W., Kolsch, P. & Avhale, A. (2005b) Influence of Si/Al ratio, pre-treatment and measurement conditions on permeation properties of MFI membranes on metallic and ceramic supports. Microporous and Mesoporous Materials, 82, 147-157.

Noble, R. D., Koval, C. A. & Pellegrino, J. J. (1989) Facilitated transport membrane systems. Chemical Engineering Progress, 85, 58-78.

Ohtaa, Y.; Takababb, H.; Nakao, S. A (2007) combinatorial dynamic Monte Carlo approach to finding a suitable zeolite membrane structure for CO2/ N2 separation. Microporous Mesoporous Mater., 101, 319

Pandey, P. & Chauhan, R. S. (2001) Membranes for gas separation. Progress in Polymer Science, 26, 853-893.

Pedroli, B., Elbersen, B., Frederiksen, P., Grandin, U., Heikkilä, R., Krogh, P. H., ... & Spijker, J. (2013). Is energy cropping in Europe compatible with biodiversity?–Opportunities and threats to biodiversity from land-based production of biomass for bioenergy purposes. Biomass and Bioenergy, 55, 73-86.

Perathoner S, Centi G. 2014 A new scenario for green & sustainable chemical production.

Pera-Titus, M. (2014), Porous inorganic membranes for CO2 capture: Present and prospects. Chem. Rev., 114(2), 1413-1492

Pereira, C. C., Nobrega, R., Peinemann, K. V. & Borges, C. P. (2003) Hollow fiber membranes obtained by simultaneous spinning of two polymer solutions: a morphological study. Journal of Membrane Science, 226, 35-50.

Ping, E., Zhou, R., Funke, H., Falconer, J., Noble, R. (2012) Seeded-gel synthesis of SAPO-34 single channel and monolith membranes, for CO2/CH4 separations. Journal of Membrane Science, 415-416, 770-775.

Pires, J. C. M., Martins, F. G., Alvim-Ferraz, M. C. M., & Simões, M. (2011). Recent developments on carbon capture and storage: an overview. Chemical Engineering Research and Design, 89(9), 1446-1460.

Poshusta, J. C., Noble, R. D. & Falconer, J. L. (1999) Temperature and pressure effects on CO2 and CH4 permeation through MFI zeolite membranes. Journal of Membrane Science, 160, 115-125.

Poshusta, J. C., Noble, R. D., & Falconer, J. L. (2001), Characterization of SAPO-34 membranes by water adsorption. J. Membr. Sci., 186, 25.

Poshusta, J.C., Tuan, V.A., Falconer, J.L., & Noble, R.D. (1998), Synthesis and permeation properties of SAPO-34 tubular membranes. Ind. Chem. Res., 37, 3924-3929.

Powell, C.E., & Qiao, G.G. (2006), Polymeric CO2/N2 gas separation membranes for the capture of carbon dioxide from power plant flue gases. J. Membr. Sci., 279, 1-49.

Rackley, S. (2009). Carbon capture and storage. Gulf Professional Publishing.

Rahamana S.A.M., Cheng L-H., Zhang, L., Chena, H-L, 2011, A review of carbon dioxide capture and utilization by membrane integrated microalgal cultivation processes., Renewable and Sustainable Energy Reviews Volume 15, Issue 8, Pages 4002–4012

Ruthven, D.M., (1984) Principles of Adsorption Processes J Wiley & Sons Inc.: Canada.

Sakamoto, K., Obata, K., Hirata, H., Nakajima, M., & Sakurai, H. (1989), Chemistry of organosilicon compounds. 257. Novel anionic polymerization of masked disilenes to polysilylene high polymers and block copolymers. J. Am. Chem. Soc., 111 (19), 7641-7643. DOI: 10.1021/ja00201a070

Salomon, M. A., Coronas, J., Menendez, M. & Santamaria, J. (2000) Synthesis of MTBE in zeolite membrane reactors. Applied Catalysis A: General, 200, 201-210.

Sato, K., & Nakane, T. (2007), A high reproducible fabrication method for industrial production of high flux NaA zeolite membrane. J. Membr. Sci., 301, 151-161.

Shin, D. W., Hyun, S. H., Cho, C. H. & Han, M. H. (2005) Synthesis and CO2/N2 gas permeation characteristics of ZSM-5 zeolite membranes. Microporous and Mesoporous Materials, 85, 313-323.

Sipahutar, R., Bernas, S. M., & Imanuddin, M. S. (2013). Renewable energy and hydropower utilization tendency worldwide. Renewable and Sustainable Energy Reviews, 17, 213-215.

Sjöberg, E., Barnes, S., Korelskiy, D., Hedlund, J. (2015) MFI membranes for separation of carbon dioxide from synthesis gas at high pressures. Journal of Membrane Science 2015, 486, 132-137.

Skoulidas, A. I., Bowen, T. C., Doelling, C. M., Falconer, J. L., Noble, R. D. & Sholl, D. S. (2003) Comparing atomistic simulations and experimental measurements for CH4/CF4

mixture permeation through silicalite membranes. Journal of Membrane Science, 227, 123-136.

Sloan, E. D. (2003). Fundamental principles and applications of natural gas hydrates. Nature, 426(6964), 353-363.

Snyder M.A., & Tsapatsis M. (2007), Hierarchical Nanomanufacturing: From Shaped Zeolite Nanoparticles to High Performance Separation Membranes. Angew. Chem. Int. Ed, 119, 7704–7717.

Solangi, K. H., Islam, M. R., Saidur, R., Rahim, N. A., & Fayaz, H. (2011). A review on global solar energy policy. Renewable and sustainable energy reviews, 15(4), 2149-2163.

Sommer, S., Melin, T., Falconer, J. L. & Noble, R. D. (2003) Transport of C6 isomers through ZSM-5 zeolite membranes. Journal of Membrane Science, 224, 51-67.

Songolzadeh, M., Soleimani, M., Ravanchi, T.M., Songolzadeh, R. (2014), Carbon Dioxide Separation from Flue Gases: A Technological Review Emphasizing Reduction in Greenhouse Gas Emissions. The Sci. World J. http://dx.doi.org/10.1155/2014/828131 accessed 20/04/2015

Soria, R. (1995) Overview on industrial membranes. Catalysis Today, 25, 285-290.

Stickler, C. M., Coe, M. T., Costa, M. H., Nepstad, D. C., McGrath, D. G., Dias, L. C., ... & Soares-Filho, B. S. (2013), Dependence of hydropower energy generation on forests in the Amazon Basin at local and regional scales. Proceedings of the National Academy of Sciences, 110(23), 9601-9606.

Tang, Z., Kim, S., Reddy, G., Dong, J., Smirniotis, P. (2010) Modified zeolite membrane reactor for high temperature water gas shift reaction. Journal of Membrane Science, 354, 114-122.

Tavolaro, A. & Drioli, E. (1999) Zeolite Membranes. Advanced Materials, 11, 975-996.

Thielemann, T., Schmidt, S., & Gerling, J. P. (2007). Lignite and hard coal: Energy suppliers for world needs until the year 2100—An outlook. International Journal of Coal Geology, 72(1), 1-14.

Tin, P. S., Chung, T. S., Liu, Y., Wang, R., Liu, S. L. & Pramoda, K. P. (2003) Effects of cross-linking modification on gas separation performance of Matrimid membranes. Journal of Membrane Science, 225, 77-90.

Tsai, C.-Y., Tam, S.-Y., Lu, Y. & Brinker, C. J. (2000) Dual-layer asymmetric microporous silica membranes. Journal of Membrane Science, 169, 255-268.

Tuan, V.A., Li, S., Noble, R.D., & Falconer, J.L. (2001), Preparation and pervaporation properties of a MEL-type zeolite membrane. Chem. Commun., 583-584. DOI 10.1039/B008547M

Urry, J. (2013). Societies beyond oil: Oil dregs and social futures. Zed Books.

Van De Graaf, J. M., Kapteijn, F. & Moulijn, J. A. (1999) Modeling permeation of binary mixtures through zeolite membranes. AIChE Journal, 45, 497-511.

Van De Graaf, J. M., Kapteijn, F. & Moulijn, J. A. (2000) Diffusivities of light alkanes in a silicalite-1 membrane layer. Microporous and Mesoporous Materials, 35-36, 267-281.

Van De Graaf, J. M., Van Der Bijl, E., Stol, A., Kapteijn, F. & Moulijn, J. A. (1998) Effect of operating conditions and membrane quality on the separation performance of composite silicalite-1 membranes. Industrial & Engineering Chemistry Research, 37, 4071-4083.

van den Bergh, J., Zhu, W., Gascon, J., Moulijn, J. A., & Kapteijn, F. (2008) Separation and permeation characteristics of a DD3R zeolite membrane. J. Membr. Sci. 316, 35

Van Den Broeke, L. J. P., Kapteijn, F. & Moulijn, J. A. (1999b) Transport and separation properties of a silicalite-1 membrane-II. Variable separation factor. Chemical Engineering Science, 54, 259-269.

Van Dyk, L., Lorenzen, L., Miachon, S.,& Dalmon, J. (2005), Xylene isomerization in an extractor type catalytic membrane reactor. Catal. Today, 104, 274-280

Van Vuuren, D. P., van Vliet, J., & Stehfest, E. (2009). Future bio-energy potential under various natural constraints. Energy Policy, 37(11), 4220-4230.

Vandezande, P., Lieven, E., & Vankelecom F. (2008), Solvent resistant nanofiltration: separating on a molecular level. Chem. Soc. Rev., 37, 365-405.

Verweij, H. (2003) Ceramic membranes: Morphology and transport. Journal of Material Science, 38, 4677-4695.

Verweij, H., Lin, Y. S. & Dong, J. (2006) Microporous silica and zeolite membranes for hydrogen purification. MRS Bulletin, 31, 756-764.

Vroon, Z. A. E. P., Keizer, K., Burggraaf, A. J. & Verweij, H. (1998) Preparation and characterization of thin zeolite MFI membranes on porous supports. Journal of Membrane Science, 144, 65-76.

Vroon, Z., Keizer, K., Gilde, M. J., Verweij, H. & Burggraaf, A. J. (1996) Transport properties of alkanes through ceramic thin zeolite MFI membranes. Journal of Membrane Science, 113, 293-300.

Wei, Q., Ding, Y., Nie, Z., Liu, X., Li, Q. (2014) Wettability, pore structure and performance of perfluorodecyl-modified silica membranes. Journal of Membrane Science, 466, 114-122.

Xiao, J. & Wei, J. (1992) Diffusion mechanism of hydrocarbons in zeolites--I. Theory. Chemical Engineering Science, 47, 1123-1141.

Xomeritakis, G. & Lin, Y. S. (1996) Fabrication of a thin palladium membrane supported in a porous ceramic substrate by chemical vapor deposition. Journal of Membrane Science, 120, 261-272.

Xomeritakis, G., Gouzinis, A., Nair, S., Okubo, T., He, M. Y., Overney, R. M. & Tsapatsis, M. (1999) Growth, microstructure, and permeation properties of supported zeolite (MFI) films and membranes prepared by secondary growth. Chemical Engineering Science, 54, 3521-3531.

Xomeritakis, G., Lai, Z. P. & Tsapatsis, M. (2001) Separation of xylene isomer vapors with oriented MFI membranes made by seeded growth. Industrial & Engineering Chemistry Research, 40, 544-552.

Xu, W., Dong, J., Li, J., & Wu, F. (1990), A novel method for the preparation of zeolite ZSM-5. J. Chem. Soc. Chem. Commun., 10, 755-756.

Yang, H., Chen, H., Du, H., Hawkins, R., Craig, F., Ring, Z., Omotoso, O., Munoz, V., & Mikula, R.(2009), Incorporating platinum precursors into a NaA-zeolite synthesis mixture promoting the formation of nanosized zeolite. Micropor. and Mesopor. Materi., 117, 33–40

Yang, H., Xu, Z., Fan, M., Gupta, R., Slimane, R.B., Bland, A.E., & Wright, I. (2008), Progress in carbon dioxide separation and capture: A review. J. Env. Sci., 20, 14-27

Yang, M., Crittenden, B. D., Perera, S. P., Moueddeb, H. & Dalmon, J. A. (1999) The hindering effect of adsorbed components on the permeation of a non-adsorbing component through a microporous silicalite membrane: the potential barrier theory. Journal of Membrane Science, 156, 1-9. 299

Yang, R.T., (1997) Gas separation by Adsorption Processes. Imperial College Press: London

Zah, J., Krieg, H., & Beytenbach, J, (2007), Single gas permeation through compositionally different zeolite NaA membranes: Observation on the intercrystalline porosity in an unconventional, semicrytalline layer. J. Membr. Sci., 287, 300-310.

Zhang, C., Hong, Z., Chen, J., Gu, X., Jin, W., Xu, N. (2012) Catalytic MFI zeolite membranes supported on α-Al2O3 substrates for m-xylene isomerization. Journal of Membrane Science, 389, 451-458.

Zhang, X., Singh, B., He, X., Gundersen, T., Deng, L., & Zhang, S. (2014). Post-combustion carbon capture technologies: Energetic analysis and life cycle assessment. International Journal of Greenhouse Gas Control, 27, 289-298.

Zhang, X., Tang, D., & Jiang, G. (2013), Synnthesis of zeolite NaA at room temperature: The effect of synthesis parameters on crystal size and its size distribution. J. Membr. Sci., 24, 689-696.

Zhang, Y., Avila, A., Tokay, B., Funke, H., Falconer, J., Noble, R. (2010) Blocking defects in SAPO-34 membranes with cyclodextrin. Journal of Membrane Science, 358, 7-12.

Zhang, Y., Wu, Z., Hong, Z., Gu, X., Xu, N.(2012) Hydrogen-selective zeolite membrane reactor for low temperature water gas shift reaction. Chemical Engineering Journal, 197, 314-321.

Zhao, L., Rienche, E., Menzer, R., Blum, L., & Stolten, D. (2008), A parametric study of CO2/N2 gas separation membrane processes for post-combustion capture. J. Membr. Sci., 325, 284-294.

Zhao, Z., Ma, X., Li, Z., Lin,Y.S.(2011) Synthesis and Characterisation of MOF-5 Membranes. Journal of Membrane Science, 382, 82-90.

Zhao,Z., Ma, X., Kasik, A., Li, Z., Lin, Y.S. (2013) Gas separation properties of metal organic framework (MOF-5) Membranes. Industrial and Chemical Engineering Research, 52, 1102-1108.

Zheng, J., Lee, Y. K., Babu, P., Zhang, P., & Linga, P. (2016). Impact of fixed bed reactor orientation, liquid saturation, bed volume and temperature on the clathrate hydrate process for pre-combustion carbon capture. Journal of Natural Gas Science and Engineering.

Zhou, H., Korelskiy, D., Sjöberg, E., Hedlund, J. (2014) ultrathin hydrophobic MFI membranes. Microporous and Mesoporous Materials, 192, 76-81.

Zhou, W., Yoshino, M., Kita, H. & Okamoto, K.-I. (2003) Preparation and gas permeation properties of carbon molecular sieve membranes based on sulfonated phenolic resin. Journal of Membrane Science, 217, 55-67.

Zhou, Z.; Yang, J.; Zhang, Y.; Chang, L. (2007), Sun, W.; Wang, J. NaA zeolite/carbon nanocomposite thin films with high permeance for CO2/N2 separation. Sep. Purif. Technol., 55, 392

Zhu, M., Kumakiri, I., Tanaka, K., Kita, H. (2013) Dehydration of acetic acid and esterification product by acid-stable ZSM-5 membrane. Microporous and Mesoporous Materials, 181, 47-53.

Zhu, W., Hrabanek, P., Gora, L., Kapteijn, F. & Moulijn, J. A. (2006) Role of adsorption in the permeation of CH4 and CO2 through a silicalite-1 membrane. Industrial & Engineering Chemistry Research, 45, 767-776.

# Appendix 1

## Matlab modelling code

.

**Appendix 1**

```
%%Start of Experimental Data Declaration%%

t = [298 375 423 473 523];
PermeanceCO2 = [0.246e-6 0.15e-6 0.1256e-6 0.1186e-6 0.109e-
6];

%%End of Experimental Data Declaration%%

%%Start of Variable Declaration for Maxwell Stefan (MS)
Model%%

R = 8.315; % Ideal gas constant  in J/molK
Csat1 = 4.52; % Concentration of CO2 in SAPO-34 membrane in
mol/Kg
rho = 2260;% Density of SAPO-34 in Kg/m3
E = 0.55; % Porosity of the SAPO-34 membrane
Di1 = 0.00000008; % Maxwell Stefan diffusivity @ zero coverage
for CO2 in m2/s
tor = 2.5; % Tortuosity
l = 0.732095;%Equivalent SAPO-34 membrane thickness in micro
meters, fitted parameters ;
Temp = [298 375 423 473 523]; % Temperature is from 280 to
480K
Pr = 121325; % Retentate pressure in Pa
Pp = 101325; % Permeate pressure in Pa
Po = 101325; % Reference to atmospheric pressure (101325Pa)
SAE1 = -58.07; % Standard adsorption entropy for CO2 in J/molK
DAE1 = 1200; % Diffusion activation energy for CO2 in J/mol
SAD1 = -8200; % Standard adsorption enthalpy for CO2 in J/mol

%% End of Variable Declaration for MS Model%%

%% Expression for Maxwell Stefan Model for CO2 %%

term11 = Csat1*rho*E*Di1;
term12 = tor*l;
term1 = term11*term12.^-1;
term21 = (1 + (Pr*Po.^-1)*exp((SAE1- R)*R.^-1 -
(SAD1*(R*Temp).^-1)));
term22 = (1 + (Pp*Po.^-1)*exp((SAE1- R)*R.^-1 -
(SAD1*(R*Temp).^-1)));
term23 = term22.^-1 ;
term2 = log (term21.*term23);
term31 = -(DAE1)*(R*Temp).^-1 ;
term3 = exp(term31);
fPermeanceCO2 =  term1.*term2.*term3;
%end
```

```
%% SECTION TITLE
% DESCRIPTIVE TEXT
%% Expression for Output : MS Model %%
plot (Temp,fPermeanceCO2,'b-*', t,PermeanceCO2,'r*'),
xlabel('Temperature, (K) '),ylabel('Permeance(molm-2s-1Pa-1)')
grid on,
legend show
```

# Appendix 2

Research paper